

**The Dissertation Committee for Dennis Patrick Dunn Certifies
that this is the approved version of the following dissertation:**

**XENOLITH MINERALOGY AND GEOLOGY OF THE
PRAIRIE CREEK LAMPROITE PROVINCE, ARKANSAS**

Committee:

Douglas Smith, Supervisor

William D. Carlson

J. Richard Kyle

Fred W. McDowell

Steven C. Bergman

Tom E. McCandless

**XENOLITH MINERALOGY AND GEOLOGY OF THE
PRAIRIE CREEK LAMPROITE PROVINCE, ARKANSAS**

by

Dennis Patrick Dunn, B.S., M.S.

Dissertation

Presented to the Faculty of the Graduate School of

The University of Texas at Austin

in Partial Fulfillment

of the Requirements

for the Degree of

Doctor of Philosophy

The University of Texas at Austin

December, 2002

Dedication

This dissertation is dedicated to my wife Anita who stood by me these last five years and to my father Joseph who could not be here for its completion.

Acknowledgements

I would like to acknowledge the Arkansas State Parks Commission for their enlightened support of the 1990's evaluation at the Crater of Diamonds State Park and recognize the Arkansas Diamond Development Company and Texas Star Resources and Morgan Worldwide Mining Company for their participation in this project. I would also like to acknowledge Mike Waldman, Doug Duskin, and Larry Dusak for providing unpublished data and/or discussion of ideas which assisted with development of this topic.

Special recognition is warranted by Arkansas Diamond Development Company (ADDC) for funding the diamond evaluation which generated many of the xenoliths in this study and to Michael McMurrough for his permission to publish the data. I wish to acknowledge Texas Star for access to the heavy media plant and permission to collect additional xenoliths as available. I express my personal gratitude to Mike Waldman, who provided xenoliths for this study collected during Superior Minerals Twin Knobs 1 diamond evaluation, Steve Bergman who provided microprobe data of sample bl4f, Fred McDowell who provided K-Ar isotopic age dating of amphibolite composition crustal xenoliths, Greg Thompson for thin sections and Kitty Miliken for assistance with the microprobe. Finally, special thanks to Doug Smith for his encouragement, patience, support and ideas that went into this publication.

XENOLITH MINERALOGY AND GEOLOGY OF THE PRAIRIE CREEK LAMPROITE PROVINCE, ARKANSAS

Publication No. _____

Dennis Patrick Dunn, Ph.D.

The University of Texas at Austin, 2002

Supervisor: Douglas Smith

Abstract

Three new Arkansas lamproites were delineated and evaluated during the 1980's. The intrusions were emplaced during the Middle Cretaceous Period based on stratigraphic relationships and published isotopic ages. Geological relationships record a dominant crater facies lamproite with minimal vent erosion. A 260 tonne sample taken from the two larger lamproite vents recovered 5 macro diamonds (>0.5mm) yielding a sub-economic diamond grade of ~0.04 carats per 100 tonnes. A diamond evaluation program undertaken at the Prairie Creek vent by the Arkansas State Parks Commission in the 1990's resulted in mapping of four major rock types: epiclastic rocks, olivine lamproite, phlogopite-rich tuff and olivine-rich tuff. Significant diamond contents were found only within the phlogopite-rich tuff (~0.11 carat/100 t) and olivine-rich tuff (~1.1 carat/100 t). Stratigraphic relationships indicate that the diamondiferous

tuffs have undergone <50 meters of erosion. Extrapolation of the surface rock units and their diamond contents to the pre-erosion surface suggests that ~93,000 carats of diamonds were liberated and then concentrated as a natural surface enrichment.

Mantle xenoliths recovered from the Black Lick and Twin Knobs lamproite vents were analyzed for major element compositions. Their data were used to calculate a pressure-temperature array that record maximum pressures of ~5 GPa and maximum temperatures of ~1000°C for the xenolith source region. Comparisons between calculated pressures and olivine compositions indicate relatively shallow fertile mantle overlying more depleted mantle lithosphere. The two layers of mantle lithosphere may represent different ages based on their olivine composition. Crustal xenoliths include near-surface sedimentary rocks and abundant amphibolite with granitoids and rare meta-sedimentary and meta-volcanic rocks. K-Ar dates of 1.48-1.31 Ga were obtained from four amphibolite xenoliths. The cooling ages confirm that continental crust of ~1.42 Ga in age extends beneath southwestern Arkansas and that thermal effects of the younger Grenville and Ouachita orogenies were insufficient to reset the amphibole K-Ar systems. Xenolith data and published results are used to test two models for development of the Ouachita system. The first model proposes that the Ouachita trough is part of a mid-continent failed rift; the second model suggests the Ouachita System was formed at the rifted oceanic margin of the continental craton. The xenolith data support the intra-craton rift model over the oceanic-margin model.

Table of Contents

LIST OF TABLES	X
LIST OF FIGURES	XI
LIST OF FIGURES	XI
CHAPTER 1: REGIONAL SETTING	1
CHAPTER 2: GEOLOGY OF THREE NEW LAMPROITE OCCURRENCES	9
Exploration History	9
Geology	12
Petrology	15
Diamond Bulk Testing	17
Xenoliths, Megacrysts and Xenocrysts	19
CHAPTER 3: DIAMOND ECONOMICS OF THE PRAIRIE CREEK LAMPROITE	27
Introduction	27
Mining History	27
Prairie Creek Geology	28
<i>In-Situ</i> Diamond Distribution	30
Model and Erosional History	32
Surface Concentration	34
Economic Considerations	38

CHAPTER 4: MANTLE XENOLITHS	44
Xenolith Petrology	44
Dunite	45
Harzburgite	45
Wehrlite	45
Garnet Websterite	46
Eclogite	46
Low-Cr Spinel Lherzolite	46
Mid-Cr Spinel Lherzolite	47
High-Cr Spinel Peridotite	47
Garnet/Spinel Lherzolite	48
Garnet Lherzolites	48
Mineral Chemistry of Peridotite Xenoliths	49
Analytical methods	49
Olivine	49
Orthopyroxene	50
Clinopyroxene	51
Spinel	52
Garnet	53
Pressure-Temperature Calculations	54
Method	54
Results	55
Discussion of Results	57
CHAPTER 5: CRUSTAL XENOLITHS	97
Xenolith Petrology	97
Near-Surface Lithologies	98
Amphibolite	98

Granitic and Rhyolitic Rocks	99
Epidote-rich Rocks	100
Pelitic Metamorphic Rocks	102
K-Ar Dating	103
Discussion of Results	103
CHAPTER 6: SUMMARY AND CONCLUSIONS	124
APPENDIX A: MICROPROBE RESULTS FOR MANTLE XENOLITHS	129
APPENDIX B: MICROPROBE RESULTS FOR CRUSTAL XENOLITHS	130
REFERENCES	131
VITA	146

List of Tables

Table 4-1:	Mineral Rim Compositions Used in P-T Calculations.....	68
Table 4-2:	Selected Mineral Compositions Sensitive to Melt Depletion	77
Table 4-3:	Calculated pressure and temperature for garnet-bearing xenoliths ..	78
Table 4-4:	Calculated temperature for spinel peridotite at assumed pressure ...	79
Table 4-5:	Eclogite Temperature and Depletion Criteria	80
Table 5-1:	Mineral Compositions of Selected Crustal Xenoliths	115
Table 5-2:	K-Ar Data.....	117
Table 5-3:	Comparisons of Ouachita Model Expectations.....	117

List of Figures

Figure 1-1: Geographic map of south-central United States.....	5
Figure 1-2: Interpreted basement geology of south-central United States.....	6
Figure 1-3: Simplified geologic map of Arkansas	7
Figure 1-4: Location of known Prairie Creek lamproite occurrences.....	8
Figure 2-1: Surface geological interpretation of the Black Lick lamproite	20
Figure 2-2: Geological cross-section of the Black Lick lamproite	21
Figure 2-3: Surface geological interpretation of the Twin Knobs 2 lamproite ...	22
Figure 2-4: Geological cross-section of the Twin Knobs 2 lamproite	23
Figure 2-5: Surface geological interpretation of the Timberlands lamproite.....	24
Figure 2-6: Geological cross-section of the Timberlands lamproite.....	25
Figure 2-7: Diamonds recovered during bulk sampling evaluation.....	26
Figure 3-1: Simplified surface geology of the Prairie Creek lamproite.....	41
Figure 3-2: Recovered diamond grade within the Prairie Creek lamproite	42
Figure 3-3: Erosion profile across the Arkansas lamproite province.....	43
Figure 4-1: Selected backscatter electron images of xenoliths	81
Figure 4-2: Selected backscatter electron images of xenoliths	82
Figure 4-3a: Compositional zoning in a high-Cr garnet lherzolite	83
Figure 4-3b: Compositional zoning in a high-Cr spinel lherzolite	84
Figure 4-4a: Compositional zoning in a low-Cr spinel lherzolite	85

Figure 4-4b: Compositional zoning in a low-Cr spinel lherzolite.....	86
Figure 4-5a: Compositional zoning in a high-Cr garnet lherzolite	87
Figure 4-5b: Compositional zoning in a low-Cr garnet/spinel lherzolite	88
Figure 4-6a: P-T xenolith array utilizing T BKN @ P BKN	89
Figure 4-6b: P-T xenolith array utilizing T BKpx @ P BKN	90
Figure 4-6c: P-T xenolith array utilizing T Krogh @ P BKN	91
Figure 4-6d: P-T xenolith array utilizing T Nimis @ P Nimis	92
Figure 4-7: Comparison of forsterite content in olivine and pressure	93
Figure 4-8: Comparison of Cr ₂ O ₃ in spinel and Al ₂ O ₃ in orthopyroxene	94
Figure 4-9: Comparison of forsterite content in olivine and pressure (PBKN) ..	95
Figure 4-10: Idealized section of sub-continental mantle lithosphere	96
Figure 5-1: Photomicrographs thin sections in plane polarized light	117
Figure 5-2: Location map of the lithospheric transect of Mickus and Keller ...	118
Figure 5-3: Detailed crustal section beneath Prairie Creek lamproite province	119
Figure 5-4: Aulacogen model of Ouachita System (Lowe, 1985)	120
Figure 5-5: Rifted margin model of Ouachita System (Lowe, 1985)	120
Figure 5-6: Simplified lithospheric transect model (Mickus and Keller, 1992)	121
Figure 5-7: Idealized basement geology for the Ouachita aulacogen model	122

Chapter 1

REGIONAL SETTING

Several occurrences of diamond-bearing olivine lamproite are located in Pike County, Arkansas, USA (Scott-Smith and Skinner, 1984a). Pike County is located in the southwestern part of the state and straddles the geologic and physiographic boundary between the Gulf Coastal Plain and the Ouachita Mountains (Figure 1-1). The Gulf Coastal Plain is characterized by gently south-dipping Cretaceous sedimentary rocks that onlap and lie unconformably over the intensely folded and faulted east-west trending Paleozoic sedimentary rocks of the Ouachita Mountains (Miser and Purdue, 1929).

The existence of diamondiferous lamproites within such a young tectonic province located at the southern margin of the continental craton is unique and enigmatic. Most primary diamondiferous kimberlites are located within well exposed stable cratons of Precambrian age, such as those in South Africa, Siberia Australia and western Canada. A possible explanation for this occurrence is that the Ouachita Mountains may have been thrust onto and overlie the southern margin of the North American craton which represents a preserved boundary between continental and oceanic crust (Lillie, 1985). The age of the craton in this area is uncertain, although areas 300 km to the west (Oklahoma) and north (Missouri) contain rocks of the 1.3 to 1.5 Ga granite-rhyolite terrane of the mid-continental craton (Van Schmus and others, 1986). Precambrian rocks exposed in the Llano uplift of central Texas, located about 500 kilometers to the southwest, record ages from 1.38 to 1.07 Ga (Mosher, 1998). The Llano area lies south of the Llano deformation front, which is equivalent to the Grenville deformation front,

and extends northeastward from central Texas towards southwestern Arkansas (Figure 1-2).

The Prairie Creek lamproite, the largest intrusion within the Prairie Creek lamproite province, is wholly enclosed within the “Crater of Diamonds” State Park and has been determined to have a K-Ar age of 97-106 Ma (Zartman, 1977; Gogineni and others, 1978). Cretaceous lamproite intrusions were apparently injected along a zone of structural weakness related to the Gulf Coast hinge line (Baksi, 1997). The northeast alignment is also sub-parallel to the northeast-trending Reelfoot Rift located approximately 100 km east of the intrusions. Numerous syenite intrusions also of Cretaceous age, at least one with a carbonatite core (Magnet Cove), were emplaced along the trace of the Reelfoot Rift (Figure 1-3). Other Cretaceous age intrusions exist in southeastern Arkansas beneath the Mississippi Embayment (Moody, 1949).

The Prairie Creek lamproite province consists of seven known diamondiferous lamproite vents which extend for 5 km in a northeasterly direction from the largest of the vents, Prairie Creek (Figure 1-4). Three previously unexplored Arkansas lamproites were delineated and evaluated during the 1980's. The three vents – Black Lick (10 hectares), Twin Knobs 2 (2 hectares) and Timberlands (<1 hectare) -- were intruded into the Lower Cretaceous Trinity Formation and are overlain unconformably by the Late Cretaceous Tokio Formation rocks. These stratigraphic relationships, first described in detail in Chapter 2, are used in conjunction with published economic data to re-evaluate the diamond distribution at the “Crater of Diamonds” State Park in Chapter 3.

Xenoliths of mantle and crustal rocks were recovered from the Black Lick and Twin Knobs 2 lamproites during Arkansas Diamond Development Company's (ADDC) diamond bulk test. Xenoliths are pieces of foreign or country rocks that become

entrained within the volcanic host rock at any point during the ascent of magmas from their mantle lithosphere source regions. These small fragments of rock can reveal information as to the composition, age and geological history of the mantle and crustal lithosphere beneath southwestern Arkansas. This xenolith suite is of particular importance as no previous xenolith studies have focused on the Prairie Creek lamproite province, simply because no quantity of xenoliths has ever been recovered.

Approximately 1.5 kilograms of xenoliths were recovered from 260 tonnes of lamproitic material treated in a diamond recovery plant near Sloan, Colorado. An additional one kilogram of xenoliths was supplied by Mike Waldman; the latter were derived from Superior Mineral's economic evaluation of the Twin Knobs 1 lamproite from 170 tonnes treated at the same Colorado recovery plant a few years earlier. This recovery process involves progressive crushing, screening and heavy media separation resulting in xenoliths in the 0.5 to 3.0 centimeter size range.

The 2.5 kilograms of xenoliths represent less than 0.0006 % of the total lamproite processed. Approximately $\frac{3}{4}$ of the xenoliths recovered are of probable crustal origin. Half of these crustal xenoliths consist of near-surface lithologies including shale, sandstone and quartzite. The deep crustal xenoliths are dominantly amphibolite, with lesser quantities of granite and rare meta-sedimentary, meta-volcanic and micaceous rocks. The mantle xenoliths include dunite, harzburgite, websterite, eclogite and both spinel and garnet lherzolite.

Compositions of mantle-derived xenoliths (Chapter 4) record a P-T array indicating a calculated geotherm of $\sim 40 \text{ mW/m}^2$. Analysis of the depletion index and recorded pressures of xenoliths indicate the presence of a two layer mantle lithosphere. The majority of the deep crustal xenoliths (Chapter 5) are amphibolites with lesser

amounts of granite which generally are extensively altered to epidote-rich rock. K-Ar isotopic dates of the amphibolites record an average age of 1.42 Ga. These new xenolith data have significant implications for the generation of continental lithosphere in this region.

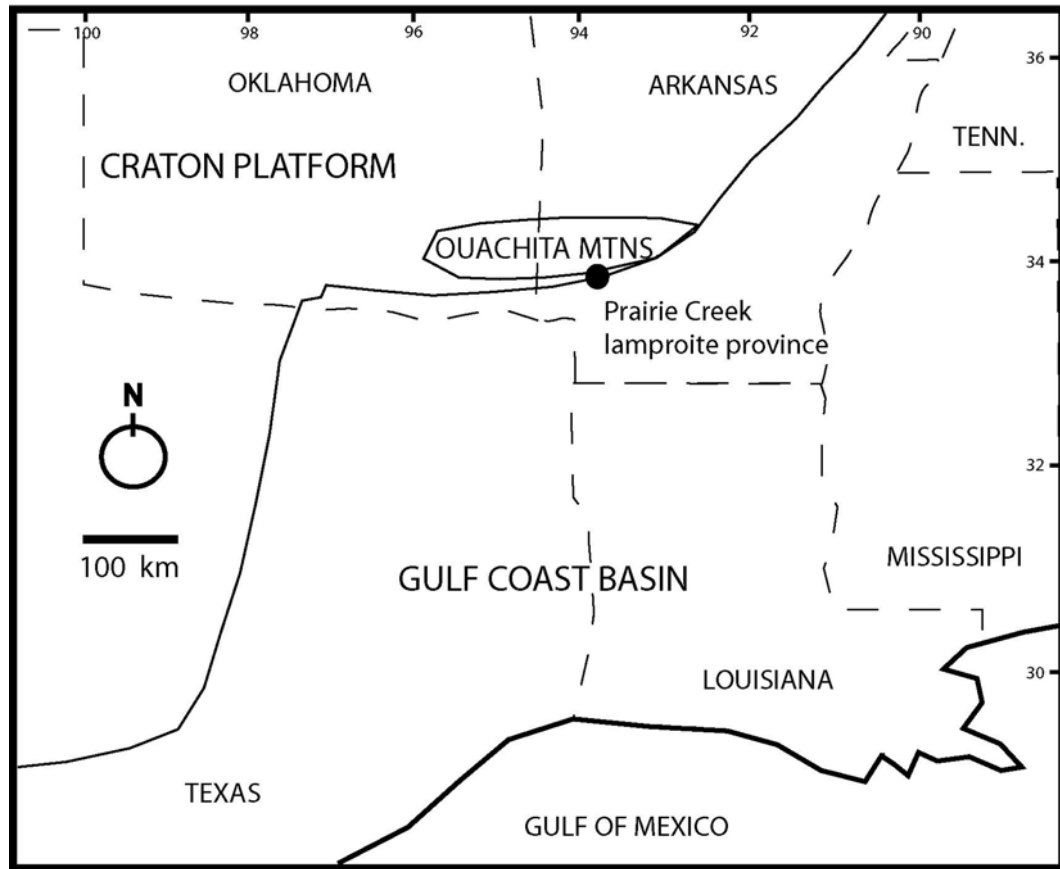


Figure 1-1: Geographic map of south-central United States. The location of the Prairie Creek lamproite province is shown in relation to selected geologic elements.

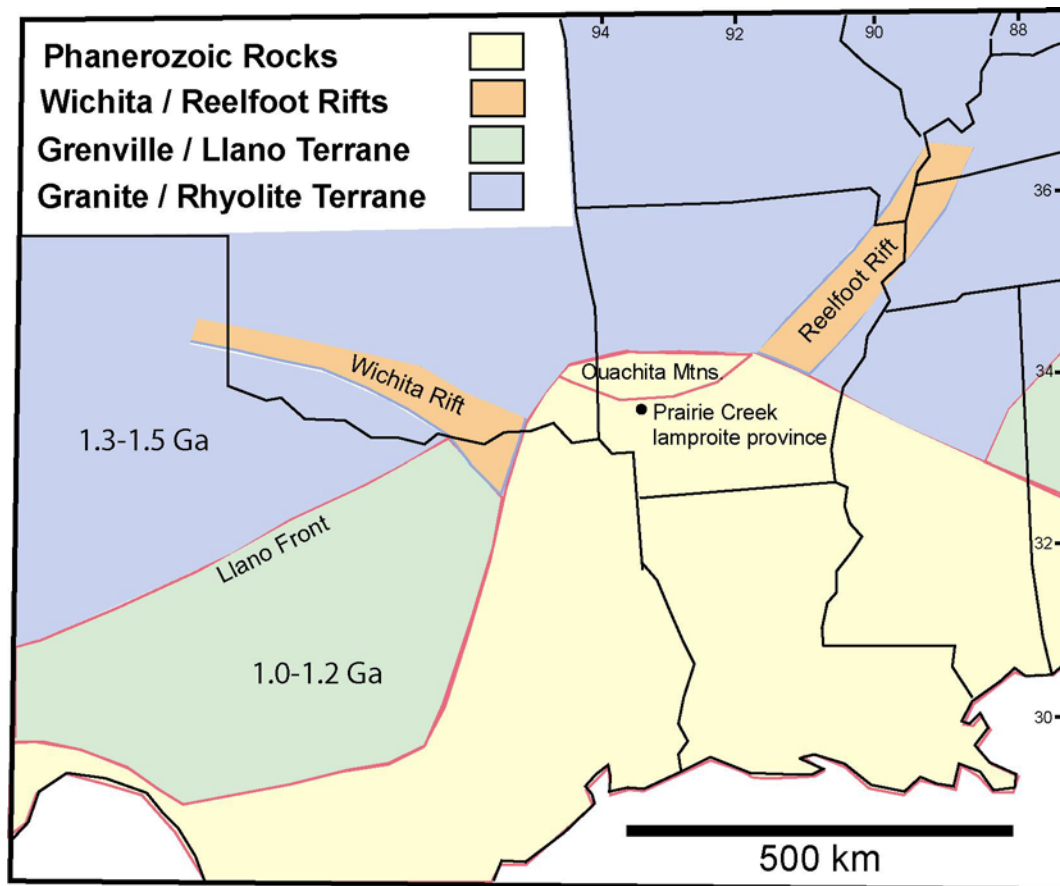


Figure 1-2: Interpreted basement geology of south-central United States (Van Schmus and others, 1986). The Llano front separates 1.3-1.5 Ga granite-rhyolite terrane from 1.0-1.2 Ga Llano terrane. No known basement rocks exist beneath the Prairie Creek lamproite province.

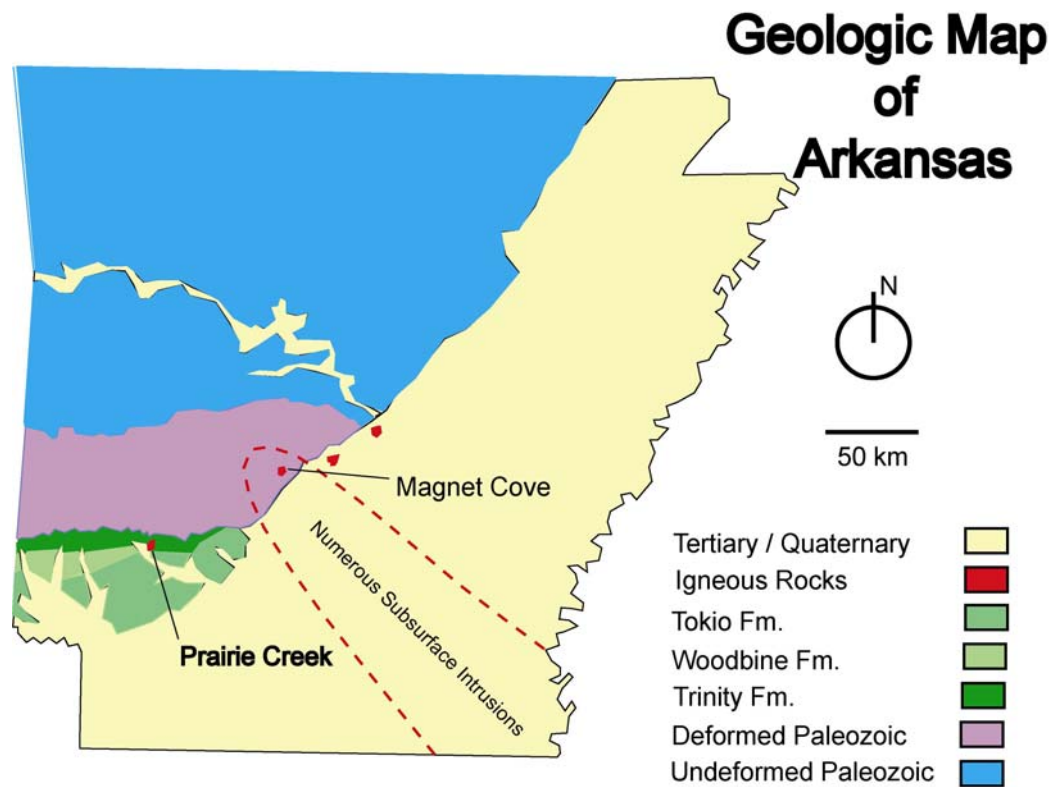


Figure 1-3: Simplified geologic map of Arkansas. The Prairie Creek lamproite province is located in the southwestern part of the state; other known Cretaceous igneous rocks are exposed in the central and southeastern part of the state.

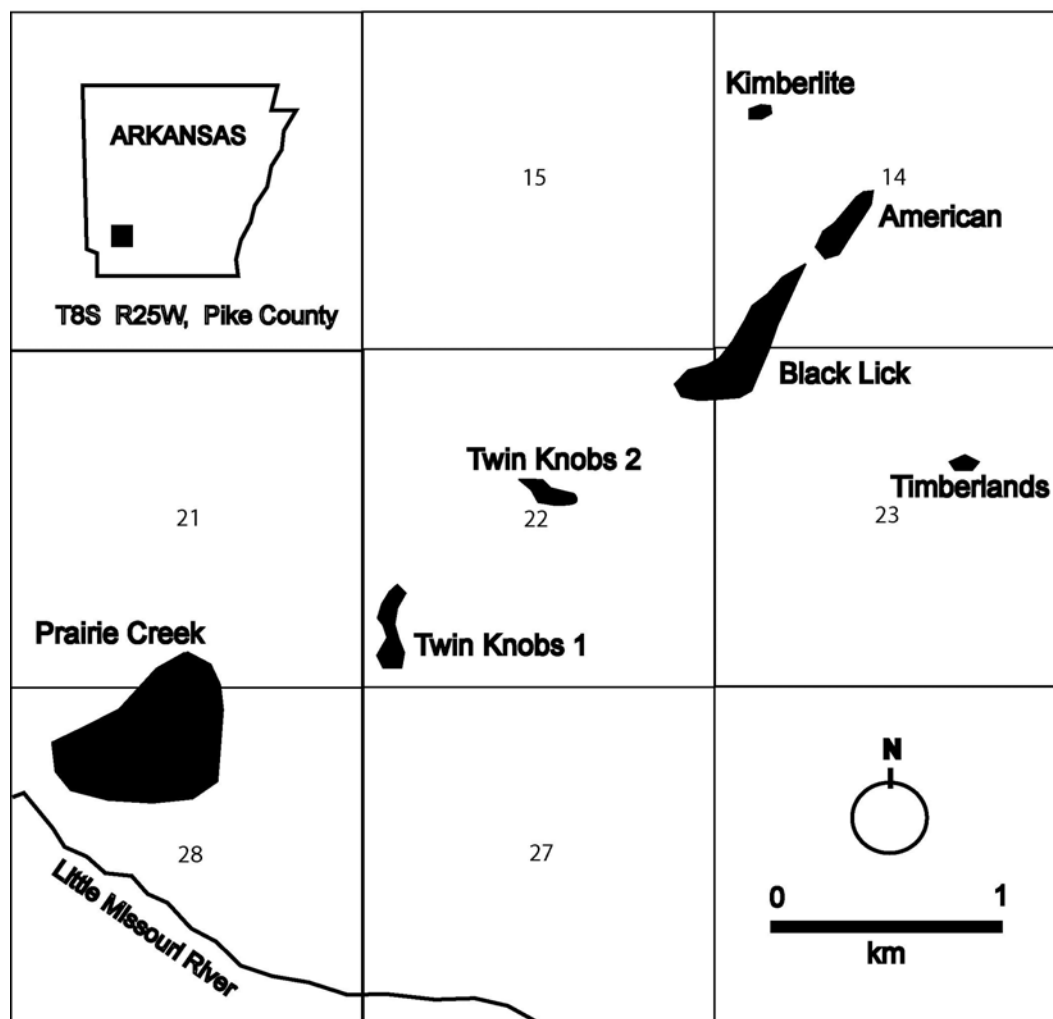


Figure 1-4: Location of known Prairie Creek lamproite occurrences.

Chapter 2

GEOLOGY OF THREE NEW LAMPROITE OCCURRENCES

EXPLORATION HISTORY

The Black Lick vent, the largest of the three intrusions, was originally described by Miser (1913) as two small peridotite outcrops located on the side of a hill about five kilometers northeast of the Prairie Creek intrusion. Black Lick was acquired by American Selection Trust (Amselco) in 1979. Their exploration efforts in the early 1980's determined the size of the intrusion more accurately and culminated with a rotary pan diamond bulk test. Doug Duskin (personal communication, 1993) reported that approximately 1000 tonnes of material was tested without the recovery of any macro-diamonds. However, the intrusion is diamondiferous, because samples collected from Amselco's pan tailings contained abundant micro-diamonds (McCandless and others, 1994).

Arkansas Diamond Development Company (ADDC) reviewed an aeromagnetic Dighem survey flown by General Crude Oil (GCO) Minerals in 1982. This review, in 1987, revealed a weak one to two gamma airborne anomaly near the vicinity of the Black Lick intrusion. A ground magnetic survey was completed using a Geometric proton magnetometer with diurnal corrections applied to data gathered along a 15 m x 30 m tape and compass grid. The resulting magnetic survey map revealed magnetic anomalies of between 10 and 50 gammas over background (Dunn and Taylor, 1988a). The geophysical anomaly was investigated using a buggy-mounted rotary drilling rig as much

of the surface was overlain by a thin veneer of younger Tokio Formation gravel. Twenty-nine shallow drill holes were used to outline the 10 hectare area of the Black Lick lamproite vent (Dunn and Taylor, 1989).

The Twin Knobs 2 intrusion was originally described by Miser (1913) as a peridotite tuff located on the side of a hill about three kilometers northeast of the Prairie Creek intrusion. In the same document, Miser described a similar occurrence of peridotite tuff in the well on the “old Riley place” just east of the main intrusion. This occurrence was delineated by Superior Minerals and described as the Twin Knobs #1 lamproite by Waldman and others (1987).

The Twin Knobs 2 lamproite was further characterized in an ADDC review of the Dighem aeromagnetic survey that revealed a weak one gamma airborne anomaly on the side of the Twin Knobs hill. Ground exploration discovered evidence of the original excavations that Miser completed during the 1910’s. ADDC explored the area of the aeromagnetic anomaly using both ground geophysics and soil geochemistry. The resulting magnetic survey map revealed magnetic anomalies of between 10 and 50 gammas (Dunn and Taylor, 1988a). The largest anomalies were later determined to be associated with two east trending magmatic lamproite dikes, which probably correspond to two ultramafic dikes found in the area by Superior Minerals in 1982 (Mike Waldman, 1989, personal communication).

A soil geochemical survey was completed concurrently over the same survey grid. One pound samples were collected from the clay-rich B-soil horizon for analysis of exchangeable magnesium (Mg), nickel (Ni), chromium (Cr) and niobium (Nb). These elements had proved useful in a test survey performed at an adjacent lamproite (Gregory and Tooms, 1969). A significant geochemical anomaly was observed proximal to the

ground magnetic anomaly (Dunn and Taylor, 1988a). The results of this ADDC geochemical soil survey indicated that the Twin Knobs 2 intrusion was best defined by the dispersal of nickel and niobium within the overlying soils. Background nickel values were <20 parts per million (ppm) whereas a peak value of ~ 300 ppm was observed. Background niobium values were <15 ppm whereas a peak value of 120 ppm was observed. Threshold values for nickel and niobium were approximately 80 and 60 ppm, respectively. The geochemical anomalies defined by chromium and magnesium were relatively weaker, less defined, and had a greater down-slope dispersion. Threshold values for chromium and magnesium were 300 and 8000 ppm, respectively. Geochemical soil anomalies at the Twin Knobs 2 lamproite are slightly stronger, but comparable to those reported for the Twin Knobs 1 lamproite (Waldman and others, 1987). The coincident geophysical and geochemical anomalies were investigated using a buggy-mounted rotary drilling rig in 1988. Fourteen shallow drill holes were used to define a 2 hectare vent (Dunn and Taylor, 1988b).

The Timberlands occurrence was discovered by GCO Minerals in 1982 by ground follow-up of their aeromagnetic Dighem survey. The Dighem survey revealed a <1 gamma magnetic airborne anomaly, which when followed up on the ground corresponded to a very small (~15 meter) anomaly with a magnitude of about 50 gammas. Three of eight drill holes penetrated sections of lamproite. ADDC acquired the mineral rights and exploration data from GCO Minerals and three of seven additional drill holes defined a buried (~12 meters deep) <1 hectare size lamproite (Dunn and Taylor 1988c). No economic evaluation was undertaken due to its small size and depth of burial.

GEOLOGY

All three igneous complexes were intruded into the Upper Early Cretaceous Trinity Group (~120 Ma) and unconformably overlain by the Lower Late Cretaceous Tokio Formation (~85 Ma). The Tokio Formation was deposited directly above of all three lamproite vents. The existence of this caprock indicates that little or no erosion of the lamproite has occurred since Cretaceous time. The exposed stratigraphic relationships are consistent with a Mid Cretaceous age of intrusion. This timing is in agreement with the 97 to 106 Ma K-Ar isotopic age range determined for the Prairie Creek intrusion by Zartman (1977) and Gogineni and others (1978).

Lamproite field relationships were documented during trenching and were interpreted from drill cuttings. A border facies, consisting of sandy tuffs and fine-grained lapilli tuffs with minor amounts of epiclastic rocks, commonly occurs at the margins of the lamproitic vents. This border facies appears to be transitional to, and to be intruded by, later coarser-grained lapilli tuffs and more massive autolithic breccias near specific loci within the vents. The autolithic breccias have been interpreted by Waldman and others (1987) as representing proximity to the vent. The pyroclastic material was intruded by late-stage dikes of hypabyssal olivine lamproite. The contacts of some larger hypabyssal dikes have transition zones of auto-brecciated lamproite near their margins. This auto-brecciated lamproite may result from volatile exsolution from the magma and/or phreatic fragmentation of magmatic debris (Mitchell and Bergman, 1991). Some of the hypabyssal lamproite may have reached the surface as lava flows as indicated by samples of olivine lamproite with vesicles found on the surface of the Black Lick vent. The observed

eruptive relationship is in good agreement with the idealized eruptive sequences of lamproites described by Mitchell and Bergman (1991).

The geological relationships appear the same for all three lamproites, although the ratio and volume of specific rock types vary within any individual vent. The Black Lick lamproite has a well-defined border facies consisting of sandy tuffs and fine-grained pyroclastic tuffs with a larger volume of coarse-grained pyroclastic lapilli tuffs (Dunn and Taylor, 1989). Specific areas within the vent, generally associated with a stronger magnetic signature, contain more massive autolithic breccia which appears to have been intruded into coarse-grained pyroclastic tuffs. A surface geological interpretation of the Black Lick lamproite is shown in Figure 2-1. The large size of the vent is suggestive of a relatively complex eruptive history with a characteristic champagne glass shape. The moderate dip of the vent contact shown in the representative north-south cross-section (Figure 2-2) is in agreement with the dip of the contact determined by deep drilling at the Prairie Creek intrusion (Morgan Worldwide Mining Consultants, 1997). Moderately dipping contacts also are associated with the diamondiferous lamproites of Western Australia (Atkinson and others, 1984).

The Twin Knobs 2 lamproite consists of fine-grained pyroclastic rocks such as sandy and lapilli tuffs with only a few small coarse-grained pyroclastic centers (Dunn and Taylor, 1988b). Two late-stage hypabyssal dikes (defined by magnetic anomalies) penetrate the vent. A surface geological interpretation of the Twin Knobs 2 lamproite is shown in Figure 2-3. In the representative northwest-southeast cross-section of the vent (Figure 2-4), the very shallow dipping contact is consistent with the abundance of “crater facies” pyroclastic tuffs. The Timberlands vent appears to be a small, near-vertical intrusion of hypabyssal olivine lamproite with only minor amounts of auto-brecciation associated with margin contacts (Figure 2-5). In the

subsurface geological interpretation (Figure 2-6), the Timberlands vent is shown as a small intrusion of less than a hectare in size emanating from an east-trending lamproite dike (Dunn and Taylor, 1988b). Fine-grained pyroclastic tuffs were not observed, although the top of the intrusion shows oxidation and soil development probably due to sub-aerial exposure in Cretaceous time.

The wide diversity of vent shapes and petrological facies within this small lamproite province is ascribed to structural controls on magma emplacement. The relative locations of the seven known vents within the province define a strong southwest-northeast alignment. This alignment is best represented by the nearly continuous lamproite outcrop between the Black Lick and the American vents which appear to be enlargements within a subsurface dike structure. This SW-NE alignment is strongly suggestive of a deep-seated structural control parallel to the Reelfoot Rift located ~100 kilometers east of this lamproite province. The three vents described in this paper also show an internally consistent west-east orientation. This is most apparent within hypabyssal lamproite intruded in the form of dikes. This west-east orientation is probably imposed on the magmas as they follow W-E oriented thrust faults, common features at depths of >60 meters, contained within rocks of the underlying Ouachita Mountains structural province.

The large variation in relative amounts of crater facies and hypabyssal facies is best explained by variations in magma interaction with groundwater at the time of intrusion. The lamproite magmas were apparently intruded into a near-surface water-saturated coastal environment represented by the Trinity Group marls with a 30-meter thick basal gravel. Much of the volcanic activity was phreatomagmatic in origin, as is consistent with the large amounts of pyroclastic debris within the crater vents. Areas with less pyroclastic debris such as the Timberlands lamproite may have been intruded into an area of less groundwater saturation and

decreased basal gravel thickness. Variation in the amount and textures of pyroclastic material within the vents appear to be related to the amount of interaction with near surface water in Cretaceous time.

PETROLOGY

The observed petrology and mineralogy within the three lamproites is in good agreement with more detailed studies reported for the Prairie Creek intrusion (Gogineni and others, 1978; Bolivar and Brookins, 1979; Scott-Smith and Skinner, 1984a) and with other lamproites within the district (Scott-Smith and Skinner, 1984b; Waldman and others, 1987). Velde (2000) has studied the reaction zones of mafic xenoliths within the hypabyssal olivine lamproite and found that they contain almost all of the characteristic lamproitic mineral phases such as potassium-richterite, priderite, jeppeite and haggertyite. The two major igneous rock types observed include a diverse textural range of pyroclastic materials and hypabyssal olivine lamproite.

Hypabyssal Olivine Lamproite

The hypabyssal olivine lamproite is dark green to black and is hard and dense in hand sample. I estimate it comprises about 25% of the volume of the diatremes. Phenocrysts of olivine and pseudomorphs of olivine altered to serpentine constitute up to 20% of the rock and are subhedral (~2mm). The rock contains about 10% relatively large (~1mm) poikilitic phenocrysts of pale mica, probably tetraferriphlogopite, judging from its characteristic reverse pleochroism of

brown to orange. Megacrysts of olivine and ilmenite are common. The groundmass consists of abundant laths of phlogopite, serpentine replacing olivine, clinopyroxene, amphibole, perovskite, and lesser amounts of apatite and spinel in a devitrified glass consisting largely of a fine-grained clay mineral. Potassium-richterite and priderite were identified only in selvages surrounding ultramafic xenoliths. Microprobe analyses of mineral phases are in good agreement with those found by previous authors at other vents within the lamproite province. Xenoliths of sedimentary rocks are common giving some rock a brecciated appearance in hand sample.

Pyroclastic Rocks

About 75% of the surface area of the lamproites consists of pyroclastic rocks including autolithic breccias, lapilli tuffs, and sandy tuffs. The pyroclastic rocks are quite variable in composition and texture and commonly appear interbedded with gradational contacts. Sub-rounded breccias, massive to thinly bedded lapilli tuffs and sandy tuffs with rare epiclastic rocks were observed. The sandy tuffs and epiclastic rocks are generally finer-grained, and more extensively reworked, and they may represent a more distal pyroclastic facies. Veinlets of secondary calcite and barite commonly cut through all pyroclastic rock types.

Autoliths of lamproite are common among the autolithic breccias and lapilli tuffs. The autoliths consist of pyroclastic material with a rounded accretionary form, but they have different grain sizes from the surrounding matrix. Altered olivine and pale phlogopite micro-phenocrysts are set in a fine-grained groundmass of serpentine, clinopyroxene, perovskite, carbonate, and altered glass. Xenoliths of sandstone, shale, and marl are common.

DIAMOND BULK TESTING

Both the Black Lick and Twin Knobs 2 lamproites were bulk-tested by ADDC for diamond content utilizing at least four trenches within pyroclastic rocks from each vent (trench locations shown in figure 2-1 and 2-3). The top three meters of each trench was spoiled and only the lower 2 meters of material from each pit was shipped for processing. The material was transported via covered truck to a recovery plant near Sloan, Colorado. The plant utilized a jaw crusher, scrubber, washer and various screens to produce a consistent feed into a heavy media circuit. The diamonds were recovered from the heavy media concentrate using both “SORTEX” and grease table technology for redundancy. Test diamonds and density tracers were utilized to assure good diamond recovery.

Three macro diamonds in excess of 0.5 mm were recovered from the 155 tonnes of material from the Black Lick lamproite (Figure 2-7). Total weight of the three stones was approximately 0.045 carat. Three of the four pits at Black Lick yielded one stone each. The calculated diamond grade throughout the Black Lick lamproite was approximately 0.03 carats per 100 tonnes. The first diamond found is a clear white to light gray modified octahedron about 1.5 mm on a side. The stone displayed abundant surface trigons and other features. The stone had a large area of embayment and/or cleavage with about 25% of the original crystal missing. The stone might be classified as gem quality weighing 0.015 carat. The second diamond is a slightly included brown dodecahedron about 1.5 mm on the longest side. The diamond has a naturally polished rounded surface except for a cleavage where about 40% of the original stone is missing.

The stone might be classified as a near gem weighing 0.02 carat. The third diamond found is an included brown octahedron about 1.5 mm on the longest side. The stone indicates the presence of partly resorbed surface growth lines. The crystal is embayed along a cleavage and about 30% of the original stone is missing. The diamond would be classified as an industrial stone weighing 0.01 carat.

Two additional macro diamonds in excess of 0.5 mm were recovered from the 105 tonnes of material from the Twin Knobs 2 lamproite (Figure 2-7). Total weight of the two stones was 0.04 carat. Both diamonds were recovered from the northern pits (coarse pyroclastics), whereas the southern pits (fine pyroclastics) did not yield macro diamonds. The calculated diamond grade throughout the Twin Knobs 2 lamproite was approximately 0.04 carats per 100 tonnes. The first diamond recovered was a brown-white modified octahedron about 1 mm on a side. The stone displays surface trigons, although they are extensively corroded. The stone has abundant inclusions including some attached lamproite. The stone would be classified as industrial grade weighing about 0.01 carat. The second diamond recovered was a clear white tetrahedron about 2 mm on a side. The diamond had sharp growth features and trigons and appeared to be a cleavage representing about 70% of the original stone. The stone had a piece of attached lamproite and would be classified as a small gem weighing about 0.03 carat. The calculated average diamond content of both intrusions was an order of magnitude less than that observed at the Prairie Creek lamproite which yielded an average diamond grade of 0.57 carats per 100 tonnes (Morgan Worldwide Mining Consultants, 1997), and for the Twin Knobs 1 lamproite which yielded a grade of 0.17 carats per 100 tonnes (Waldman and others, 1987).

XENOLITHS, MEGACRYSTS AND XENOCRYSTS

Rare xenoliths of mantle and crustal rocks have been recovered from the Black Lick and Twin Knobs 2 lamproites. Approximately 1.5 kilograms of xenoliths were recovered from 260 tonnes of lamproitic material treated for the diamond bulk sample. Approximately $\frac{3}{4}$ of the xenoliths recovered are of probable crustal origin. Half of these crustal xenoliths consist of near-surface lithologies including shale, sandstone and quartzite. The deeper crustal xenoliths are dominantly amphibolite, with lesser quantities of granitic and volcanic rock and rare mica-rich rocks. The mantle xenoliths include dunite, harzburgite, websterite, wehlite, eclogite and both spinel and garnet lherzolite. In addition, megacrysts of olivine, clinopyroxene, ilmenite, spinel and garnet have been recovered. Microprobe analysis of these indicator minerals is in good agreement with the analysis reported by Waldman and others (1987). A comparable suite of deep-seated xenoliths was observed within the Twin Knobs 1, but no detailed description of their mineralogy has been published.

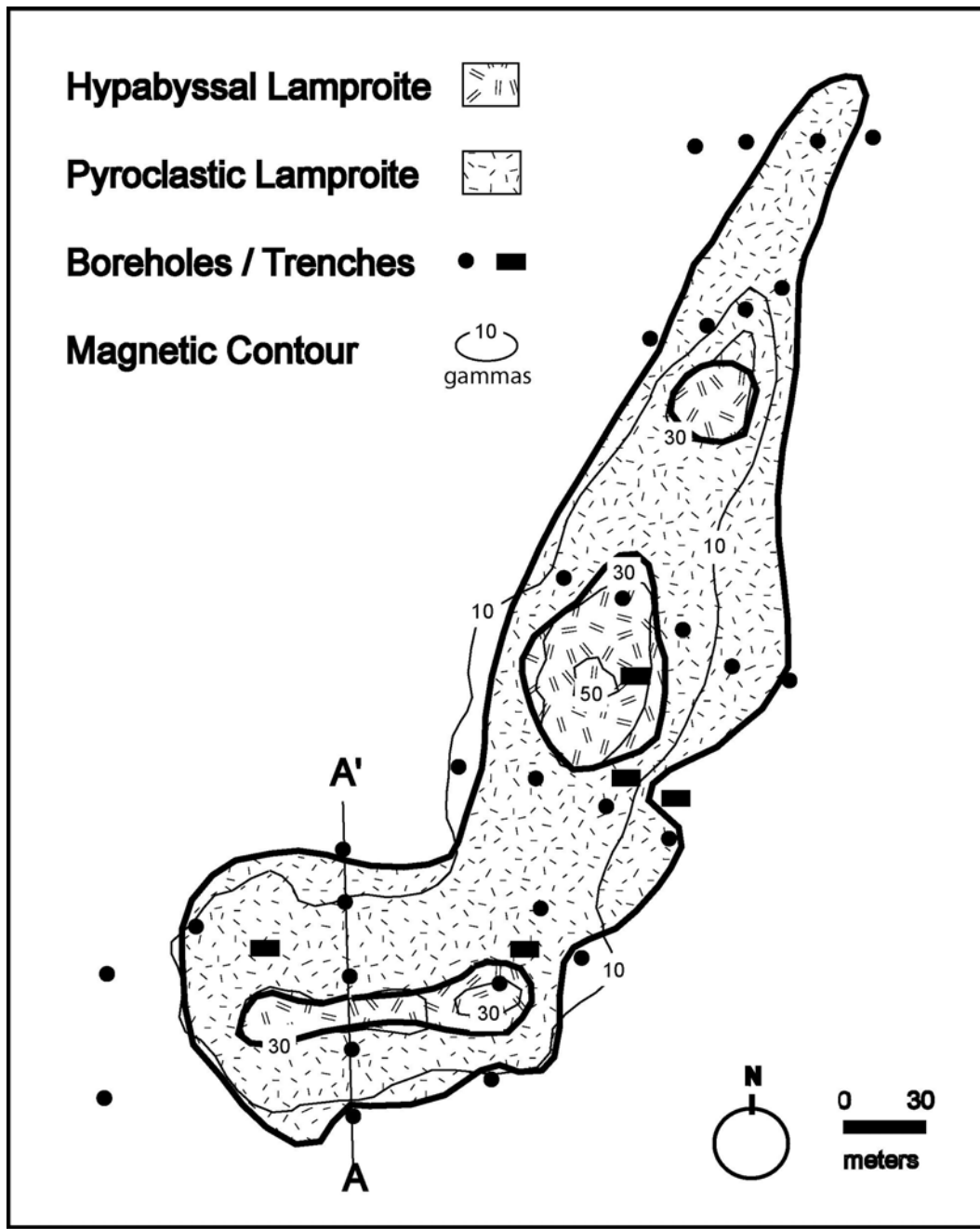


Figure 2-1: Surface geological interpretation of the Black Lick lamproite.

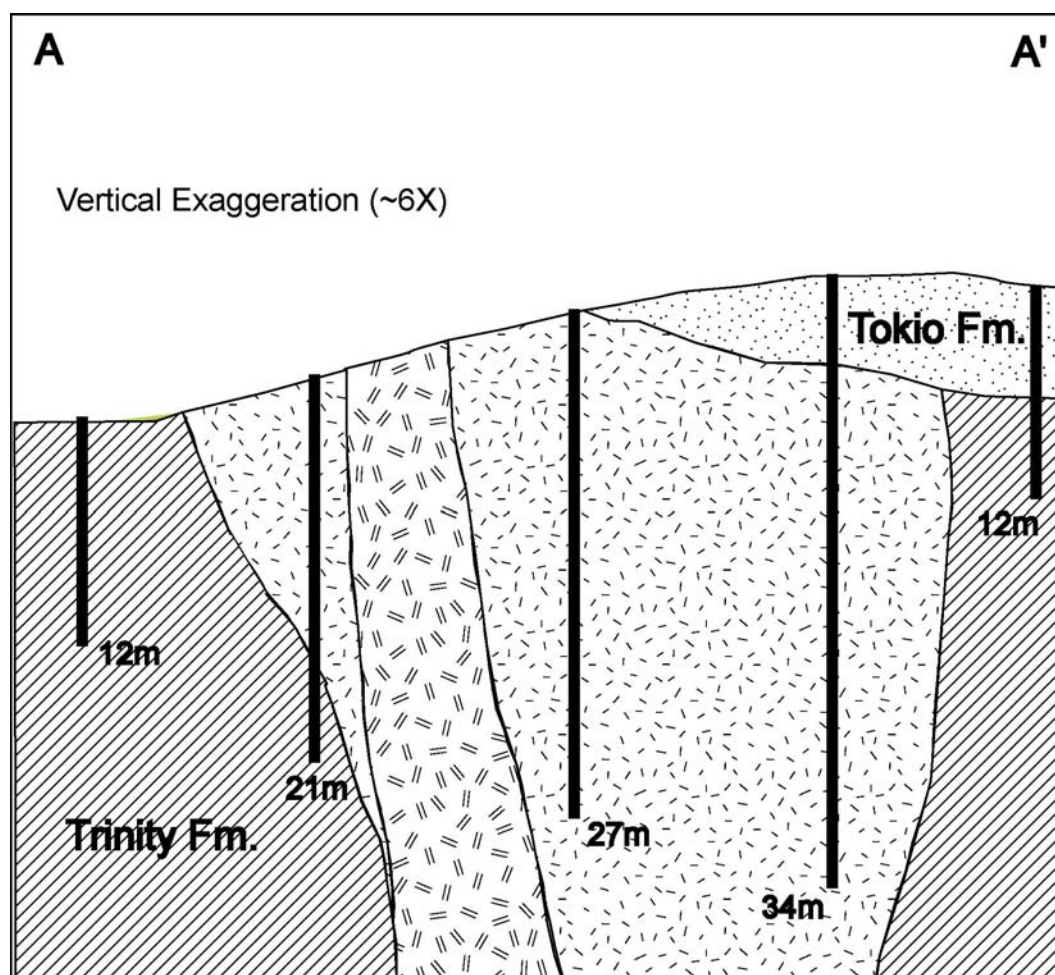


Figure 2-2: Geological cross-section of the Black Lick lamproite. Exploration boreholes are shown with depth in meters.

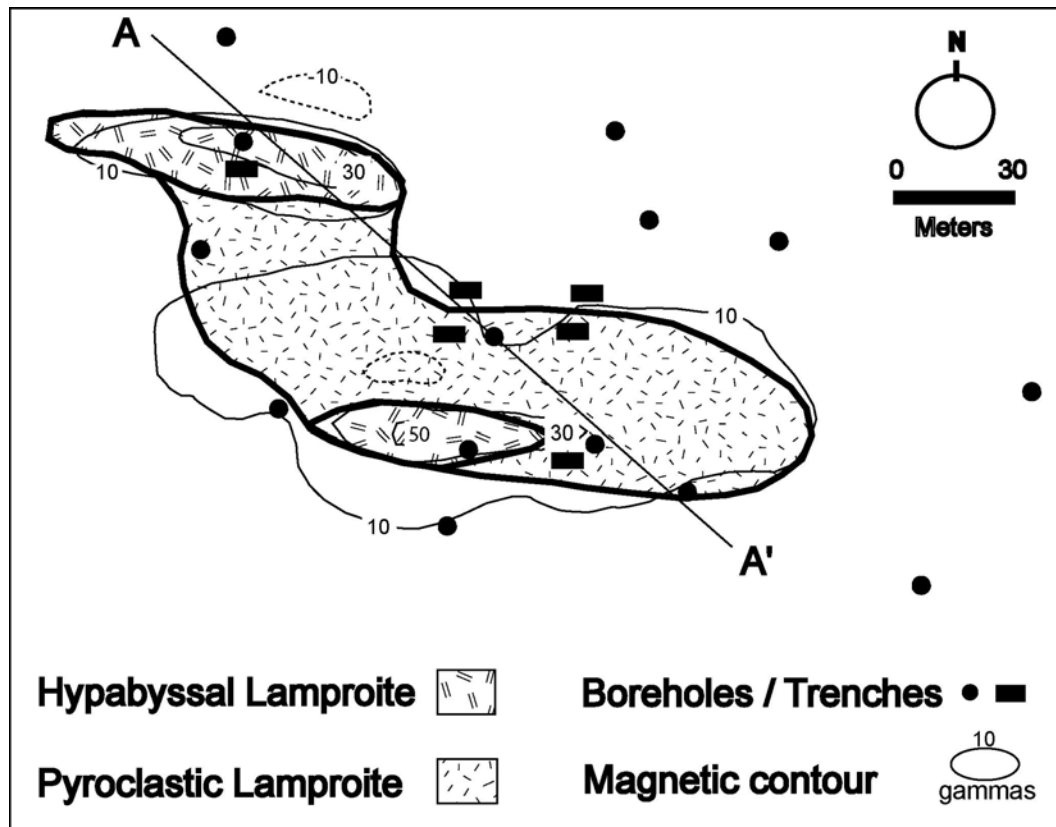


Figure 2-3: Surface geological interpretation of the Twin Knobs 2 lamproite.

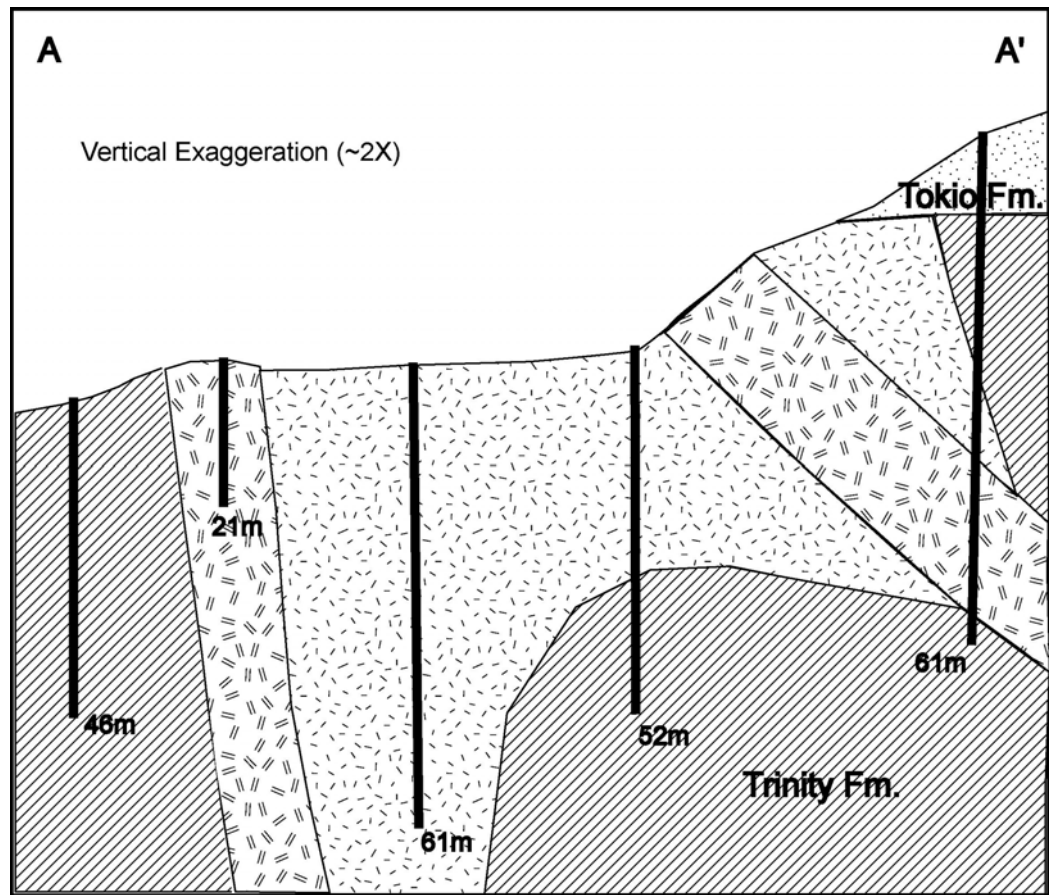


Figure 2-4: Geological cross-section of the Twin Knobs 2 lamproite. Exploration boreholes are shown with depth in meters.

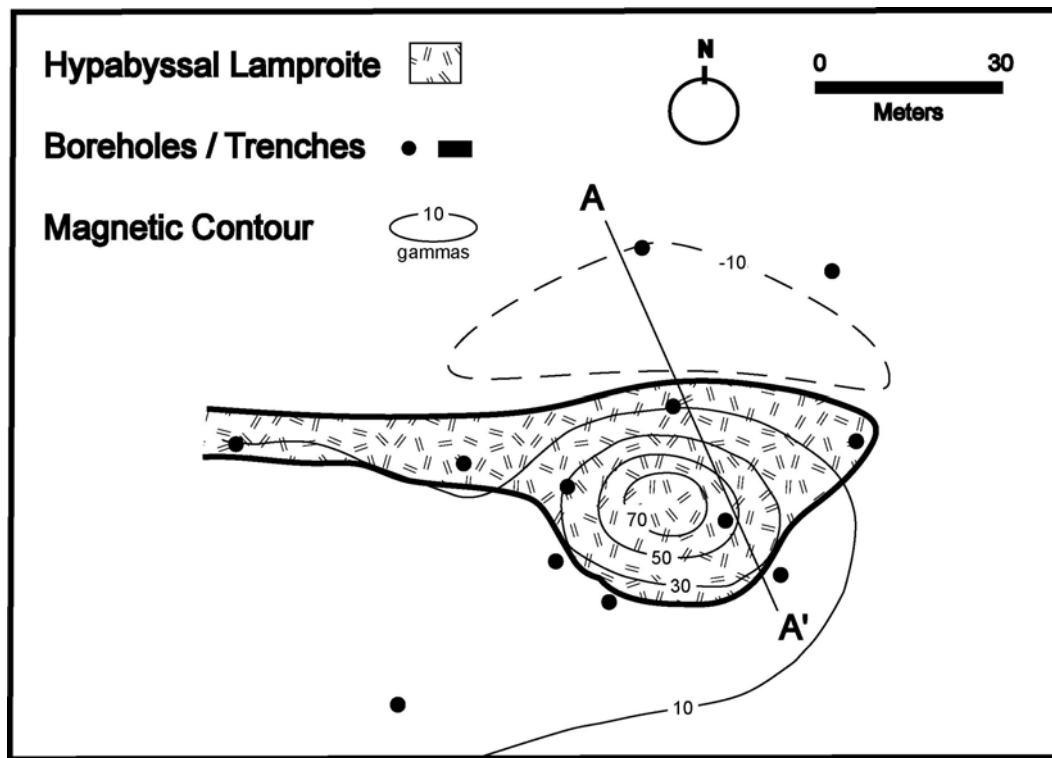


Figure 2-5: Subsurface geological interpretation of the Timberlands lamproite.

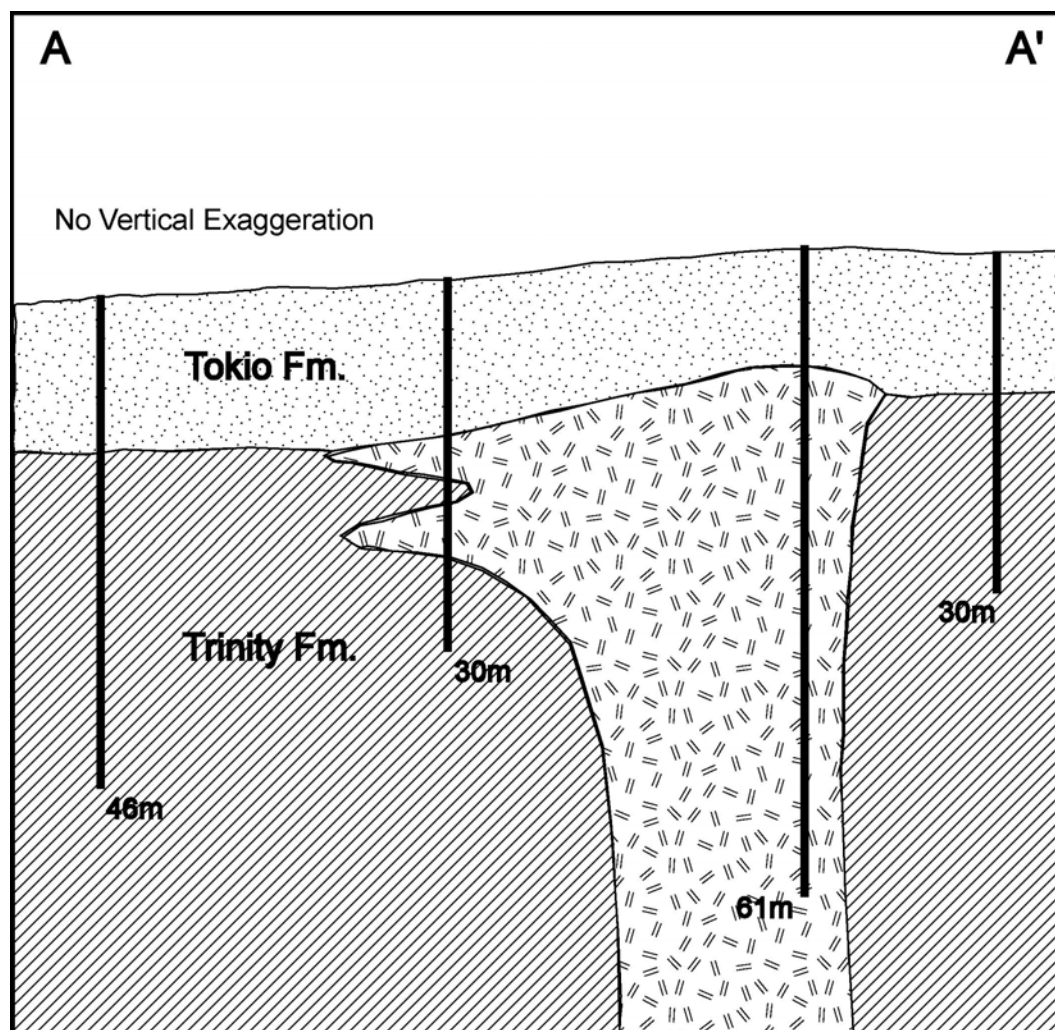


Figure 2-6: Geological cross-section of the Timberlands lamproite. Exploration boreholes are shown with depth in meters.

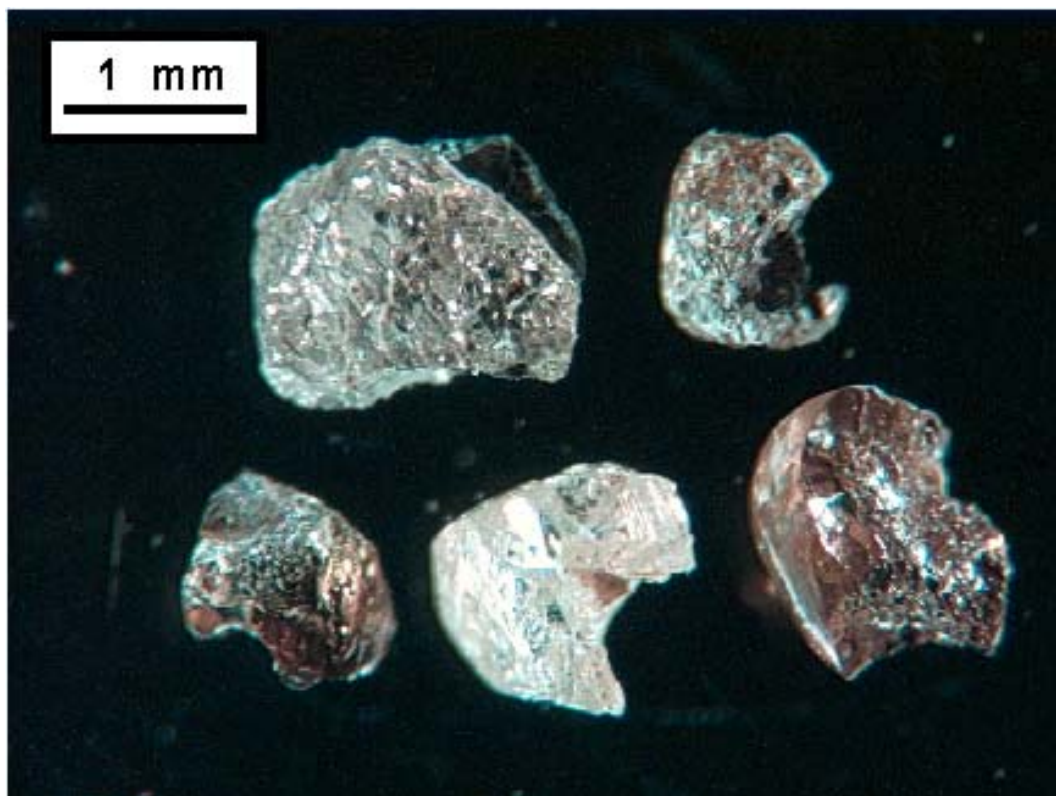


Figure 2-7: Diamonds recovered during bulk sampling evaluation. The top two diamonds are recovered from Twin Knobs 2; the three lower diamonds are from the Black Lick lamproite.

Chapter 3

DIAMOND ECONOMICS OF THE PRAIRIE CREEK LAMPROITE

INTRODUCTION

The discovery of economic diamond deposits in the late 1970's within Western Australia lamproitic intrusions generated renewed interest in the Arkansas lamproite province and resulted in reevaluation of the diamond potential of the region. The purpose of this paper is to utilize the geologic setting and recent diamond evaluation results at the Prairie Creek Lamproite within the Crater of Diamonds State Park to constrain estimates of the post-erosion diamond distribution. This model is then used to provide an estimation of the diamond distribution within and immediately adjacent to the diamondiferous lamproite. This model provides insight into the future economic potential of the intrusion as both a commercial mine and as a tourist attraction. In addition, the model helps to explain and clarify past mining history that has been poorly documented in the literature.

MINING HISTORY

Diamonds were first found on this property on August 1, 1906, by the owner John W. Huddleston. Immediately after confirmation of the diamond find, the majority of the property was optioned and eventually sold to a consortium that organized into the

Arkansas Diamond Company. Arkansas Diamond Company production was initiated in 1907 and continued until the end of 1912. In 1919, the mining operation was reorganized as Arkansas Diamond Mining Corporation of Virginia, and a larger washing plant was constructed. Production in the 1920's appears to have been plagued by various problems, but production continued until 1927 when the property was sold under threat of foreclosure. Small scale operations were reinitiated in 1928 and continued until stopped by the Great Depression in 1931 (Kidwell, 1990).

In 1944, the Bureau of Mines evaluated the property as a source of industrial diamonds. Their report published in 1949 indicated only low-grade diamond reserves. In 1948, Glenn Martin leased the diamond property and erected a washing plant to test the recently consolidated diamond deposit. This test returned only 246 carats of diamonds from approximately 112,000 tonnes of material. The State of Arkansas purchased the land in 1972 and named it the "Crater of Diamonds State Park". Since that time, numerous improvements have been made on the property to facilitate its operation as a tourist attraction. Approximately 500 diamonds, with a total carat weight of nearly 50 carats, are recovered annually by tourists within the State Park.

PRAIRIE CREEK GEOLOGY

A review of the early mining history revealed that the only available subsurface information on the lamproite intrusion was from three holes described by Fuller in 1909 and by Thoenen and others (1949) in the U.S. Bureau of Mines investigation of 1943-1944. This drilling was to a maximum depth of 63 meters with an average depth of less than 10 meters. Few if any of the borings intersected the intrusive contact at depth, and

therefore they provided no significant data on the size or shape of the diamond resource at depth. The Phase 1 evaluation of the vent was undertaken in 1990 by the State Parks Commission to provide this subsurface data.

The Phase 1 Evaluation Program involved vertical and angled diamond drilling in order to determine the subsurface shape of the lamproite intrusion. At various locations around the intrusion both vertical and 45° diamond drill holes were drilled that, when used with the known surface outcrop location, provided a three point intrusive contact surface. The results of this drilling revealed that the sides of the intrusion dip inward with depth at an approximate 45° angle mimicking the shape of a martini glass as indicated on cross-sections generated during the Phase 1 evaluation program (Morgan Mining & Environmental Consultants, 1993). This morphology is typical for high level crater facies lamproitic vents (Mitchell and Bergman, 1991).

The Phase 1 Evaluation Program resulted in a clearer understanding of the surface geology and its three-dimensional projection into the subsurface. Four main rock types were identified and mapped (Figure 3-1). The first rock type is hypabyssal magmatic olivine lamproite which forms nearly half of the surface vent exposure. It is a very hard, dense, greenish-black olivine porphyry lamproite with contact-metamorphosed near-surface sedimentary xenoliths. This unit was previously described by Miser and Purdue as “magmatic”. The second mapped unit was “maar epiclastics” which likely formed in shallow crater lakes during periods between eruptions. The epiclastics largely consist of medium-grained quartz sandstone and appear to have been preserved near the margins of the intrusion. The distribution of epiclastic rocks is erratic as the unit thickness changes rapidly over short distances. Estimated mapped surface exposure is

about 5% of the area and total volume of the “epiclastics” within the vent is estimated as less than 10% (MMEC, 1993).

In addition, two types of pyroclastic lamproite were observed and mapped. The first type is a phlogopite-rich tuff which is generally finer-grained and was previously mapped by Miser and Purdue (1929), and subsequent workers as “tuffs”. Although the geologic contact between the two types of lamproite tuff are not very well defined, due to a transitional nature, the phlogopite-rich tuffs are believed to make up approximately 20% of the surface outcrop. The second type, olivine-rich lamproite tuff occupies much of the visitor search area and was previously mapped in 1929 as “breccia”. The textures observed do not resemble “breccias” because clasts are not angular in nature, but rather coarse-grained tuffs and lapilli tuffs with rounded fragments. The surface extent of the olivine-rich tuffs can be estimated from the map of surface geology as approximately 30% of the 32 hectare vent.

***IN-SITU* DIAMOND DISTRIBUTION**

The four major rock types were bulk tested for diamond content as part of the Phase 2 Evaluation Program completed by the State Parks Commission in 1997. The purpose of the evaluation was to determine the diamond grade and value of the diamond-bearing lamproite. This evaluation utilized 14 trenches throughout the vent, each consisting of a 600 tonne bulk sample. Approximately 3 meters of surface overburden was removed for backfill and the in-situ lamproite was shipped to an off-site heavy media plant for diamond concentration and recovery (Morgan Worldwide Mining Consultants, 1997). It should be noted that some researchers question the validity of the 1990’s

evaluation (Howard, 2000); however, the reported diamond grades appear to be validated by the data comparison discussed below.

Estimated diamond grades can be applied to these four rock types based on results of the bulk diamond testing. The specific diamond content of the magmatic olivine lamproite that forms about 45% of the surface outcrop was never definitively determined. Miser and Purdue (1929) reported that only a few small diamonds have ever been found within this unit. Because the massive resistant rock is not conducive to rotary pan concentration or crushing and heavy media separation, the rock type has never been bulk tested economically. However, petrological observations by Roger Mitchell (MMEC, 1993) revealed reaction rims around the large olivine megacrysts and poikilitic phlogopite phenocrysts which indicate a relatively slow cooling. Mitchell suggested that few diamonds would survive this slow cooling event under conditions outside of the diamond stability field. Both of these lines of evidence suggest that the *in-situ* diamond content of the magmatic olivine lamproite is insignificant.

The epiclastics are generally fine-grained clay to sandy sedimentary rocks that also have not been definitively sampled. Trench 3-B was largely in the epiclastics of the border zone and although described as “sandy tuffs”, it yielded no diamonds from a 240 tonne bulk sample. In contrast, the relatively fine-grained border facies described as sandy tuffs within the diamondiferous Australian lamproite province is described as having relatively high grade diamond contents. Due to the barren epiclastic deposit sampled during the Phase 2 testing, the volumetrically small amount of “epiclastics” is considered barren of diamonds.

The phlogopite-rich tuffs commonly appear somewhat transitional between the border “epiclastics” and the central olivine-rich tuffs and are found interbedded with both

units. Phlogopite-rich tuffs are mostly found on West Hill and the eastern flanks of Middle Hill adjacent to the western edge of the visitor search area. Four of the bulk sample trenches were at least in part finer-grained phlogopite-rich tuffs. Evaluation of the diamond-content of the *in-situ* phlogopite-rich tuffs yielded two trenches barren of diamonds and two other trenches with less than 0.11 carats per 100 tonnes (0.11 cpht). To estimate maximum reasonable diamond contents, it is assumed that the fine-grained phlogopite-rich tuffs have an average diamond content of 0.11 cpht.

The olivine-rich tuffs tend to be coarse-grained due to the presence of rounded lamproite lapilli. The olivine-rich tuffs are found throughout most of the visitor search area and represent the source of most of the visitor diamonds. The majority of the diamond evaluation efforts were concentrated within its outcrop areas and the *in-situ* diamond distribution is fairly well defined. Results from the Phase 2 evaluation show that the majority of the olivine-rich lapilli tuffs have a diamond grade of ~1.1 cpht. Material from the northern and southern margins of the visitor search areas show evidence of dilution by other rock types and yield average diamond grades of about 0.33 cpht (Figure 3-2). In order to place an upper limit on the reasonable diamond content, the olivine-rich lapilli tuffs were assumed to have an average grade of 1.1 cpht.

MODEL AND EROSIONAL HISTORY

The unique stratigraphic relationship in which the Arkansas lamproites were intruded into the Upper Early Cretaceous Trinity Group, eroded, and then capped by the Lower Late Cretaceous Tokio Formation allows accurate estimation of the time of intrusion. Furthermore, the elevation of this regional unconformity permits an accurate

determination of the amount of lamproite erosion since Late Cretaceous time. An adjacent lamproitic intrusion (Twin Knobs 2), located approximately 1.5 kilometers northeast of the Prairie Creek vent, reveals the cross-cutting relationship of the lamproites with the host stratigraphy (Dunn and Taylor, 2001). The top of the intrusion is eroded and the basal gravel of the Tokio Formation was deposited nearly horizontally on the eroded surface. The elevation of this erosional surface is ~150 meters above mean sea level. This erosional surface exists at similar elevations at both the Black Lick and American lamproite vents further northeast along the trend of the intrusions.

Extrapolation of this disconformity to the southwest reveals that the Prairie Creek pipe within the Crater of Diamonds State Park was probably buried by the Tokio Formation during the Late Cretaceous Period. It was only exhumed by erosion in recent geologic time by the action of the Little Missouri River at an elevation of 150 meters above sea level (Figure 3-3). The highest elevation within the park today is the East Hill (elevation of ~140 meters) which is capped by erosion-resistant magmatic olivine lamproite. The elevation of this resistant topographic feature tends to reinforce the approximate exhumation elevation of 150 meters for the Prairie Creek vent. The average elevation of the visitor search area at the Crater of Diamond State Park is just higher than 100 meters above sea level indicating that the average thickness removed by erosion of the diamondiferous intrusion in recent geologic time is less than 50 meters (Dunn, 2000).

This erosion depth, the area of intrusion, and the approximate diamond grade of the removed rock yields an estimate of the total volume of original diamonds liberated by erosion. The density of *in-situ* weathered lamproite during the Phase 2 evaluation was found to be ~1.65 tonnes per cubic meter. The geologic mapping indicated about 20% of the surface area (6.4 hectares or 64,000 square meters) to be phlogopite-rich lamproite

with an average diamond content of 0.11 cpht. Assuming a maximum erosion depth of 50 meters, the total eroded volume of phlogopite-rich tuffs is 3,200,000 cubic meters or ~5,280,000 tonnes of material. If this material contained an average grade of 0.11 cpht, a total of ~5,800 carats of diamond would have been liberated.

The same calculation for the olivine-rich pyroclastics that cover 30% of the mapped vent yields 9.6 hectares of exposure or 96,000 square meters of olivine-rich pyroclastics. This number multiplied by a maximum erosion depth of 50 meters yields a total volume of 4,800,000 cubic meters or ~7,920,000 tonnes. If this material contained an average grade of 1.1 cpht, a total of ~87,000 carats of diamond would have been liberated. All of the diamondiferous material eroded since exhumation of the deposit would yield an estimated 93,000 carats of diamond (Dunn, 2000).

SURFACE CONCENTRATION

Southwestern Arkansas experiences warm and humid summers and cool to mild winters, with almost a sub-tropical climate and over 125 cm of rain per year. The local climate results in development of pedalfer to lateritic soil horizons with well-developed thick organic-rich residual black topsoil. The surface layer or organic-rich A-layer is known to contain mainly resistate minerals which are not easily weathered or eroded and have accumulated over time within the soil. These surface soils develop by extensive chemical weathering and dissolution of the underlying ultrabasic rock (saprolite). This process is demonstrated by the deep leaching and extensive saprolite development (depths > 30 meters) found during drilling and by the low density of lamproite during the bulk testing.

Chemical weathering is expected to predominate over physical transport of material in a low-relief sub-tropical environment. Thoenen and others (1949) stated that “The greatest concentration of diamonds appears to have been found in the black ground capping the brecciated peridotite. This averaged about 2.5 feet thickness and yielded a diamond concentration of approximately 0.844 carat per cubic yard” (~50 cpht). During the Phase 2 evaluation program, an absence of original organic-rich surface layer was observed over the entire intrusion, even in areas which overlay “barren” magmatic lamproite rock types. Earliest mining operations most probably removed and exploited the natural surface concentration of diamonds. Early recovery methods were designed for extremely soft weathered material, and large crushers were not utilized during these operations. A report by an employee of the Arkansas Diamond Company, indicated that existing mining operations were recovering ~15 cpht with an average stone size of 0.35 carats (Fuller, 1931).

Rotary pan concentration techniques used in the old mining operations had relatively poor recovery rates especially for smaller stones because insignificant weight differences did not allow for gravity separation of small diamonds. A cumulative plot of actual diamond size distribution for the Phase 2 diamond evaluation reveals that nearly 50% of the diamond content by carat weight is in the size fraction of less than 0.3 carats (MWMC, 1997). The average size of recovered diamond was just over 0.2 carats. Reported diamond grades during the early mining years may have been underreported by as much as 50% due to non-recovery of smaller diamonds. Actual diamond contents within the surface soil concentration mined in the early stages of commercial operations may have had diamond grades in excess of 30 cpht. This hypothesis is borne out by the fact that in the 1980’s the majority of diamonds reported as finds at the Crater of

Diamonds State Park was by artisan miners who were working the old tailings near the southern edge of the visitor search area. In addition, the majority of these stones were less than 0.3 carat in size. It is proposed that the vast majority of these diamonds were non-recoverable during early commercial production.

Records of the early diamond production are sparse, with the most complete review of diamond production and grades that of Fuller (1931). Fuller suggested that at least two grades of ore were processed. The first ore type was rich in diamonds and yielded recovered diamond grades of 15 cpht with actual total diamond contents possibly in excess of 30 cpht. The second reported ore grade encompassed over 50% of the material processed for the period 1919 to 1925. This material yielded 176 carats of diamonds from ~20,000 cubic meters of material. The combination yields an average recovered ore grade of approximately 0.5 cpht. Compensating for a 50% loss of small stones yields an average ore grade of about 1.0 cpht.

The U.S. Bureau of Mines evaluation during the 1940's consisted of 54 large diameter holes drilled from the surface, yielding ~240 cubic meters or 395 tonnes of material. Processing of this material yielded 32 stones weighing a total of 8.41 carats for an average grade of 2.1 cpht and an average size of 0.25 carats (Theonen and others, 1949). This ore grade is slightly higher than the Glenn Martin bulk test results where a large bulk sample from the consolidated mining properties produced about 246 carats from approximately 112,000 tonnes of material (St. Clair, 1956). The calculated ore grade during this evaluation is approximately 0.22 cpht. It has been noted that no small stones were recovered during this test so consideration for poor recovery during processing yields approximate diamond grades of up to 0.44 cpht.

Review of the Crater of Diamonds State Park mining history and the results of the 1996 Phase 2 evaluation suggest that two types of diamond resources were encountered at the Prairie Creek Lamproite. The first ore type was relatively rich in diamonds with recovered ore grades in excess of 15 cpht and probable actual diamond contents near 30 cpht. This material constituted the bulk of the material washed in the earliest mining operations until 1912 and at least part of the material processed during the 1920's. During the 1920's two ore grades can be distinguished. The higher-grade ore had grades comparable to those of earlier mined surface enrichments and was probably constituted from the same material. The lower grade ore processed appears to represent *in-situ* pyroclastic lamproite and yielded diamond contents averaging <1.0 cpht. By the late 1920's, nearly all of the surface-enriched material had been processed. The *in-situ* material at that time was found to be too low grade and sub-economic, and the commercial operation failed and was abandoned by 1931.

Later economic evaluations at the Prairie Creek vent specifically evaluated the *in-situ* lamproite as the enriched surface material had been depleted. The U.S. Bureau of Mines test, which may have included some surface material, yielded average diamond contents of 2.1 cpht. Glenn Martin's large scale evaluation in 1948 yielded average grades of about 0.44 cpht, and the 1997 Phase 2 evaluation yielded an average grade of 0.57 cpht. When viewed in retrospect, the mining history and reported diamond grades appear consistent with the current geologic understanding and erosion processes at work in the area.

ECONOMIC CONSIDERATIONS

The mining history and economic evaluation of the *in-situ* Prairie Creek lamproite vent proves that it has limited commercial economic potential even utilizing modern large-scale bulk mining equipment. The Phase 2 evaluation proved that although the total resource size is significant, the *in-situ* diamond grade is too low for economic consideration. However, a review of the results of the Phase 2 evaluation in conjunction with the sparse mining records suggests that early mining grades were significantly higher due to weathering and diamond concentration in the soil overburden. Diamond concentrations exceeded economic diamond ore grades for that time. Unfortunately, the natural high-grade concentration in the surface soil was volumetrically small for a commercial mining operation and was essentially depleted by the end of the 1920's.

The commercial alluvial potential of diamonds derived from the Prairie Creek lamproitic vent can be determined utilizing the erosional model. Erosion estimates for this vent indicate that a maximum of 50 meters of erosion has occurred since the Cretaceous. Previous calculations have revealed that the pyroclastic lamproite eroded from the vent would have yielded approximately 93,000 carats of diamonds. Diamonds recovered from the surface lag concentrations which were less than a meter thick and covered the 16 hectares of the intrusion and had an estimated diamond grade of 30 cpht would have yielded approximately 58,000 carats of diamonds. Of this amount of diamond, it is estimated that ~ 29,000 carats of the larger stones were recovered by early mining operations and another ~29,000 carats of the smaller stones were lost to the tailings.

This calculation reveals that approximately 35,000 carats of diamonds could have been removed from the vent area. These diamonds would be contained in adjacent eluvial deposits and small erosion channels, and they would ultimately be delivered to the Little Missouri River for transport and fluvial concentration. Using the average value of diamonds recovered during the Phase 2 evaluation (\$12.30 per carat), the potential value of all the Prairie Creek intrusion alluvial diamonds is approximately US \$430,000. Obviously, commercial alluvial diamond deposits along the Little Missouri River are not economically feasible. The lack of alluvial diamond potential is supported by two lines of evidence. The first is the near total lack of diamonds found immediately downstream of the vent. Furthermore, American Selection Trust (AMSELCO) is known to have evaluated the alluvial potential of the Little Missouri River approximately 10 kilometers downstream. No diamonds were recovered from at least one large tonnage gravel sample (Doug Duskin, personal communication, 1991).

The diamond resource provided by eluvial diamonds adjacent to the vent can be estimated utilizing the erosion model. Approximately 35,000 carats of diamonds are estimated to have been removed from the surface of the vent. Of this value, many of these diamonds have probably not been transported far (due to lateritic soils) and may be contained in eluvial deposits adjacent to the vent. Artisan miners discovered two diamond-rich eluvial stream channels (east and west drains) during the late 1980's and extensively worked these channels until they were exhausted. The "drains" were essentially buried ephemeral streams which ran from the center of the vent to the Little Missouri River. Furthermore, Phase 2 evaluation tested some eluvial material formed by downslope creep off the southern margin of the vent in trench 3A. This material had small pebbles and gravel, and despite being of eluvial nature, yielded two diamonds from

a relatively small sample. This sample demonstrates that the eluvial material and/or terrace alluvium mapped adjacent to the vent may still contain some surface concentrations of diamonds that were not previously recovered. These deposits adjacent to the intrusion may provide promising targets for further tourist development within the park (Dunn, 2000).

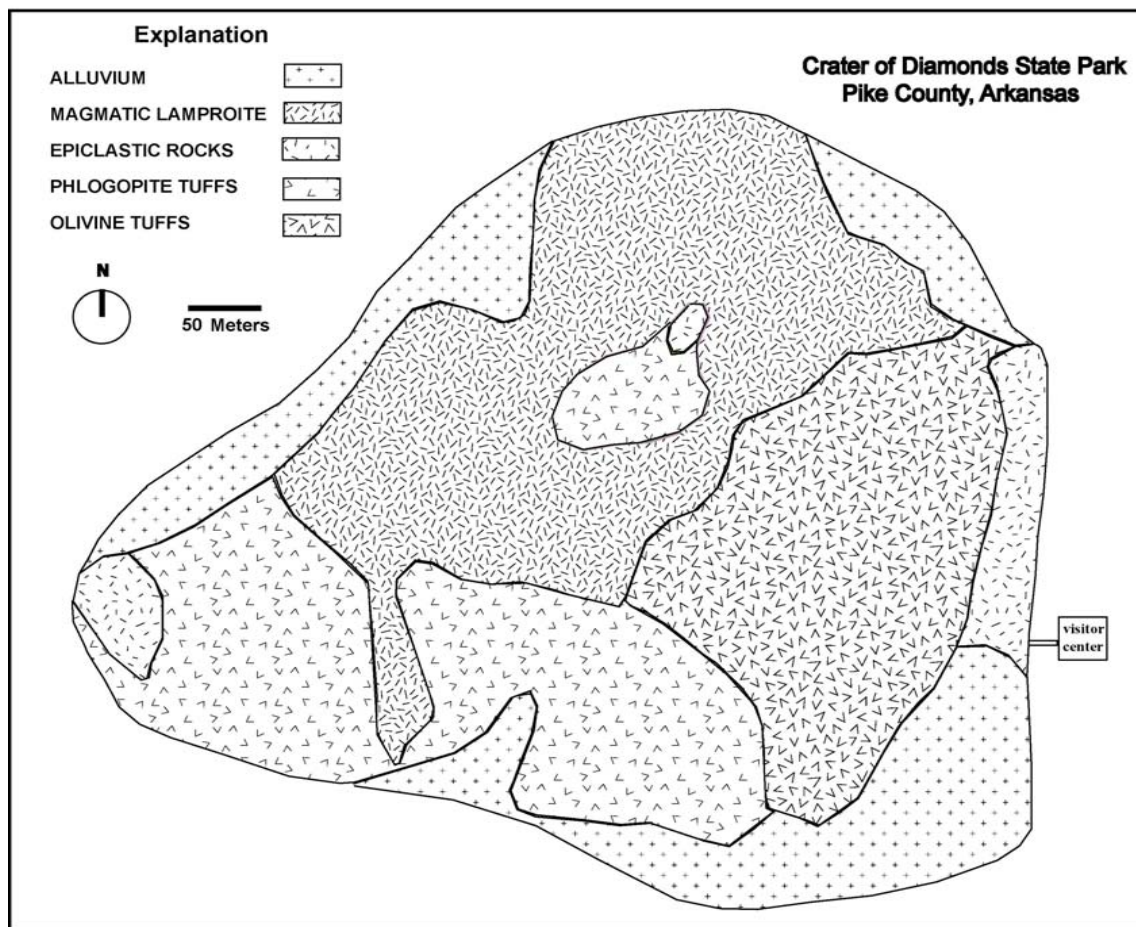


Figure 3-1: Simplified surface geology of the Prairie Creek lamproite. The four mapped volcanic rock types are indicated. Modified from MMMC (1997).

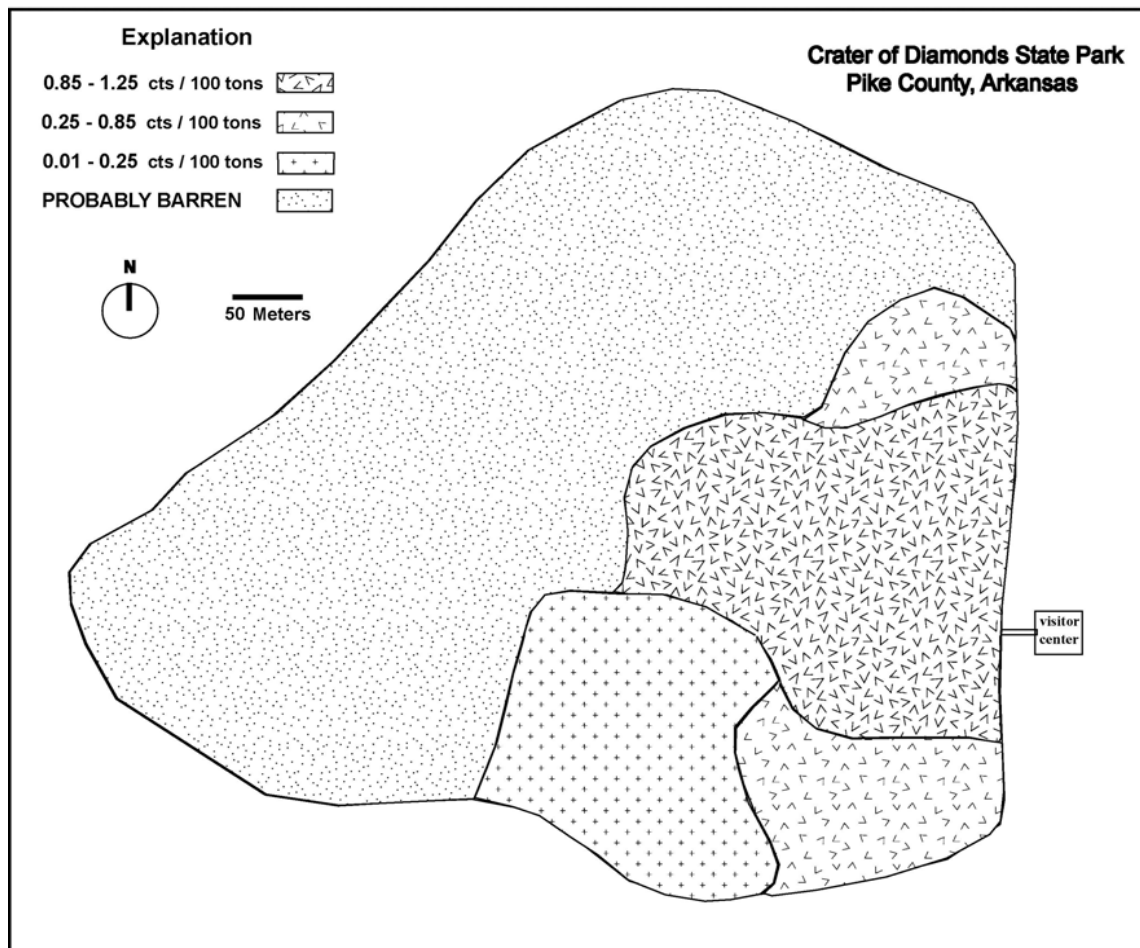


Figure 3-2: Recovered diamond grade within the Prairie Creek lamproite. Modified from MWMC (1997).

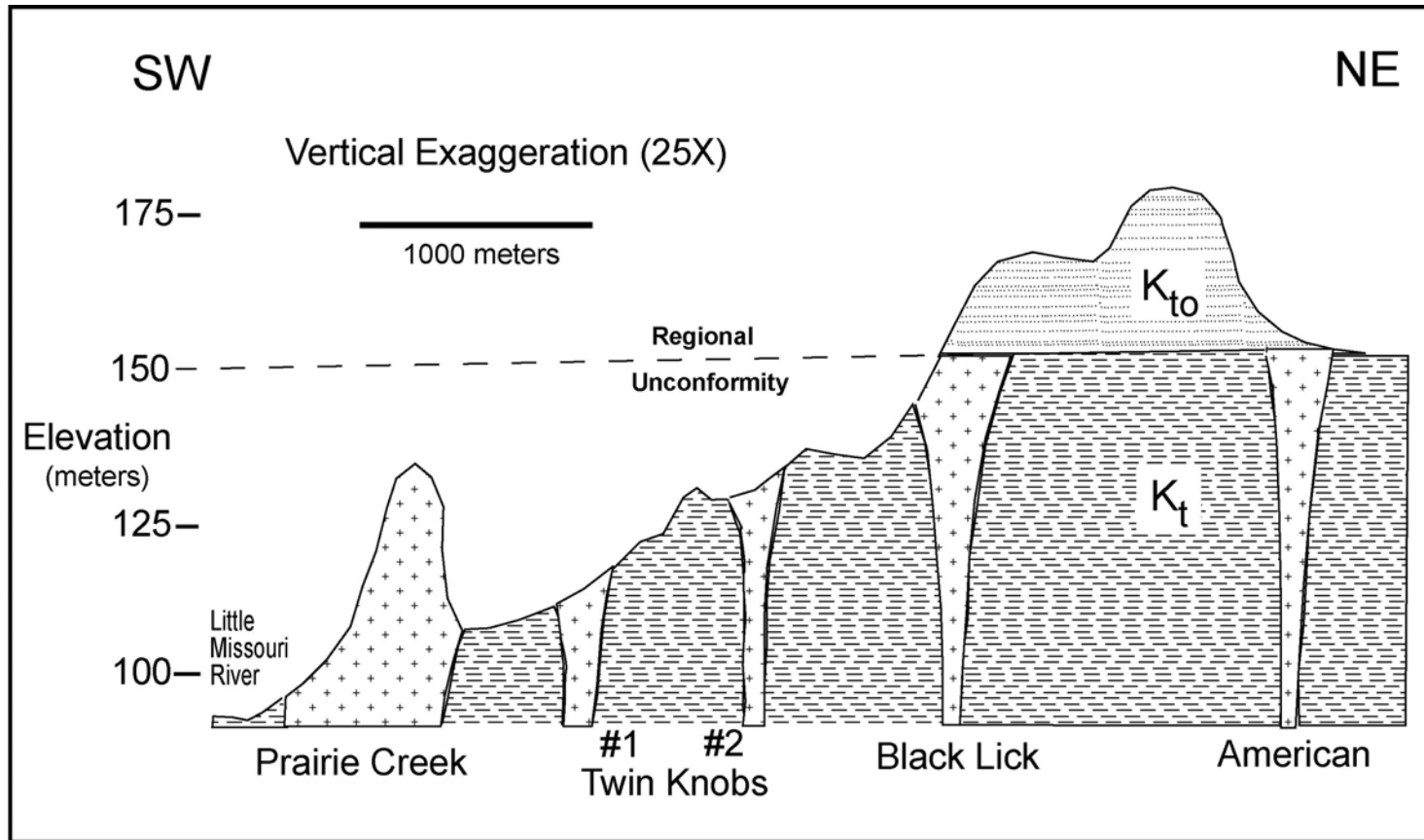


Figure 3-3: Erosion profile across the Arkansas lamproite province. Estimated level of erosion of the Prairie Creek lamproite below the below regional unconformity is indicated. K_t indicates the Early Cretaceous Trinity Group and the K_{to} indicates the Late Cretaceous Tokio Formation.

Chapter 4

MANTLE XENOLITHS

XENOLITH PETROLOGY

The xenoliths, recovered as crushed heavy media concentrate (<3cm), were initially sorted by their probable crustal or mantle origin and by major compositional rock groups. Representative xenoliths of each major compositional group were selected for thin sections based on their relative abundance and lack of visible alteration as determined by binocular microscope examination. Ultramafic xenoliths were of particular interest because multiphase xenoliths can be used to estimate mantle pressure and temperature conditions. Detailed mineralogy was determined by thin section analysis. Xenoliths consisting of two or more minerals were selected for microprobe analysis to determine mineral compositions. Polished thin sections were carbon coated, and areas of interest were marked using ink to assist in future location and identification.

This study is based on ~40 mantle xenoliths ranging in size from 0.5 cm to 3.0 cm in size. Megacrysts were recovered, but are not described in this study as they have been adequately addressed previously (Waldman and others, 1987). The mantle xenolith suite includes the following rock types (lithologic nomenclature of Le Bas and others, 1986) with approximate proportion: dunite (20%), harzburgite, (10%), wehrlite (5%), eclogite (10%), spinel lherzolite (30%), garnet/spinel lherzolite (10%) and garnet lherzolite (15%).

Dunite

Dunite xenoliths are composed predominantly of olivine with at least some of the olivine altered to serpentine. This alteration initiated along fractures and expanded outward until many of the dunite xenoliths are predominantly serpentine and secondary Fe-oxides. Most dunite xenoliths are coarse-grained (>1 cm) with some grains possibly originating as olivine megacrysts. Many of the coarse olivine grains are wholly or partially recrystallized to clear equant (0.5 mm) polygonal olivine neoblasts.

Harzburgite

The harzburgite suite is represented by two samples (m12 and m36) of coarse (~6 mm) peridotite with ~75% olivine and ~20% orthopyroxene and ~5% subhedral fine (<1 mm) spinel. Sample m12 has nearly opaque spinel and sample m36 shows extensive serpentinization at grain boundaries and only rare altered spinel.

Wehrlite

Three samples containing only olivine and clinopyroxene were observed (m10, m44 and m50). However, the latter two samples may be fragments of spinel lherzolite which are lacking orthopyroxene due to their small size. The first sample (m10) may represent wehrlite as it has a much higher iron to magnesium ratio than the latter two samples. It consists of 90% olivine and 10% clinopyroxene. The sample has coarse olivine (1 cm), with one small (1 mm) very pale green clinopyroxene grain. The clinopyroxene grain is rimmed by an alteration halo of serpentine.

Garnet Websterite

Two samples of garnet websterite (m42 and m43) consist of ~70% garnet, ~20% clinopyroxene, and ~10% orthopyroxene (Figure 4-1a). The garnet is coarse-grained (~10 mm) and pink in color and it has abundant pyroxene inclusions. The clinopyroxene exists as fine-grained (2 mm) inclusions and discrete grains (4 mm) and is pale green in thin section. The orthopyroxene is fine-grained (1-2 mm), lacks visible exsolution, and occurs only as inclusions within the garnet.

Eclogite

Four eclogite samples (m26, m28, m29, and m51) contain about 75% subhedral green pleochroic clinopyroxene (10 mm) and 20% sub-rounded (5 mm) orange garnet (Figure 4-1b). Two samples include about 5% subhedral brown rutile (2 mm), and the garnet contains exsolution needles that may also be rutile (m26 and m51). All the garnets have kelyphite rims, less than 1 mm thick, surrounding the relatively inclusion-free garnets. The garnet/clinopyroxene boundary in one sample (m28) is altered to fine-grained amphibole and phlogopite near a lamproite contact. The clinopyroxene in two samples is extensively altered to clay minerals (weathering?).

Low-Cr Spinel Lherzolite

Ten low-Cr spinel lherzolite samples (m9, m17, m20, m21, m23, m24, m32, m33, m46 and m47) consist of ~45% olivine, ~30% orthopyroxene, ~15% clinopyroxene and ~10% brown spinel. The olivine is typically coarse (5 mm) and partly recrystallized to

clear equant (1 mm) olivine neoblasts. The orthopyroxene is coarse (5 mm) with good cleavage and commonly with exsolution lamellae. The clinopyroxene tends to be in fine (<2 mm) equant grains and intimately associated with second-generation spinel. The spinel is light to medium brown color and may record two episodes of growth. First-episode spinel is in fine (1 mm) subhedral grains that are commonly embayed and altered. The second-episode spinel is at grain boundaries and in an intergranular texture, commonly poikilitic, and enclosing equant grains of other minerals (Figure 4-1c). The textures may indicate re-equilibration of the spinel lherzolite to changing P-T conditions.

Mid-Cr Spinel Lherzolite

Four mid-Cr spinel lherzolite samples (m6, m30, m37, and m41) consist of ~50% olivine, ~30% orthopyroxene, ~15% clinopyroxene and ~5% brown spinel. The olivine is typically coarse (5 mm) and rarely recrystallized to clear equant (1 mm) olivine neoblasts. The orthopyroxene is coarse (5 mm) with occasional thin exsolution lamellae. The clinopyroxene generally forms fine (<2 mm) equant grains associated with the spinel. The spinel is dark brown, medium-grained (> 2 mm) with evidence of some secondary growth along grain boundaries (Figure 4-1d). The textures may indicate re-equilibration of the spinel lherzolite in changing P-T conditions.

High-Cr Spinel Peridotite

Three high-Cr spinel peridotites (m4, m12, m36,) consist of ~60% olivine, ~30% orthopyroxene, ~2% clinopyroxene and ~8% opaque spinel (Figure 4-2a). The olivine is coarse (5 mm), with no evidence of recrystallization. The orthopyroxene is coarse (5

mm) and lacks exsolution lamellae. The clinopyroxene is rare and forms (<2 mm) equant grains. The spinel is opaque in thin section and small (<1mm) equant subhedral grains.

Garnet/Spinel Lherzolite

Four garnet/spinel lherzolites (m25, m27, m31 and m49) consist of subhedral (5 mm) olivine (40%), subhedral orthopyroxene (25%), clinopyroxene (15%), brown spinel (10%), and very pale lilac garnet (10%). The garnet occurs as overgrowths (0.5 mm) on slightly to strongly corroded and embayed brown spinel with garnet growth near grain boundaries (m25 and m27) and at the apparent expense of spinel (Figure 4-2b). Most samples show evidence of growth of neoblastic (~1 mm) clinopyroxene at the expense of coarse-grained (~3 mm) orthopyroxene. Coarse grains (~5 mm) of olivine are partly recrystallized to fine-grained neoblastic olivine (~1 mm).

Garnet Lherzolites

The garnet lherzolite suite consists of seven samples (bl4f, m7, m22, m34, m35, m45 and m48) which can be separated into two groups based on the appearance of the garnet. The first group consists of four samples (bl4f, m7, m34, and m45) with coarse-grained (~3mm) olivine (45%), subhedral orthopyroxene (35%), subhedral clinopyroxene (10%) and purple garnet (10%) with kelyphite rims (Figure 4-2d). Some of the garnet is altered and has irregular shapes (m34 and m45) with thick (~50um) kelyphite rims. The second group (m22, m35, and m48) has coarse to neoblastic olivine (45%) subhedral orthopyroxene (35%), rounded clinopyroxene (10%) and pale lilac garnet (15%) without kelyphite rims (Figure 4-2c). The olivine is partly recrystallized from coarse (5 mm) to

neoblastic (1 mm) grains. Some exsolution lamellae are present in the orthopyroxene. Some of the garnet is anhedral, interstitial grains.

MINERAL CHEMISTRY OF PERIDOTITE XENOLITHS

Analytical methods

All wavelength dispersive microprobe analysis were performed on the JEOL Superprobe 733 at The University of Texas at Austin. Accelerating voltage was maintained at 15keV with a cup current of about 40 na. A beam diameter of one micron was typically used except for calibration of Na using albite, which required a 10 micron beam. Maximum counting times for both standards and unknowns were set at 40 seconds. Counts were terminated before 40 seconds if a standard deviation less than 0.3% was achieved based on counting statistics. In nearly all cases, ten elements were analyzed using the four spectrometer crystals. Energy dispersive spectrometry (EDS) was used to qualitatively confirm the mineral assemblages present and one or more backscattered electron images (BSE) were generated for each thin section analyzed. Secondary standards were analyzed prior to and upon completion of analysis of unknowns to check on accuracy of the mineral analysis. Representative mineral rim compositions used in calculation of P-T conditions are listed in Table 4-1.

Olivine

Most olivine compositions have Mg-numbers ($100 \cdot \text{Mg} / \text{Mg} + \text{Fe}$) in the range 89.5 to 93.6. The most magnesian olivine occurs in coarse garnet lherzolites (92.0 to 92.5) and in mid-Cr and high-Cr spinel lherzolites (91.4 to 93.6). Olivine in the low-Cr

spinel lherzolites, garnet/spinel lherzolites, and three recrystallized garnet lherzolites have Mg-numbers in the range 89.5 to 91.1. Olivine in a wehrlite has an exceptionally low Mg-number of 83.2. Olivine from most xenoliths have Cr, Ca, and Ti contents at or near detection limits (~ 0.01 wt %). NiO contents are between 0.35 and 0.42 wt %. MnO contents of olivine are between 0.06 and 0.15 wt % and positively correlate with FeO contents. Olivine appears homogeneous for all major elements as determined by electron microprobe traverses within grains and across grain boundaries.

Orthopyroxene

Most orthopyroxene Mg-numbers are in the range from 89.7 to 94.0 and all are higher than the corresponding olivine Mg-numbers. This relationship of Mg-number between olivine and orthopyroxene is consistent with equilibrium (Gurney and others, 1979). Orthopyroxene grains in the first group of garnet lherzolites and mid-Cr and high-Cr spinel lherzolites have the highest Mg-numbers, whereas those in the low-Cr spinel, garnet/spinel lherzolite and second group of garnet lherzolites have relatively low Mg-numbers. In a garnet websterite, orthopyroxene has an exceptionally low Mg-number of 83.2.

The Cr_2O_3 content of orthopyroxene lies in the range from 0.1% to 0.7%, but no systematic variation among xenolith groups was observed. The CaO content of most orthopyroxene is in the range 0.10% to 0.37 wt %. Trends are difficult to discern, but orthopyroxene tends to have the highest CaO values (up to 0.37%) in the first group of garnet lherzolites. Orthopyroxene in the two garnet websterites have exceptionally high CaO contents up to 1.81%. Highest Al_2O_3 contents in orthopyroxene are found in the

low-Cr spinel lherzolites (2.1% to 4.1%), whereas the lowest Al_2O_3 contents are found in the garnet-bearing lherzolites (0.47% to 1.52%) and in the high-Cr spinel lherzolites (0.47% to 0.89%). Orthopyroxene in one garnet websterite, contains an exceptional 7.35 wt % Al_2O_3 . The Cr-number ($100 \cdot \text{Cr} / (\text{Cr} + \text{Al})$) of orthopyroxene is an indicator of the melt depletion level of the rock. Orthopyroxene in the high-Cr spinel peridotites and first group of garnet lherzolites have the highest chrome numbers of all the xenoliths (Table 4-2). Orthopyroxene in high-Cr peridotite is relatively homogeneous (Figure 4-3a, b), whereas in low-Cr spinel lherzolite subtle zoning is demonstrated by electron microprobe traverses within grains and across grain boundaries (Figure 4-4a, b).

Clinopyroxene

The Mg-numbers of clinopyroxene within peridotites are in the range 92 to 96 and are higher than the Mg-numbers of corresponding olivine and orthopyroxene. Exceptional clinopyroxene mg-values between 83.1 and 89.6 are found for wehrlite and websterite and between 75 and 85 for eclogite. The titanium content of clinopyroxene ranges from below detection to 0.5 wt % TiO_2 . A high TiO_2 content of clinopyroxene is often considered an indicator of peridotite fertility. Clinopyroxene in the mid-Cr and high-Cr spinel peridotites tend to have the lowest TiO_2 content whereas clinopyroxene associated with the garnet/spinel lherzolites tend to have the highest titanium contents (Table 4-2). Chrome content of clinopyroxene ranges from 0.6 % to 2.6 wt % Cr_2O_3 , with those in the garnet-bearing lherzolites having values greater than 1.0% Cr_2O_3 and those in the spinel lherzolites generally less than 1.0 wt % Cr_2O_3 . Sodium content of clinopyroxene has a similar trend; in the garnet-bearing xenoliths the value exceeds 2.0

wt % Na₂O, whereas in the spinel lherzolites it generally is less. The alumina content of the clinopyroxene ranges between 0.8 wt % Al₂O₃ and 6.2 wt % Al₂O₃. Values in the two garnet websterites again are exceptional, between 8.0 and 11.5 wt % Al₂O₃. Clinopyroxene in coarse garnet lherzolite and mid-Cr and high-Cr spinel lherzolite generally have low (<2.0 wt %) Al₂O₃.

Compositional zoning at grain boundaries within clinopyroxene grains is rare or absent in high-Cr lherzolites (Figure 4-3a, b) and subtle within the low-Cr spinel lherzolites (Figure 4-4a, b). Clinopyroxene zoning within the low-Cr spinel lherzolites is usually near-rim depletion adjacent to orthopyroxene and near-rim enrichment adjacent to garnet. This compositional zonation is most apparent in elements with low diffusion rates (Al and Cr) and may record chemical diffusion gradients to grain boundaries.

Spinel

Spinel is readily sub-divided into high-Cr, mid-Cr and low-Cr groups. The low-Cr spinel appears red-brown in thin section and contains less than 30 wt % Cr₂O₃. Mid-Cr spinel is usually dark brown in thin section and contains between 30 and 45 wt % Cr₂O₃. High-Cr spinel is usually opaque in thin section and contains more than 50 wt % Cr₂O₃. Low-Cr spinel has between 17.0 and 19.4 wt % MgO, whereas high-Cr spinel have less than 15 wt % MgO. The Cr-number ($100 \times \text{Cr} / (\text{Cr} + \text{Al})$) in spinel is an excellent way to distinguish between the three groups of chrome spinel. Low-Cr spinels have Cr-numbers of less than 30, mid-Cr spinels have values between 30 and 60, whereas high-Cr spinels have Cr-numbers greater than 60 (Table 4-2).

Garnet

There are two distinct types of peridotite garnet based on color, texture and chemical analysis. The first type of garnet is darker red to purple in color, coarse-grained (<1 cm), sub-rounded, and is surrounded by kelyphite rims. These garnets are relatively high-Cr (3-9 wt % Cr_2O_3) pyrope garnet. Garnet of the second type is very pale lilac in color and lacks a kelyphite rim. Grains are either rounded and equant or elongated along grain-boundaries. These garnets are relatively low-Cr (1-2 wt % Cr_2O_3) pyrope garnet and found in some garnet lherzolite and garnet/spinel lherzolites. The high-Cr peridotite garnets have higher TiO_2 (0.1-0.3 wt %), higher CaO (5-9 wt %) and lower Al_2O_3 (17-21 wt %), lower FeO (7-9 wt %) when compared to low-Cr peridotite garnets. The Cr-number in garnet is considered an indicator of melt depletion of the rock. High-Cr lherzolite garnets (depleted) have Cr-numbers in excess of 8.0 whereas low-Cr lherzolite garnets (fertile) have ratios of less than 5.0 (Table 4-2).

Major element compositional zoning at grain boundaries within garnet grains is generally rare or absent in high-Cr garnet lherzolite, when excluding the kelyphite rim (Figure 4-5a). Major element compositional zoning at grain boundaries is subtle within the low-Cr garnet/spinel lherzolite (Figure 4-5b). Compositional zoning within low-Cr garnet/spinel lherzolite grains is commonly near-rim enrichment in Al_2O_3 , and near-rim depletion in CaO and MgO.

Garnet within the two garnet websterites is coarse-grained and light pink in color. This garnet has moderate Cr_2O_3 (2.73-2.81 wt %), high TiO_2 (0.99-1.14 wt %), moderate CaO (5.11-5.43 wt %) and moderate FeO (8-10 wt %) when compared to lherzolitic garnet. Garnet found in eclogite is pale orange, rounded and has a kelyphite rim. Three

of four eclogites have garnet with less than 0.1 wt % Cr_2O_3 , whereas the exception (m26) has 0.56 wt % Cr_2O_3 . Eclogite garnet has relatively high TiO_2 (0.1-0.4 wt %), high CaO (4.8-8.2 wt %), and high FeO (18-20 wt %) when compared to garnets in the Iherzolite suite.

PRESSURE-TEMPERATURE CALCULATIONS

Method

Equilibrium pressure-temperature (P-T) calculations are based on the partitioning of elements between coexisting minerals, and are an integral part of research on the upper mantle. A major advance in P-T calculations resulted from experiments utilizing naturally occurring mantle compositions. The most widely used and accepted geobarometer for mantle peridotites is that of Brey and Kohler (1990) which utilizes solubility of Al in orthopyroxene equilibrated with garnet (P BKN). Widely used geothermometers include those of Brey and Kohler (1990) which utilize a clinopyroxene-based two pyroxene thermometer (T BKN) and a calcium-in-orthopyroxene-based thermometer (T BKopx). A review of temperature and pressures of mineral equilibrium by Smith (1999) indicates that the clinopyroxene-based thermometer (T BKN) is more accurate at temperatures in excess of 900°C while the orthopyroxene-based thermometer (T BKopx) is more accurate in the range of 800°C to 900°C.

Because calculated pressure and temperatures for mantle xenoliths are based on equilibrium compositions, sufficient time and temperature at ambient mantle conditions are required to permit minerals to equilibrate by diffusion. Compositions of minerals in Arkansas xenoliths with calculated temperatures of ~900°C were found to be relatively

homogenous. Homogeneity is taken to be when the standard deviation for various analyses within a grain is approximately the standard deviation expected from microprobe counting statistics. Xenoliths that record temperatures of $\sim 800^{\circ}\text{C}$ or less may not have equilibrated to ambient mantle conditions, except very near grain contacts (Smith, 1999). Therefore, the use of line scans to determine mineral compositions near grain boundaries is a preferred analytical technique for minerals used in P-T calculations. The outermost grain boundary compositions of mineral phases, with good stoichiometric and oxide weight totals, were utilized for all calculations. Many of the analyzed xenoliths yield evidence of re-equilibration, recrystallization and secondary mineral growth. It is hoped that use of compositions near grain boundaries will most closely reproduce the ambient mantle conditions immediately prior to xenolith entrainment and eruption in Cretaceous time.

Comparison of P-T calculations utilizing different methodologies is a powerful tool for evaluation of mineral equilibrium and accuracy of results. Therefore, many different thermobarometers were used to calculate P-T conditions recorded by single xenoliths. All pressures and temperatures were calculated with the FORTRAN program TP01.v1 which is available from a web address (<http://www.geo.utexas.edu/DougSmith/>). Calculated pressures and temperatures for all orthopyroxene and garnet-bearing Arkansas xenoliths are listed in Table 4-3.

Results

Two garnet lherzolite xenoliths (bl4f and m7) record pressures of ~ 4 GPa and temperatures in excess of 900°C . Two garnet lherzolite xenoliths (m34, and m45) record

pressures of ~3 GPa and temperatures near 800°C. Seven additional xenoliths (m22, m25, m27, m31, m35, m48 and m49) record pressures of ~2.5 GPa and temperatures slightly less than 800°C. Four of these seven xenoliths contain coexisting spinel and garnet and help to define the garnet/spinel transition zone within the upper mantle. The last two P-T array points are relatively low pressure and high temperature falling well off the main trend and represent the two garnet websterite xenoliths. Calculated P-T conditions for all xenoliths with garnet and orthopyroxene, together with the graphite-diamond transition curve and typical mantle geotherms are plotted in Figure 4-6a, b, c, d. The presence of garnet rims as overgrowths on spinel within four of the xenoliths confirm that the garnet-spinel transition zone occurs between 2 and 3 GPa of pressure. These pressures are consistent with those suggested by O'Neill (1981). Likewise, calculated P-T conditions for the deepest xenoliths fall within the diamond stability field and are consistent with the presence of diamond within all the Arkansas lamproites (Dunn and Taylor, 2001). Both of these mineralogical and petrological observations are consistent with the calculated P-T values for the Arkansas xenoliths.

P-T values using the T BKN two pyroxene thermometer (Figure 4-6a) can be compared to a plot using the T BK orthopyroxene thermometer (Figure 4-6b). The two plots compare favorably at higher temperatures in excess of 800°C. Temperatures for xenoliths at lower temperatures show a good cluster for the T BKopx thermometer whereas the T BKN two pyroxene thermometer shows much greater scatter. These data support the conclusion of Smith (1999) that the T BK orthopyroxene thermometer appears more accurate than the T BKN two-pyroxene thermometer at temperatures of less than 900°C. Calculated temperatures at less than 800°C are thought to represent blocking temperatures as indicated by the increasing tendency of xenoliths at these lower

temperatures to show compositional mineral zoning (Figures 4-4a, b) and by the increasing discrepancies between different thermometers. The P-T array calculated using T Krogh (a garnet-clinopyroxene based thermometer) @ P BKN (Krogh, 1988) records slightly higher temperatures for the deep xenoliths than both the pyroxene-based thermometers. However, overall the T Krogh array is consistent with those using the T BK thermometers and is shown as Figure 4-6c. P-T values were calculated using the T Nimis @ P Nimis thermobarometer (Nimis and Taylor, 2000). This single clinopyroxene method is based on a completely different barometer using Cr in clinopyroxene. The Nimis barometer records slightly (+/-1 GPa) higher pressures for high-Cr lherzolites and slightly (+/-1 GPa) lower pressures for the low-Cr lherzolites than the P BKN barometer (Figure 4-6d). These calculated pressure differences tend to increase the scatter of data points from the average mantle geotherm when compared to the P BKN barometer. This increased scatter of data points with the Nimis barometer indicates a less robust, but viable alternative geobarometer for mantle lherzolites.

Discussion of Results

The P-T arrays calculated for Arkansas mantle xenoliths are proposed to represent equilibration to a conductive, steady state geotherm at the time of lamproite eruption (excepting two anomalous garnet websterites). In order to compare the Arkansas geotherm with those elsewhere, the calculated 40mW/m² geotherm of Pollack and Chapman (1977) and the xenolith-derived Kalahari (southern Africa) craton geotherm (Rudnick and Nyblade, 1999) are also shown in the P-T arrays (Figure 4-6a, b, c, d). The Arkansas data at pressures of less than 3 GPa plot at or above a geotherm of

$\sim 40 \text{ mW/m}^2$, whereas data at pressures greater than 3 GPa tend to plot at or below this relatively cool mantle geotherm. This result is in agreement with calculations of T, based on T_{Ni} in garnet, from ~ 100 garnets recovered at the Prairie Creek and Twin Knobs 1 lamproites which are consistent with a geotherm of $\sim 40 \text{ mW/m}^2$ (Griffin and others, 1994). Furthermore, the Arkansas P-T array is very similar to that calculated using mantle xenoliths and the same thermobarometers by Rudnick and Nyblade (1999) for the Kalahari craton.

Archean age cratons have yielded P-T xenolith arrays which indicate geotherms of $\sim 40 \text{ mW/m}^2$ or less. O'Reilly and others (2001) have used the observation that Archons (Archean cratons) typically have a geotherm of less than 40 mW/m^2 , Protons (Proterozoic cratons) have a geotherm of between $40\text{--}45 \text{ mW/m}^2$, and Tectons (cratons $< 1 \text{ Ga}$) have a geotherm of 50 mW/m^2 or more. This relationship is used to define a concept of technothermal age of the cratons which states that the older the craton, the cooler the associated geotherm. Based on these observations, the Arkansas xenolith P-T array is indicative of a stable craton of at least Early Proterozoic age. This is a surprising result, as Arkansas lamproites intrude deformed Paleozoic age rocks of the Ouachita orogeny.

The two points representing garnet websterite fall well off the main P-T array. They appear to be unrelated to the main xenolith trend and may indicate a different genesis. The pyroxenes in the garnet websterite are partly altered inclusions within the garnet. Calculated pressures and temperatures using different thermobarometers vary widely for the two garnet websterite xenoliths, suggesting lack of mineral equilibrium for these pyroxenes. However, calculated pressures are generally less than 2 GPa and temperatures in excess of 1000° C . These conditions are more representative of basaltic

magma crystallization at depth than those of a conductive mantle geotherm. These two garnet websterite xenoliths may have formed during underplating of basaltic magmas near the base of the continental crust. This hypothesis is in agreement with the proposed genesis of potassium richterite xenoliths as being cumulates within the lamproite melt (Mitchell and Lewis, 1983). The high temperatures indicated by the pyroxene compositions suggest insufficient time for conductive cooling and therefore they may be related to the Cretaceous volcanic event that generated the host lamproites.

The forsterite content of olivine can be used as a proxy for the amount of melt depletion within the mantle. There is also a strong correlation between the average forsterite content in olivine and the age of the lithospheric mantle from which the olivine is derived (Gaul and others, 2000). These authors observe that Archean age mantle lithosphere olivine is $\sim\text{Fo}_{92-93}$, Proterozoic lithosphere olivine is $\sim\text{Fo}_{91-92}$ whereas Phanerozoic mantle lithosphere olivine is $\sim\text{Fo}_{90}$. Given the importance of the forsterite content of olivine, it is included under the olivine analysis of Table 4-1 and Table 4-2.

A comparison of the forsterite content of olivine vs. calculated pressures (depth) for the xenoliths yields estimated mantle depletion with depth. Data for all xenoliths containing a geobarometer assemblage indicate a general trend of increasing mantle depletion with depth to pressures of ~ 5 GPa (Figure 4-7). Only the four garnet lherzolite xenoliths that reveal the highest pressures (3-5 GPa) have olivine more magnesian than Fo_{92} . Of greater significance, all other garnet-bearing xenoliths have olivine with a forsterite content of less than Fo_{90-91} . This gap in forsterite content represents a significant break in mantle depletion from a shallow less depleted mantle lithosphere to a relatively depleted mantle lithosphere at depths in excess of 100 kilometers.

Inclusion of the forsterite content of olivine within all spinel peridotites would add many more data points to this graph; however, spinel peridotites do not contain a reliable geobarometer. It is reasonable to assume that most typical (low-Cr) spinel peridotites have equilibrated at pressures of ~ 1.5 GPa, a value which is less than the xenolith-defined spinel-garnet transition zone which occurs at recorded pressures between 2 and 3 GPa. Ten of the 17 spinel peridotites would qualify as typical low-Cr spinel lherzolites which have forsterite contents of olivine between $\text{Fo}_{89.5}$ and $\text{Fo}_{91.2}$.

The other seven spinel peridotites are mid-Cr and high-Cr spinel peridotites (spinel with >30 wt % Cr_2O_3) with olivine in the range of $\text{Fo}_{91.4}$ to $\text{Fo}_{93.5}$. The high-Cr spinel peridotites may represent a distinct group of mantle xenoliths. Increasing the Cr_2O_3 content of spinel has been found to increase the depth of the spinel-garnet transition (O'Neill, 1981). An inverse correlation has been found between the Cr_2O_3 content of spinel and the Al_2O_3 in the orthopyroxene (Figure 4-8). All rocks containing spinel with over 30 wt % Cr_2O_3 have less than ~ 2 wt% Al_2O_3 in the orthopyroxene. Boyd and others (1999) showed that spinel peridotites containing orthopyroxene with less than 1.0 wt % Al_2O_3 may represent peridotite equilibrated at pressures within the garnet stability field. The three high-Cr spinel peridotites (m4, m12 and m36) all have less than 1.0 wt % Al_2O_3 and a Cr-number in spinel of ~ 70 . Lee and Rudnick (1999) found that a Cr-number in spinel of 70 increases the garnet-spinel transition to pressures of ~ 3.6 GPa in xenoliths from Tanzania. In other words, the three high-Cr xenoliths may represent "garnet-facies" spinel peridotites and could represent pressures as great as ~ 3.5 GPa (greater than the garnet/spinel transition zone for aluminous peridotites). The four mid-Cr spinel lherzolites have petrologic and chemical characteristics between the low-Cr and high Cr spinel lherzolites. They are assumed to represent pressures of ~ 2.5 GPa, midway

between the two groups and well within the garnet/spinel transition zone as recorded by the four garnet/spinel lherzolites. Addition of all the spinel peridotites, plotted at pressures indicated by the Cr-number in spinel to the previous plot of garnet lherzolite depletion vs. depth indicates that the trend of increasing mantle depletion with depth is still observed (Figure 4-9). The relatively sharp break between relatively fertile shallow mantle ($\text{Fo}_{91.5}$) and depleted deeper mantle (Fo_{92}) lithosphere occurs at pressures of $\sim 3\text{GPa}$.

The assumption that high-Cr spinel peridotite (orthopyroxene with <1 wt % Al_2O_3) equilibrated at pressures greater than low-Cr spinel lherzolites (orthopyroxene with >2 wt % Al_2O_3) is reasonable, given that the decreasing Al_2O_3 content of orthopyroxene in the presence of garnet with increasing pressure, is the basis for the widely used P BKN barometer in garnet lherzolite. Further evaluation that high-Cr spinel peridotites are derived from greater depths than low-Cr spinel lherzolites can be made by comparing calculated temperatures recorded by the two xenolith populations. Calculated temperatures for spinel peridotites derived from seven different thermometers are provided in Table 4-4. The high-Cr spinel peridotites generally lack clinopyroxene preventing the use of clinopyroxene-based thermometers. However, the one high-Cr spinel lherzolite and the mid-Cr spinel lherzolites generally record higher temperatures than the low-Cr spinel lherzolites. Furthermore, the olivine-spinel thermometer of Ballhaus and others (1991) can be applied to all of the spinel peridotites, and these calculations record significantly higher temperatures for the high-Cr spinel peridotites than the low-Cr spinel lherzolites. Application of the P Nimis (Cr-in-clinopyroxene) barometer to spinel lherzolite also indicates that the high- and mid-Cr groups generally record higher pressures than the low-Cr spinel lherzolites.

A plot of xenolith abundance and mineralogy used in conjunction with estimated pressure of origin yields a theoretical depth profile of the sub-continental lithospheric mantle beneath southwestern Arkansas at the time of eruption (Figure 4-10). The lowermost part of the section is dominated by relatively depleted high-Cr spinel harzburgite and high-Cr garnet lherzolite, whereas the uppermost mantle section consists of relatively fertile low-Cr spinel lherzolites and a higher abundance of eclogite, wehrlite and garnet websterite.

Eclogite equilibration temperatures were calculated using T Krogh at pressures of 1.5 GPa (Table 4-5). The four eclogites can be divided into low temperature and high temperature groups and plotted according to their recorded temperatures on the T Krogh P-T array geotherm of $\sim 45 \text{ mW/m}^2$ (Figure 4-6c). This exercise indicates that the two higher temperature eclogites were derived from depths of ~ 3 GPa and hence their equilibrium temperatures were recalculated to those pressures. After placing all xenoliths at their estimated depths, a relatively sharp break between the two chemically different mantle volumes appears at a pressure of ~ 3 GPa.

The crust-mantle boundary is at depths of 30-35 kilometers based on seismic reflection interpretation beneath the Prairie Creek lamproite province (Mickus and Keller, 1992). This shallow boundary is consistent with more detailed crustal models which indicate that much of the Gulf Coast has a crustal thickness of less than 40 kilometers (Chulick and Mooney, 1998). The gravity data indicate the presence of low density upper mantle ($\sim 3.30 \text{ gm/cm}^3$) suggesting the presence of a Mg-rich depleted mantle beneath the region. Two different methodologies (Boyd and McCallister, 1976; Lee and others, 2001) were used to estimate the density of the Arkansas mantle lherzolites. These calculations indicate a relatively low upper mantle density of $3.34\text{-}3.36 \text{ g/cm}^3$. Grand

(1994) also found evidence for the presence of anomalous mantle to a depth of 175 kilometers as indicated by anomalously high shear velocities more typical of highly depleted Archean age shield areas beneath Arkansas. This suggestion is compatible with Re-Os isotope studies of the Prairie Creek lamproites which find that the mantle source rocks of the Arkansas lamproites had sub-chondritic Re/Os ratios that are best satisfied by a refractory (harzburgitic) mantle source (Lambert and others, 1995). Lamproite magmas were probably generated at depths of ~6 GPa and temperatures in excess of 1200°C, based on maximum recorded xenolith pressures and extrapolation of the ~40 mW/m² mantle geotherm.

Both xenolith abundance (mantle section) and depletion plots (olivine F_0) indicate the existence of a two-part mantle lithosphere beneath the Prairie Creek lamproite province in Cretaceous time. The upper part of the mantle lithosphere consists predominantly of relatively fertile peridotite with an olivine content of ~Fo₉₀. In contrast, the lower part of the mantle lithosphere is relatively depleted with an olivine content of Fo₉₂₋₉₃. Griffin and others (1998a) used the forsterite content of mantle olivine to help define the tectonothermal age of the craton. Application of their criteria to the two part mantle lithosphere observed beneath the Prairie Creek lamproite province indicates the shallow mantle lithosphere has a Tecton (<1.0 Ga) age, whereas the deeper, depleted mantle lithosphere might be an Archon (>2.5 Ga).

The finding of a shallow fertile mantle lithosphere overlying a deeper depleted mantle lithosphere is in contrast to mantle sections proposed for most other sub-continental lithospheric mantle of Archean age. Kopylova and others (1998) found that the Canadian Slave Province has a relatively depleted upper lithosphere and a much more fertile, metasomatized, lower mantle lithosphere. Griffin and others (1998a) found

similar layering in the Siberian craton, and Rudnick and Nyblade (1999) summarized earlier data to show that the Kalahari craton had increasing mantle fertility at depth due to metasomatism within the asthenosphere. Evidence for this type of deep lithosphere metasomatism may be indicated by Arkansas garnet xenocryst data (Griffin and others, 1994), which are used to calculate olivine equilibrium compositions and which indicate an increase in olivine Mg-numbers down to a pressure of ~ 5 GPa but show a slight decrease in olivine Mg-numbers at pressures between 5-6 GPa (Bill Griffin, personal communication, 2002). Olivine inclusions found within Arkansas diamonds have Mg-numbers of 91.7 and 92.2 and could be interpreted to show a slight decrease in Mg-number at these higher pressures (Pantaleo and others, 1979).

The finding of fertile mantle lithosphere overlying depleted mantle lithosphere is more common in Proterozoic age cratons. This sub-continental mantle lithospheric structure is similar to sections based on xenoliths of Shandong Province in China (Griffin and others, 1998b), and the Colorado Plateau of the western U.S. (Roden and Shimizu, 1993). The Gawler craton of Australia is similar in that there is a sharp boundary between the upper and lower mantle layers which may suggest a two-stage construction of that mantle lithosphere (Scott-Smith and others, 1984).

The presence of a two-part mantle lithosphere with relatively young fertile material overlying a relatively cool, depleted ancient mantle lithosphere located in a Paleozoic age tectonic belt on the southern margin of the North American craton is problematic. Two possible emplacement scenarios are consistent with available data. The first proposed model is that an allochthonous terrane of either Archean or Lower Proterozoic age was incorporated into the southern margin of the North American craton before the development of the mid-continent granite-rhyolite terrane of 1.3 to 1.5 Ga.

Such a region would have a depleted lithospheric keel which would be extremely stable (low density) and difficult to destroy by delamination (Jordan, 1978). Parts of this old allochthonous terrane would have to survive the forces associated with the granite-rhyolite terrane development leaving some relatively pristine depleted lithosphere keel at depth. A similar scenario has been proposed for the eastern Sino-Korean craton where thickened mantle lithosphere with extensional tectonics resulted in partial rejuvenation to a younger more fertile lithosphere (Griffin and others, 1998b). It is possible that small regions of relatively intact depleted mantle lithosphere could have been preserved and sampled by the Prairie Creek lamproite province. Evidence that is consistent with such a scenario is U-Pb dating of one zircon recovered from concentrates from the Prairie Creek lamproite that records a 1.85 Ga isotopic age which is older than any known crustal rocks in the region (Reichenback and Parrish, 1988). Also, Nelson and DePaolo (1985) have determined Sm-Nd crustal formation ages for several clustered samples from the granite-rhyolite terrane in southern Oklahoma to be from 1.81 to 1.98 Ga in age. It is possible that these ~1.9 Ga ages could represent a sample of preserved allochthonous terrane located within the southern edge of the mid-continent craton.

A second model for the presence of the two layer mantle lithosphere involves tectonic emplacement of relatively old (Archean?) depleted mantle lithosphere beneath younger (Upper Proterozoic) more fertile continental lithosphere by subduction within a large scale continent-continent collision. Mosher (1998) has proposed that the Grenville-Llano deformation front separating a 1.3-1.5 Ga granite-rhyolite terrane from the ~ 1.1 Ga age Grenville-Llano terrane to the south continues northeast from central Texas toward the Arkansas border. K-Ar ages of four amphibolite xenoliths recovered from the Prairie Creek lamproite province yields ages of 1.48 Ga, 1.43 Ga, 1.43 Ga, and 1.31 Ga

(Dunn and others, 2000). These ages are suggestive of an association with the mid-continent granite-rhyolite terrane and indicate that the region was inboard and thermally isolated from the major continent-continent collision associated with the Grenville-Llano orogeny. Based on paleomagnetic data, it has been proposed that the continent-continent collision which generated this Grenville deformation resulted from collision of the southern margin of the North American craton with the Kalahari craton (Dalziel and others, 2000). Preservation of part of this Archean craton may have occurred due to tectonic stacking of depleted mantle lithosphere which would probably preserve an Archean lithosphere keel (Poudjom Djormani and others, 2001). It may be more than coincidental that the xenolith-defined mantle geotherms of Arkansas and the Kalahari craton are similar. Other evidence for possible juxtaposition of mantle lithosphere comes from isotope studies. Lambert and others (1995) have used Re-Os isotopic studies of the Prairie Creek lamproite to obtain a lithosphere separation model age of ~1.2 Ga. However, they suggest that subduction-related processes associated with Grenville-Llano tectonics may have juxtaposed younger(?) lithosphere under the Middle Proterozoic age craton. Alibert and Albarede (1988) used Sr, Nd and Pb isotope data to determine that the Prairie Creek lamproite shows a major contribution of ancient recycled sediments in its mantle source in contrast to North American “kimberlites”. Both low and high temperature eclogites have been recorded and their presence may suggest a possible tectonic emplacement of this two layer mantle boundary. The observed presence of both peridotite and eclogite-suite minerals as inclusions within Arkansas diamonds (Pantaleo and others, 1979) helps support the role of subduction-related tectonics in the generation of Arkansas diamonds.

Arkansas mantle xenoliths reveal the existence of a shallow fertile mantle layer above a deeper depleted mantle layer, with a relatively sharp contact between the two types of sub-continental mantle lithosphere. This juxtaposition of mantle lithosphere suggests a two-stage construction of the sub-continental mantle lithosphere beneath southwestern Arkansas. It is proposed that this juxtaposition was tectonically emplaced either by incorporation of an older allochthonous terrane within the southern margin of the North American craton or by tectonic stacking of sub-continental mantle lithosphere during a continent-continent collision. A similar tectonic emplacement scenario might be applicable to other areas with comparable structured sub-continental lithospheric sections such as the southern Australian craton.

TABLE 4-1

Mineral Rim Compositions used in Pressure-Temperature Calculations

	m7					bl4f			
	Olivine	OPX	gtlz CPX	Garnet		Olivine	OPX	gtlz CPX	Garnet
SiO ₂	41.47	57.76	54.71	41.89		40.74	57.44	54.66	40.68
TiO ₂	0.02	0.03	0.09	0.22		nd	0.07	0.18	0.29
Al ₂ O ₃	nd	0.57	1.88	16.95		nd	0.47	1.98	17.15
Cr ₂ O ₃	0.03	0.32	2.6	8.43		0.03	0.28	2.01	3.94
FeO*	7.58	4.65	2.04	7.33		7.56	5.17	2.34	8.17
MnO	0.12	0.11	0.06	0.45		0.10	0.10	0.06	0.46
MgO	51.05	35.33	15.76	18.04		51.71	36.51	16.26	19.82
CaO	0.01	0.32	19.32	7.05		0.03	0.37	19.81	4.89
Na ₂ O	nd	0.10	2.65	0.04		0.05	0.13	2.29	0.08
K ₂ O	nd	nd	nd	nd		nd	nd	nd	nd
NiO	0.37	0.08	0.06	0.03		0.37	0.08	nd	0.05
Total	100.6	99.27	99.17	100.43		100.6	100.62	99.59	95.53
mg#	0.923	0.931	0.932	0.814		0.924	0.926	0.925	0.812

	m34					m45			
	Olivine	OPX	gtlz CPX	Garnet		Olivine	OPX	gtlz CPX	Garnet
SiO ₂	41.49	58.39	55.13	41.88		41.49	57.5	55.82	41.26
TiO ₂	0.03	0.07	0.31	0.11		0.01	0.08	0.17	0.38
Al ₂ O ₃	nd	0.69	2.80	21.26		nd	1.08	1.62	17.67
Cr ₂ O ₃	0.03	0.23	1.92	3.05		nd	0.37	2.11	6.61
FeO*	7.72	4.97	1.70	8.56		7.59	4.96	2.02	7.81
MnO	0.10	0.10	0.01	0.50		0.11	0.11	0.10	0.45
MgO	51.00	36.03	15.59	19.23		51.51	35.51	16.49	18.91
CaO	0.01	0.19	21.22	5.24		0.02	0.33	20.07	6.24
Na ₂ O	nd	nd	2.12	0.02		nd	0.09	2.04	0.04
K ₂ O	nd	nd	nd	nd		nd	nd	nd	nd
NiO	0.36	0.07	0.03	0.02		0.36	0.13	0.14	0.01
Total	100.75	100.76	100.83	99.87		101.11	100.16	100.58	99.38
mg#	0.922	0.928	0.942	0.800		0.924	0.927	0.936	0.812

		m22	gtlz			m35	gtlz	
	Olivine	OPX	CPX	Garnet	Olivine	OPX	CPX	Garnet
SiO2	40.09	56.70	54.48	41.51	41.54	56.89	54.58	42.03
TiO2	0.01	0.09	0.36	0.07	nd	0.07	0.35	0.06
Al2O3	0.13	1.38	3.68	21.82	nd	0.89	3.51	21.99
Cr2O3	nd	0.27	1.02	1.22	nd	0.23	1.36	1.55
FeO*	9.49	5.83	2.27	10.28	8.94	5.70	2.05	10.35
MnO	0.10	0.10	0.04	0.43	0.09	0.10	0.01	0.46
MgO	48.35	34.28	15.17	18.61	49.58	34.79	14.85	18.97
CaO	0.03	0.22	20.32	4.62	0.01	0.22	19.81	4.64
Na2O	nd	0.03	2.55	0.03	nd	0.04	2.78	nd
K2O	nd	nd	nd	nd	nd	nd	nd	nd
NiO	0.35	0.11	0.02	0.01	0.38	0.04	0.02	nd
Total	98.55	99.01	99.91	98.60	100.57	98.97	99.32	100.07
mg#	0.901	0.913	0.923	0.763	0.908	0.916	0.928	0.766

		m48	gtlz			m25	gtsplz		
	Olivine	OPX	CPX	Garnet	Olivine	OPX	CPX	Garnet	Spinel
SiO2	41.18	58.09	55.41	41.48	40.02	56.16	52.35	40.83	nd
TiO2	nd	0.09	0.40	0.05	nd	0.09	0.42	0.06	0.17
Al2O3	nd	1.06	3.77	22.05	nd	1.13	6.02	21.68	45.20
Cr2O3	nd	0.28	1.28	1.60	nd	0.20	0.87	0.98	19.03
FeO*	8.95	5.83	2.02	10.19	9.25	5.86	2.11	10.74	14.95
MnO	0.08	0.11	0.04	0.47	0.06	0.08	0.04	0.53	0.14
MgO	49.75	35.09	14.67	19.09	49.20	34.69	14.21	18.37	17.20
CaO	0.01	0.21	20.09	4.57	nd	0.25	20.84	4.53	nd
Na2O	nd	nd	2.36	0.03	nd	0.04	2.01	nd	nd
K2O	nd	nd	nd	nd	nd	nd	nd	nd	nd
NiO	0.44	0.07	0.05	0.03	0.37	0.08	0.04	0.01	0.28
Total	100.42	100.85	100.19	99.56	98.91	98.58	98.91	97.74	96.98
mg#	0.908	0.915	0.928	0.770	0.905	0.913	0.923	0.753	0.672

		m27		gtsplz			m42		gtweb
	Olivine	OPX	CPX	Garnet	Spinel		OPX	CPX	Garnet
SiO2	40.38	57.25	52.50	41.98	0.03		51.83	49.13	41.76
TiO2	nd	0.10	0.49	0.06	0.14		0.38	1.52	1.14
Al2O3	nd	1.52	5.00	22.54	48.17		7.35	8.07	19.72
Cr2O3	nd	0.26	0.77	1.17	17.07		0.68	0.59	2.73
FeO*	9.58	5.72	2.12	10.21	13.96		8.57	5.74	10.05
MnO	0.09	0.09	0.04	0.47	nd		0.25	0.22	0.29
MgO	49.37	34.84	14.77	18.41	17.57		29.17	16.10	19.12
CaO	0.01	0.20	20.90	4.94	nd		1.81	18.04	5.43
Na2O	nd	0.03	1.85	0.03	nd		0.13	0.84	0.09
K2O	nd	nd	nd	nd	nd		nd	nd	nd
NiO	0.35	0.06	0.04	nd	0.26		na	na	na
Total	99.80	100.07	98.48	99.81	97.22		100.17	100.25	100.33
mg#	0.902	0.916	0.925	0.763	0.692		0.858	0.833	0.772

		m31		gtsplz			m43		gtweb
	Olivine	OPX	CPX	Garnet	Spinel		OPX	CPX	Garnet
SiO2	40.35	58.94	55.01	42.20	nd		57.53	45.47	41.65
TiO2	nd	0.08	0.40	0.09	0.16		nd	2.46	0.99
Al2O3	nd	0.83	3.73	22.84	50.44		2.58	11.52	20.41
Cr2O3	nd	0.11	0.78	0.91	16.79		0.13	1.11	2.81
FeO*	8.96	5.74	2.22	10.30	13.85		6.57	4.63	8.01
MnO	0.10	0.10	0.04	0.48	0.13		0.01	0.18	0.29
MgO	49.32	35.37	14.99	18.96	18.02		32.80	12.78	21.13
CaO	0.01	0.16	20.55	4.43	0.03		0.56	20.48	5.11
Na2O	nd	nd	2.82	nd	nd		nd	1.09	0.05
K2O	nd	nd	nd	nd	nd		nd	nd	nd
NiO	0.41	0.08	0.04	0.02	0.37		na	na	na
Total	99.18	101.43	100.58	100.25	99.80		100.2	99.72	100.45
mg#	0.907	0.917	0.923	0.766	0.699		0.899	0.831	0.825

	m49					m4			
	Olivine	OPX	CPX	Garnet	Spinel	Olivine	OPX	CPX	Spinel
SiO2	41.24	57.54	54.30	40.91	0.02	41.29	57.75	56.51	0.03
TiO2	nd	0.10	0.34	0.03	0.28	nd	nd	0.02	0.16
Al2O3	nd	1.01	3.35	23.07	40.77	nd	0.89	0.81	14.81
Cr2O3	nd	0.21	1.06	1.08	24.91	nd	0.28	0.61	55.61
FeO*	9.23	5.95	2.24	9.19	15.75	7.81	4.91	1.33	14.73
MnO	0.09	0.09	0.07	0.33	0.03	nd	0.10	0.06	nd
MgO	49.61	34.39	15.15	19.73	16.28	50.37	36.28	18.01	13.30
CaO	nd	0.26	20.56	4.99	nd	nd	0.13	23.99	nd
Na2O	nd	nd	2.10	nd	nd	nd	nd	0.40	nd
K2O	nd	nd	nd	nd	nd	nd	nd	nd	nd
NiO	0.45	0.09	0.02	nd	0.25	0.27	nd	nd	0.07
Total	100.63	99.66	99.19	99.35	98.31	99.75	100.34	101.74	98.73
mg#	0.905	0.912	0.923	0.793	0.648	0.920	0.929	0.960	0.617

	m6				m12		
	Olivine	OPX	CPX	Spinel	Olivine	OPX	Spinel
SiO2	41.3	57.10	55.06	0.04	41.16	58.42	0.07
TiO2	0.01	nd	0.01	0.16	0.02	0.05	0.72
Al2O3	nd	2.06	1.33	30.18	0.03	0.56	9.97
Cr2O3	nd	0.45	0.49	39.13	0.02	0.30	55.94
FeO*	8.37	5.31	1.66	14.68	6.99	4.33	18.19
MnO	0.11	0.12	0.06	0.22	0.09	0.10	nd
MgO	50.17	34.33	17.30	14.50	50.74	35.70	13.04
CaO	nd	0.28	23.62	nd	nd	0.22	nd
Na2O	nd	nd	0.18	nd	nd	0.11	nd
K2O	nd	nd	nd	nd	nd	nd	nd
NiO	0.39	0.09	0.03	0.09	0.35	0.07	0.14
Total	100.37	99.75	99.74	98.84	99.41	99.86	98.09
mg#	0.914	0.920	0.949	0.638	0.928	0.936	0.561

m30					m36			
	Olivine	OPX	CPX	Spinel	Olivine	OPX	Spinel	
SiO2	41.84	57.91	54.61	nd	41.65	58.11	0.08	
TiO2	0.01	0.07	0.16	0.31	0.02	0.02	4.95	
Al2O3	nd	2.04	2.82	36.04	nd	0.47	13.09	
Cr2O3	nd	0.37	1.07	32.36	0.04	0.37	43.12	
FeO*	7.55	4.77	1.52	13.02	7.55	4.43	21.52	
MnO	0.11	0.12	0.05	0.22	0.11	0.13	nd	
MgO	51.01	35.17	16.13	16.21	51.31	35.51	14.72	
CaO	0.02	0.23	22.48	0.03	0.01	0.32	nd	
Na2O	nd	nd	1.35	nd	nd	0.16	nd	
K2O	nd	nd	nd	nd	nd	nd	nd	
NiO	0.37	0.07	0.03	0.18	na	na	na	
Total	100.92	100.77	100.22	98.37	100.7	99.52	97.49	
mg#	0.923	0.929	0.950	0.689	0.924	0.935	0.549	

m37					m41			
	Olivine	OPX	CPX	Spinel	Olivine	OPX	CPX	Spinel
SiO2	41.55	57.66	55.75	nd	41.77	57.65	55.24	0.03
TiO2	0.01	0.02	0.03	0.22	0.02	0.01	0.09	0.10
Al2O3	0.04	1.36	1.11	22.60	nd	1.70	3.68	30.86
Cr2O3	nd	0.42	0.63	45.53	nd	0.41	1.44	39.70
FeO*	8.33	5.18	1.60	16.01	6.41	4.10	1.29	12.06
MnO	0.13	0.12	0.08	0.27	0.06	0.07	0.02	0.27
MgO	50.18	35.03	17.47	13.57	51.87	35.88	15.74	16.00
CaO	0.02	0.29	24.17	0.05	0.01	0.16	20.71	nd
Na2O	0.05	nd	0.37	nd	nd	nd	2.06	nd
K2O	nd	nd	nd	nd	nd	nd	nd	nd
NiO	0.38	0.10	0.04	0.09	0.38	0.05	0.03	0.10
Total	100.91	100.19	101.25	98.34	100.53	100.1	100.3	98.86
mg#	0.915	0.923	0.951	0.602	0.935	0.940	0.956	0.703

	m9					m17			
	Olivine	OPX	splz CPX	Spinel		Olivine	OPX	splz CPX	Spinel
SiO2	40.56	56.18	53.95	0.06		42.13	56.99	54.58	0.01
TiO2	nd	0.01	0.07	0.04		nd	0.02	0.09	0.03
Al2O3	nd	2.14	2.54	44.46		nd	2.59	2.54	49.32
Cr2O3	0.01	0.28	0.71	22.48		nd	0.29	0.49	19.13
FeO*	8.65	5.88	1.57	13.53		9.27	6.17	1.91	13.33
MnO	0.12	0.16	0.09	0.13		0.14	0.16	0.06	0.13
MgO	49.98	34.06	16.71	17.11		50.34	34.28	16.93	17.72
CaO	nd	0.26	24.15	nd		0.01	0.27	23.85	nd
Na2O	nd	nd	0.62	nd		nd	nd	0.57	nd
K2O	nd	nd	nd	nd		nd	nd	nd	nd
NiO	0.42	0.08	nd	0.18		0.37	0.08	0.03	0.25
Total	99.75	99.06	100.41	97.99		102.26	100.86	101.05	98.80
mg#	0.911	0.912	0.950	0.693		0.906	0.908	0.940	0.703

	m20					m21			
	Olivine	OPX	splz CPX	Spinel		Olivine	OPX	splz CPX	Spinel
SiO2	40.80	54.35	53.24	0.01		40.34	54.77	52.55	0.01
TiO2	0.02	0.03	0.16	0.08		nd	0.11	0.48	0.07
Al2O3	nd	3.55	4.36	47.46		nd	3.33	4.82	51.20
Cr2O3	nd	0.54	1.13	19.01		nd	0.33	0.79	14.39
FeO*	8.88	5.82	1.81	12.89		8.79	5.58	1.73	11.31
MnO	0.14	0.13	0.09	0.14		0.13	0.15	0.09	nd
MgO	48.82	33.79	15.17	17.55		48.94	33.75	14.95	19.02
CaO	0.01	0.29	22.53	nd		0.01	0.31	21.69	nd
Na2O	nd	nd	1.55	nd		nd	nd	1.64	nd
K2O	nd	nd	nd	nd		nd	nd	nd	nd
NiO	na	na	na	na		na	na	na	na
Total	98.65	98.52	100.1	97.01		98.22	98.35	98.74	96.00
mg#	0.907	0.912	0.937	0.708		0.908	0.915	0.939	0.750

	m23					m24			
	Olivine	OPX	splz CPX	Spinel		Olivine	OPX	splz CPX	Spinel
SiO2	41.00	55.42	52.12	0.02		41.58	56.51	53.45	0.04
TiO2	nd	nd	0.07	nd		nd	0.07	0.32	0.10
Al2O3	nd	2.91	3.82	53.50		nd	2.55	3.93	51.59
Cr2O3	nd	0.31	0.73	13.07		nd	0.27	0.73	15.58
FeO*	9.04	5.89	1.77	11.56		8.83	5.88	1.72	11.85
MnO	0.12	0.14	0.07	nd		0.11	0.15	0.10	nd
MgO	49.48	33.94	15.41	18.59		50.38	34.47	15.45	18.73
CaO	0.01	0.28	22.43	nd		0.01	0.24	22.37	0.07
Na2O	nd	nd	1.06	nd		nd	0.03	1.52	nd
K2O	nd	nd	nd	nd		nd	nd	nd	nd
NiO	0.40	0.08	0.04	0.26		0.39	0.07	0.05	0.28
Total	100.06	99.00	97.52	97.02		101.31	100.24	99.64	98.25
mg#	0.907	0.911	0.939	0.741		0.910	0.913	0.941	0.738

	m32					m33			
	Olivine	OPX	splz CPX	Spinel		Olivine	OPX	splz CPX	Spinel
SiO2	41.10	56.22	53.78	0.02		41.1	56.28	53.82	0.01
TiO2	nd	0.06	0.42	0.07		nd	0.03	0.13	0.03
Al2O3	nd	3.88	5.37	56.63		nd	2.42	3.26	51.77
Cr2O3	nd	0.26	0.62	10.58		nd	0.25	0.61	16.27
FeO*	9.61	6.29	2.11	12.02		8.84	5.73	1.73	12.41
MnO	0.14	0.14	0.08	nd		0.14	0.12	0.07	nd
MgO	48.84	33.64	15.11	19.33		49.81	34.23	15.81	18.48
CaO	0.01	0.10	21.34	nd		nd	0.22	23.36	nd
Na2O	nd	nd	2.73	nd		nd	nd	1.22	nd
K2O	nd	nd	nd	nd		nd	nd	nd	nd
NiO	0.40	nd	nd	0.35		0.40	0.06	0.04	0.27
Total	100.12	100.59	101.56	99.02		100.29	99.36	100.05	99.24
mg#	0.901	0.905	0.927	0.741		0.909	0.914	0.942	0.726

	m46					m47			
	Olivine	OPX	splz CPX	Spinel		Olivine	OPX	splz CPX	Spinel
SiO2	40.36	54.98	52.38	0.07		41.26	56.17	53.66	0.02
TiO2	nd	0.04	0.33	0.14		nd	0.07	0.31	0.05
Al2O3	nd	4.07	5.97	55.27		nd	3.50	5.14	57.69
Cr2O3	0.05	0.33	0.75	9.97		0.06	0.21	0.58	9.47
FeO*	10.14	6.28	2.14	12.82		10.21	6.82	2.22	12.12
MnO	0.13	0.15	0.08	0.10		0.15	0.17	0.06	0.09
MgO	48.47	32.86	14.39	19.03		48.94	33.55	15.16	19.32
CaO	0.01	0.27	21.36	0.08		0.01	0.21	20.69	0.02
Na2O	nd	0.03	1.76	nd		nd	nd	1.70	nd
K2O	nd	nd	nd	nd		nd	nd	nd	nd
NiO	na	na	na	na		na	na	na	na
Total	99.17	99.01	99.16	97.48		100.64	100.72	99.52	98.78
mg#	0.895	0.903	0.923	0.726		0.895	0.898	0.924	0.740

	m10			m44			m50	
	Olivine	wehr CPX		Olivine	splz? CPX		Olivine	splz? CPX
SiO2	39.14	53.88		41.29	56.01		41.27	53.54
TiO2	nd	0.08		0.03	0.35		nd	0.33
Al2O3	nd	1.52		0.03	1.88		nd	4.66
Cr2O3	nd	2.43		0.07	1.22		nd	0.89
FeO*	15.66	3.91		10.14	4.05		8.88	1.98
MnO	0.13	0.02		0.12	0.13		0.12	0.10
MgO	43.64	14.57		48.72	19.53		49.85	14.86
CaO	0.09	20.19		0.08	16.30		nd	21.58
Na2O	nd	2.28		0.03	1.51		nd	1.78
K2O	nd	nd		nd	nd		nd	nd
NiO	na	na		na	na		na	na
Total	98.71	98.88		100.51	100.9		100.13	99.72
mg#	0.832	0.869		0.895	0.896		0.909	0.930

	m39			m26			m28	
	CPX	gtlz?		CPX	eclg		CPX	eclg
		Garnet			Garnet			Garnet
SiO2	55.82	41.29		53.77	39.63		53.96	39.86
TiO2	0.20	0.64		0.06	0.10		0.40	0.39
Al2O3	1.34	18.00		1.47	21.36		4.81	21.06
Cr2O3	1.11	5.92		0.21	0.58		0.05	0.09
FeO*	2.42	7.85		5.00	19.67		7.10	19.36
MnO	0.05	0.35		0.07	0.46		0.07	0.41
MgO	17.48	17.31		15.21	12.25		12.28	11.78
CaO	21.59	8.81		21.36	4.86		16.87	6.08
Na2O	0.94	nd		1.22	nd		3.36	0.09
K2O	nd	nd		nd	nd		nd	nd
NiO	0.03	0.01		na	na		na	na
Total	100.9	100.19		98.37	98.91		98.90	99.12
mg#	0.928	0.797		0.844	0.526		0.755	0.520

	m29			m51	
	CPX	eclg		CPX	eclg
		Garnet			Garnet
SiO2	50.78	40.56		55.11	40.01
TiO2	0.37	0.08		0.17	0.06
Al2O3	4.28	22.15		8.92	21.24
Cr2O3	0.12	0.10		0.10	0.07
FeO*	6.64	18.22		3.52	17.72
MnO	0.11	0.22		0.02	0.26
MgO	13.96	11.18		10.08	11.36
CaO	22.72	8.14		15.63	7.83
Na2O	0.85	0.02		5.31	0.04
K2O	nd	nd		nd	nd
NiO	na	na		0.04	0.01
Total	99.83	100.67		98.90	98.60
mg#	0.789	0.522		0.836	0.533

FeO*: Total iron as FeO

TABLE 4-2
Selected Mineral Compositions Sensitive to Melt Depletion

Sample No.	olivineFo	cpx wt%TiO2	opx wt%Al2O3	opx (Cr#)	sp (Cr#)	gt (Cr#)
Gt. Lherz.						
bl4f	92.42	0.18	0.47	37.3	na	13.3
m7	92.31	0.09	0.57	36.0	na	25.0
m34	92.17	0.31	0.69	25.0	na	8.8
m45	92.36	0.17	1.08	25.5	na	20.1
m22	90.08	0.36	1.38	16.4	na	3.6
m35	90.81	0.35	0.89	20.5	na	4.5
m48	90.83	0.40	1.06	20.9	na	4.6
Gt/Sp Lherz.						
m25	90.46	0.42	1.23	14.6	22.0	2.9
m27	90.18	0.49	1.52	14.6	19.2	3.4
m31	90.75	0.40	0.83	11.7	18.3	2.6
m49	90.55	0.34	1.01	17.2	29.1	3.0
Gt. Webst.						
m42	na	1.52	7.35	8.4	na	8.5
m43	na	2.46	2.58	4.8	na	8.5
Hi-Cr Sphz.						
m4	92.00	0.02	0.89	23.9	71.6	na
m12	92.82	na	0.56	34.8	79.0	na
m36	92.37	na	0.47	44.0	68.8	na
Mid-Cr Splz.						
m6	91.44	0.01	2.06	17.9	46.5	na
m30	92.33	0.16	2.04	18.1	37.6	na
m37	91.48	0.03	1.37	23.6	57.5	na
m41	93.52	0.09	1.70	19.4	56.3	na
Low-Cr Splz.						
m9	91.15	0.07	2.14	11.6	25.3	na
m17	90.64	0.09	2.59	10.0	20.6	na
m20	90.74	0.16	3.55	13.2	21.2	na
m21	90.84	0.48	3.33	9.0	15.9	na
m23	90.70	0.07	2.91	9.6	14.1	na
m24	91.05	0.32	2.55	9.5	16.8	na
m32	90.06	0.42	3.88	6.3	11.1	na
m33	90.94	0.13	2.42	9.4	17.4	na
m46	89.49	0.33	4.07	7.5	10.8	na
m47	89.52	0.31	3.50	5.7	9.9	na

TABLE 4-3
Calculated Pressure and Temperature for Garnet-Bearing Xenoliths

Sample	Gpa	(°C)	Gpa	(°C)	Gpa	(°C)	Gpa	(°C)
Gt. Lhz.	PBKN	TBKN	PBKN	TBKopx	PBKN	TKrogh	PNimis	TNimis
bl4f	4.6	977	4.5	967	4.7	993	5.0	899
m7	3.9	930	3.8	907	4.5	1053	6.0	867
m34	3.1	767	3.3	798	3.3	800	2.8	686
m45	3.6	936	2.6	864	2.8	908	5.3	968
m22	2.1	757	2.2	782	2.2	767	2.4	668
m35	2.6	759	2.9	810	2.6	755	2.8	660
m48	3.2	869	2.7	790	2.5	755	2.5	769
Gt/Sp								
Lhz.								
m25	2.5	784	2.7	824	2.3	743	0.9	672
m27	2.2	805	2.0	755	2.0	759	1.2	711
m31	1.9	585	2.8	752	3.0	791	1.9	496
m49	3.1	835	3.1	845	3.4	896	2.5	749
Gt.								
Web.								
m42	1.5	1186	1.8	1253	2.3	1262	1.4	1124
m43	2.2	1045	1.7	929	1.4	1135	0.3	861

TABLE 4-4
Calculated Temperature for Spinel Peridotites at Assumed Pressures

Sample	(°C) TBKN	(°C) TBKopx	(°C) TNimis	(°C) TWells	(°C) TWES	(°C) TSeitz	(°C) TBallhaus
Hi-Cr @ 3.5 Gpa							
m4	845	749	856	884	776	1076	949
m12	na	na	na	na	na	na	991
m36	na	na	na	na	na	na	1091
Mid-Cr @ 2.5 Gpa							
m6	862	832	878	911	889	1554	779
m30	734	796	690	800	853	885	766
m37	777	858	756	841	847	1271	858
m41	889	741	811	883	889	810	na
Lo-Cr @ 1.5 Gpa							
m9	588	780	573	723	832	911	731
m17	740	783	732	829	851	1131	705
m20	562	799	510	688	991	1010	731
m21	700	810	634	774	898	935	814
m23	674	792	639	772	877	933	720
m24	616	765	565	722	841	874	748
m32	380	642	311	546	892	945	760
m33	432	752	398	610	832	927	713
m46	752	786	681	803	933	962	790
m47	909	744	853	914	859	865	749

TABLE 4-5

Eclogite Temperature and Depletion Criteria

Sample #	T Krogh (°C)	T Krogh (°C)	Atomic	cpx	cpx
Eclogite	@1.5 GPa	@3.0 GPa	gt (Cr/Cr+Al)	wt%TiO₂	wt%Na₂O
m26	624	672	1.79	0.06	1.22
m28	867	925	0.29	0.40	3.36
m29	666	710	0.30	0.37	0.85
m51	821	873	0.22	0.17	5.31

T Krogh (Krogh, 1988)

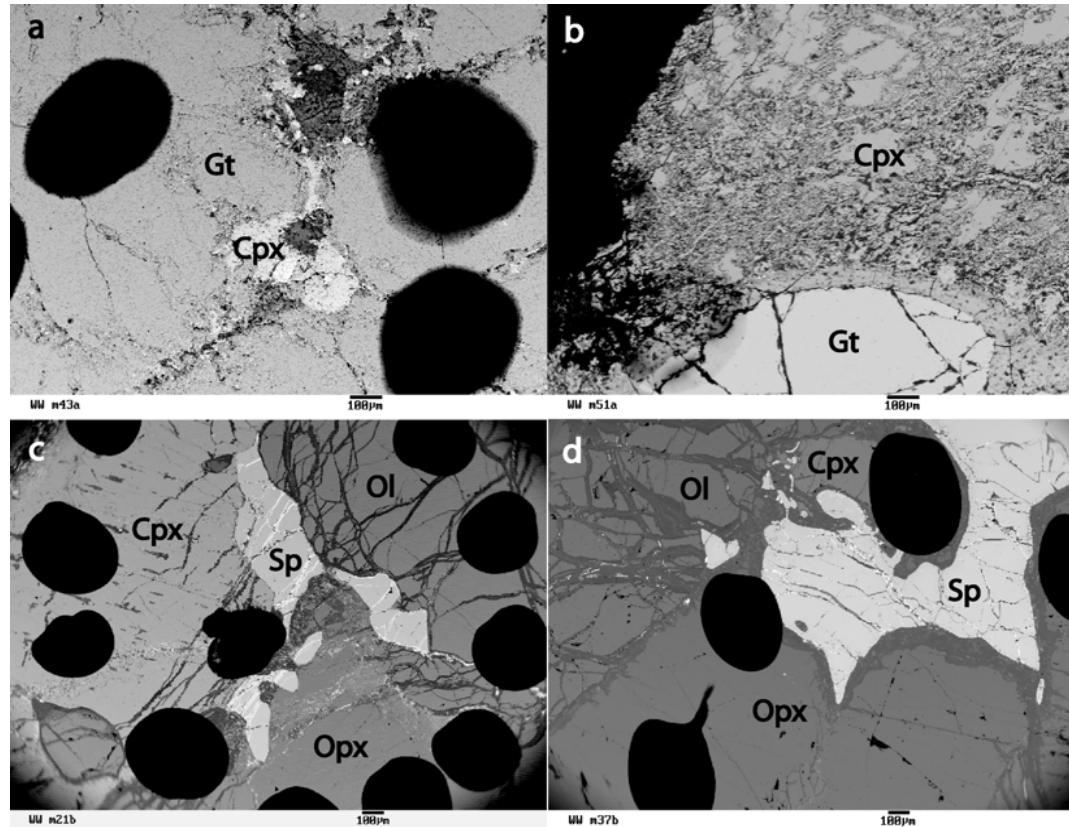


Figure 4-1: Selected backscatter electron images of xenoliths: a) garnet websterite (m43) showing pyroxene inclusions, b) eclogite (m51) showing garnet with kelyphite rim, c) low-Cr spinel lherzolite (m23) with grain boundary growth of spinel and d) mid-Cr spinel lherzolite (m37) with minor grain boundary growth of spinel. Dark circles are ink spots for navigation purposes.

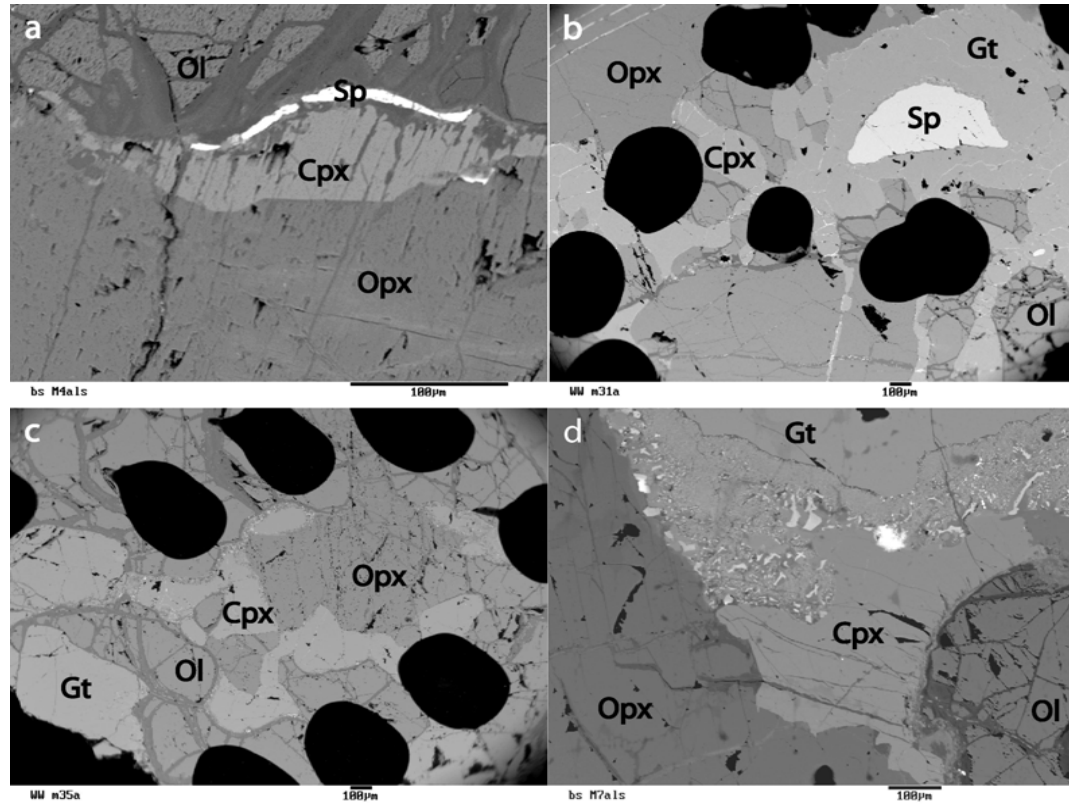


Figure 4-2: Selected backscatter electron images of xenoliths: a) high-Cr spinel peridotite (m4), b) garnet/spinel lherzolite (m31) showing garnet (no kelyphite) overgrowth of spinel c) low-Cr garnet lherzolite (m35) without kelyphite rim and d) high-Cr garnet lherzolite (m7) with kelyphite rim. Dark circles are ink spots for navigation purposes.

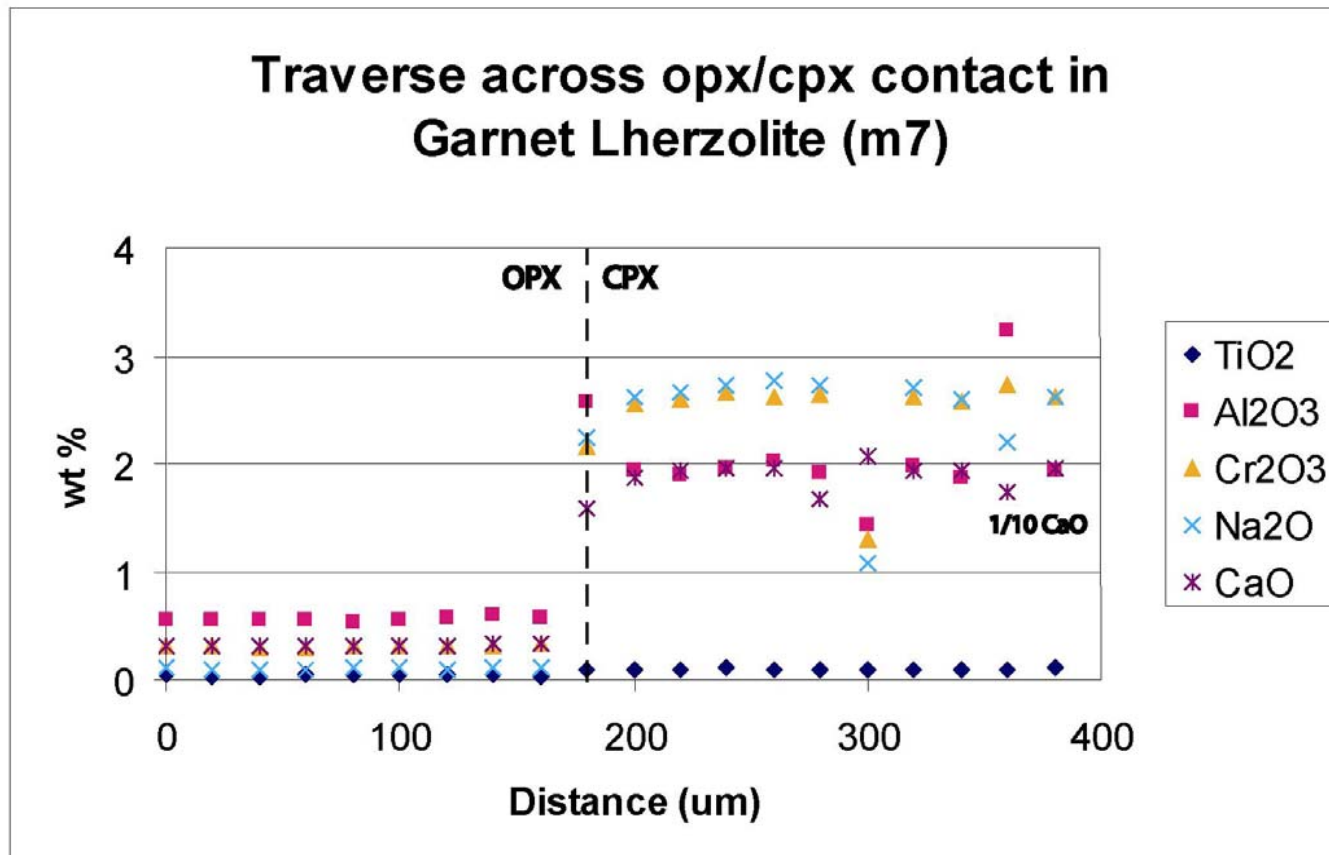


Figure 4-3a: Compositional zoning in a high-Cr garnet lherzolite. Pyroxenes appear homogeneous excluding grain boundary interferences in a traverse across an orthopyroxene/clinopyroxene grain contact.

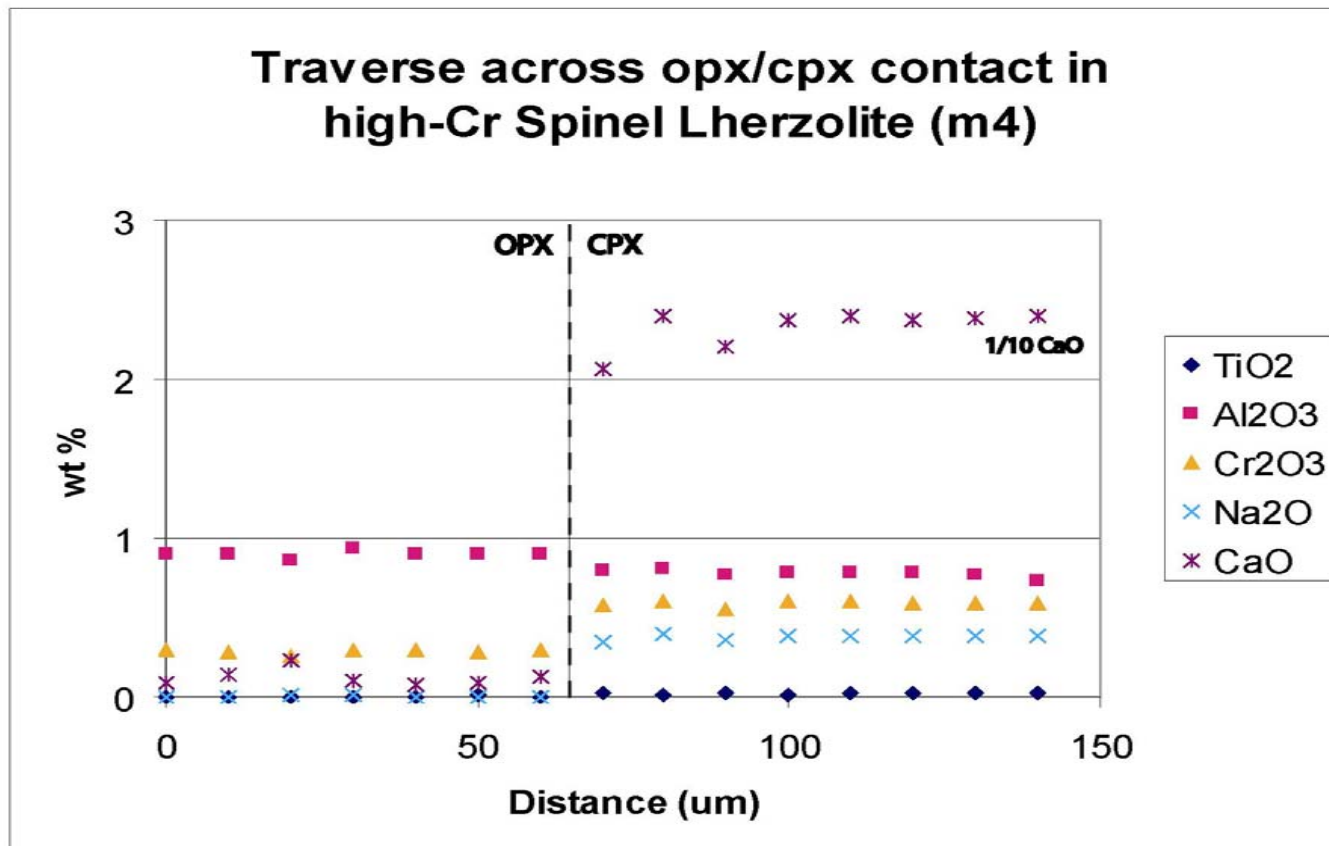


Figure 4-3b: Compositional zoning in a high-Cr spinel lherzolite. The orthopyroxene is homogeneous, whereas the clinopyroxene has a slight rim-depletion in CaO in a traverse across an opx/cpx grain contact.

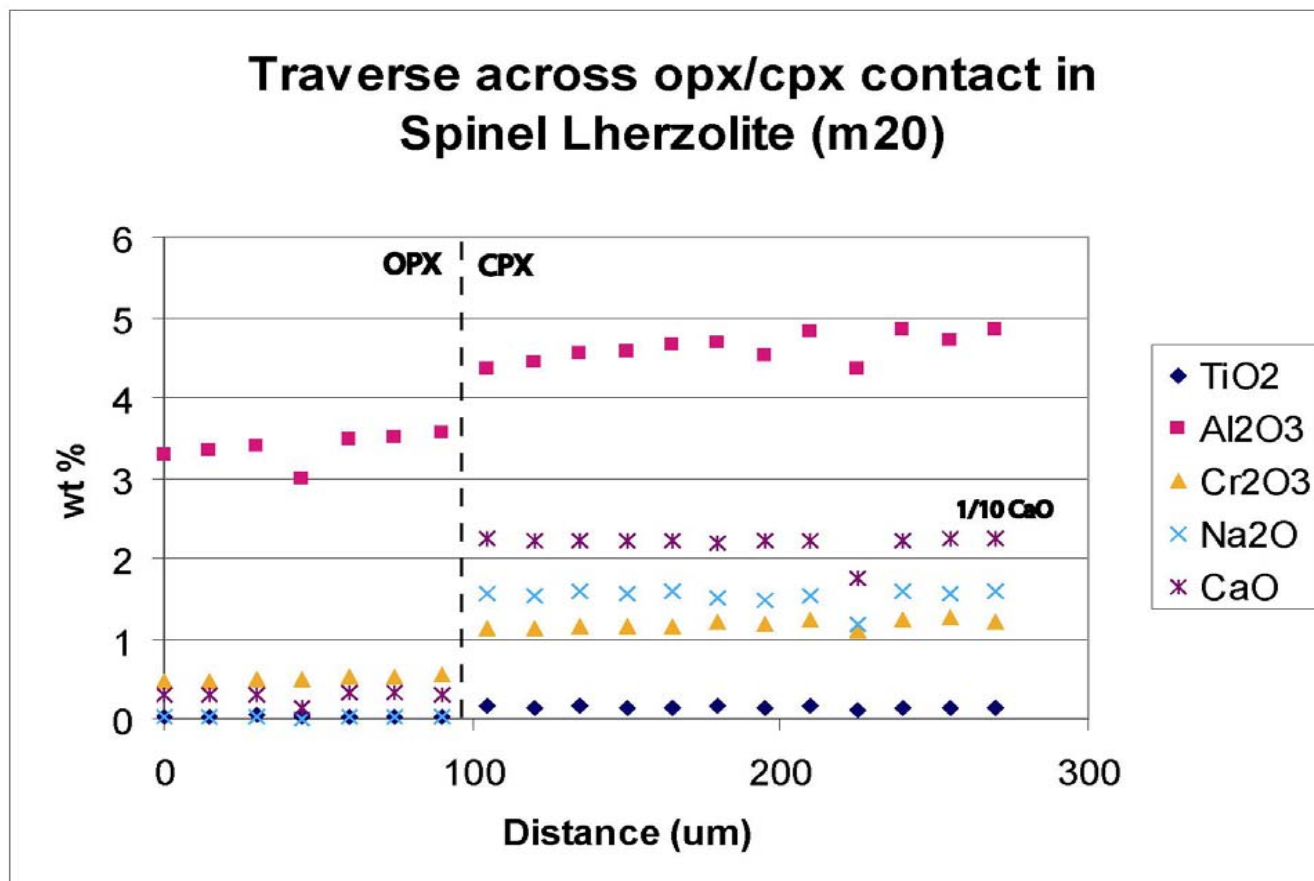


Figure 4-4a: Compositional zoning in a low-Cr spinel lherzolite. The orthopyroxene shows a rim-enrichment, whereas the clinopyroxene shows a rim-depletion in Al₂O₃ in a traverse across an opx/cpx grain contact.

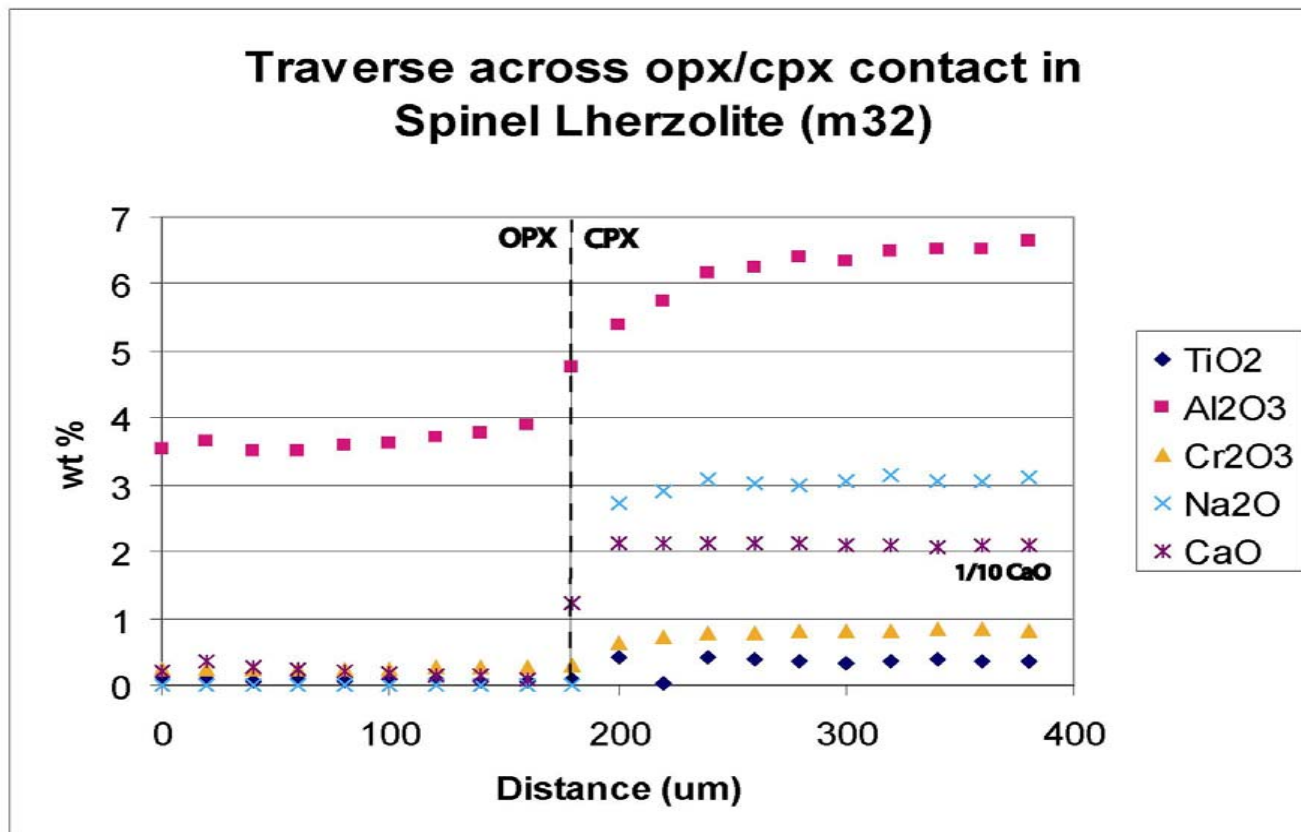


Figure 4-4b: Compositional zoning in a low-Cr spinel lherzolite. The orthopyroxene shows a progressive rim-enrichment in Al_2O_3 . The clinopyroxene shows a progressive rim-depletion in Al_2O_3 , Cr_2O_3 and Na_2O in a traverse across an orthopyroxene/clinopyroxene grain contact.

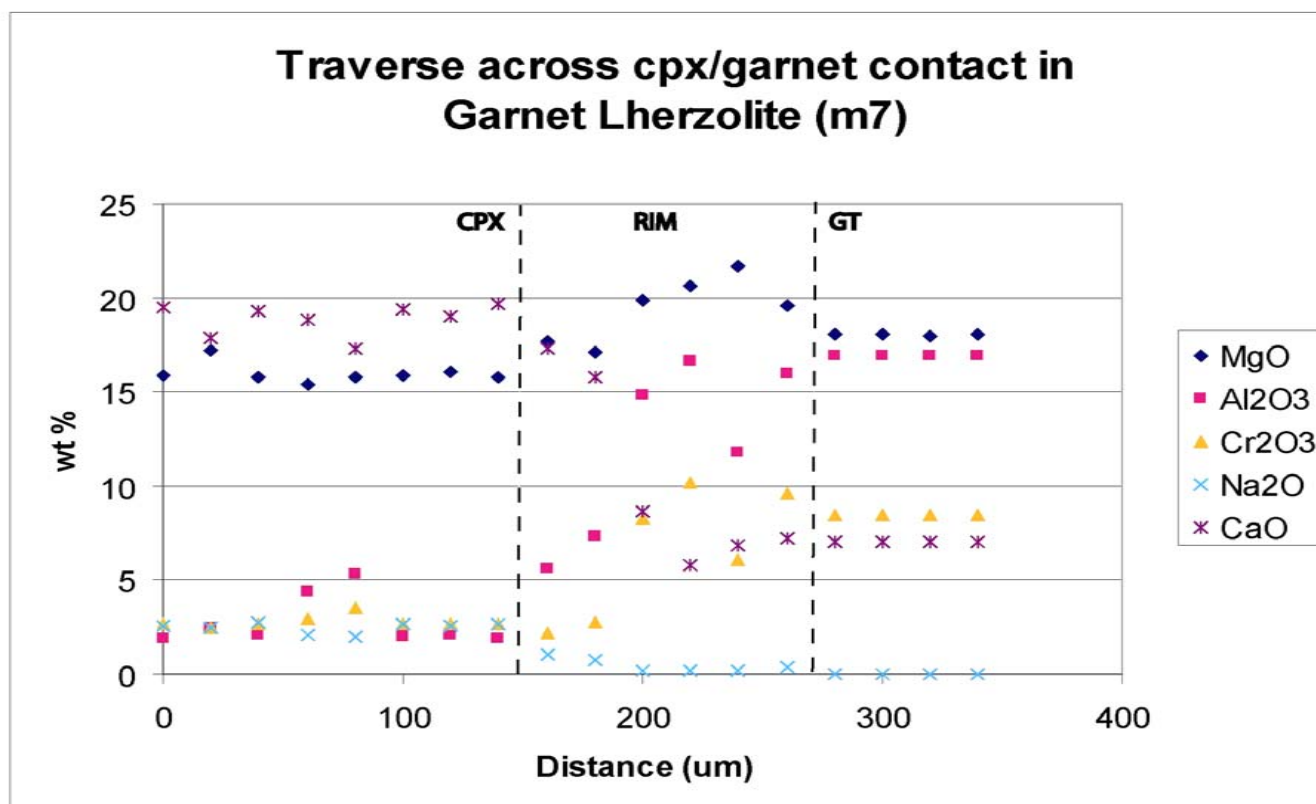


Figure 4-5a: Compositional zoning in a high-Cr garnet lherzolite. Both the clinopyroxene and the garnet show relative homogeneity near the grain boundary with the kelyphite rim (middle) which is variable in composition in a traverse across a clinopyroxene/garnet grain contact.

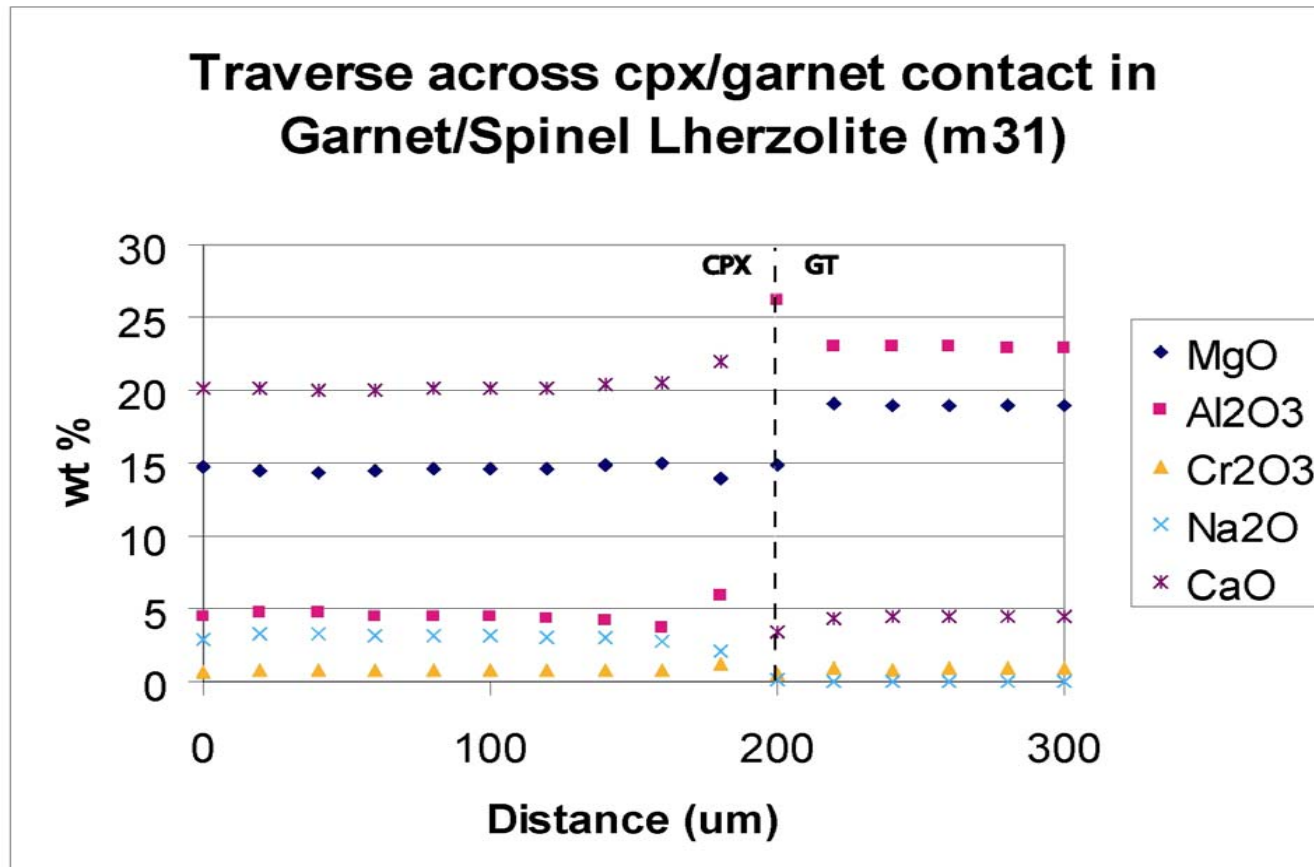


Figure 4-5b: Compositional zoning in a low-Cr garnet/spinel lherzolite. The clinopyroxene shows a rim-enrichment of CaO and Al₂O₃ and a rim-depletion in MgO and Na₂O in a traverse across a clinopyroxene/garnet grain contact.

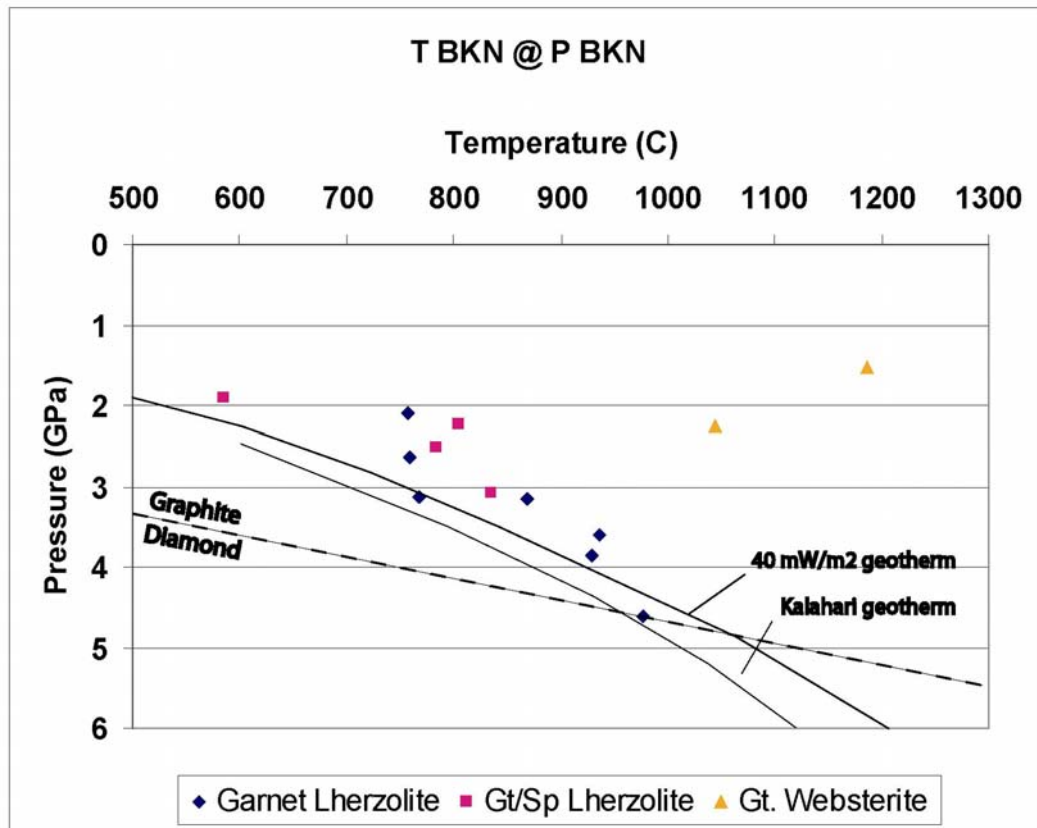


Figure 4-6a: P-T xenolith array utilizing T BKN @ P BKN. The 40mW/m² geotherm of Pollock and Chapman (1977) and the Kalahari geotherm of Rudnick and Nyblade (1999) are shown for comparison. Graphite-diamond equilibrium is according to Kennedy and Kennedy (1976). Note that all but the deepest xenoliths plot above the 40 mW/m² geotherm.

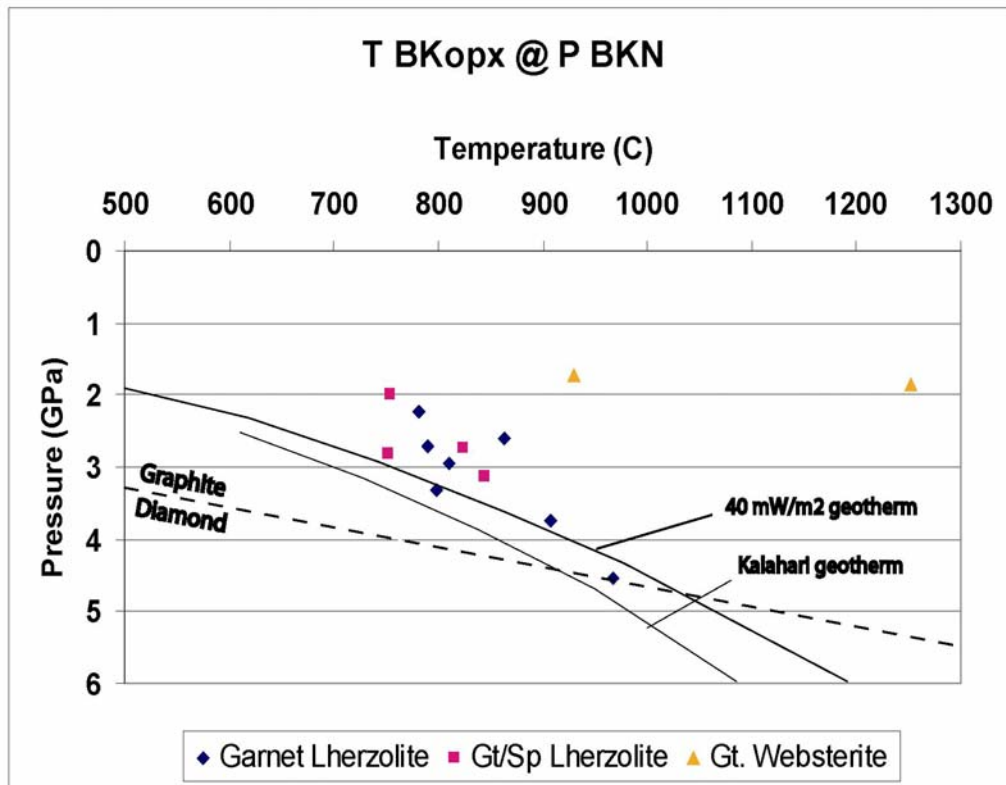


Figure 4-6b: P-T xenoliths array utilizing T BKopx @ P BKN. Note that the shallow xenoliths plot above whereas the deep xenoliths plot at or below the 40 mW/m² geotherm.

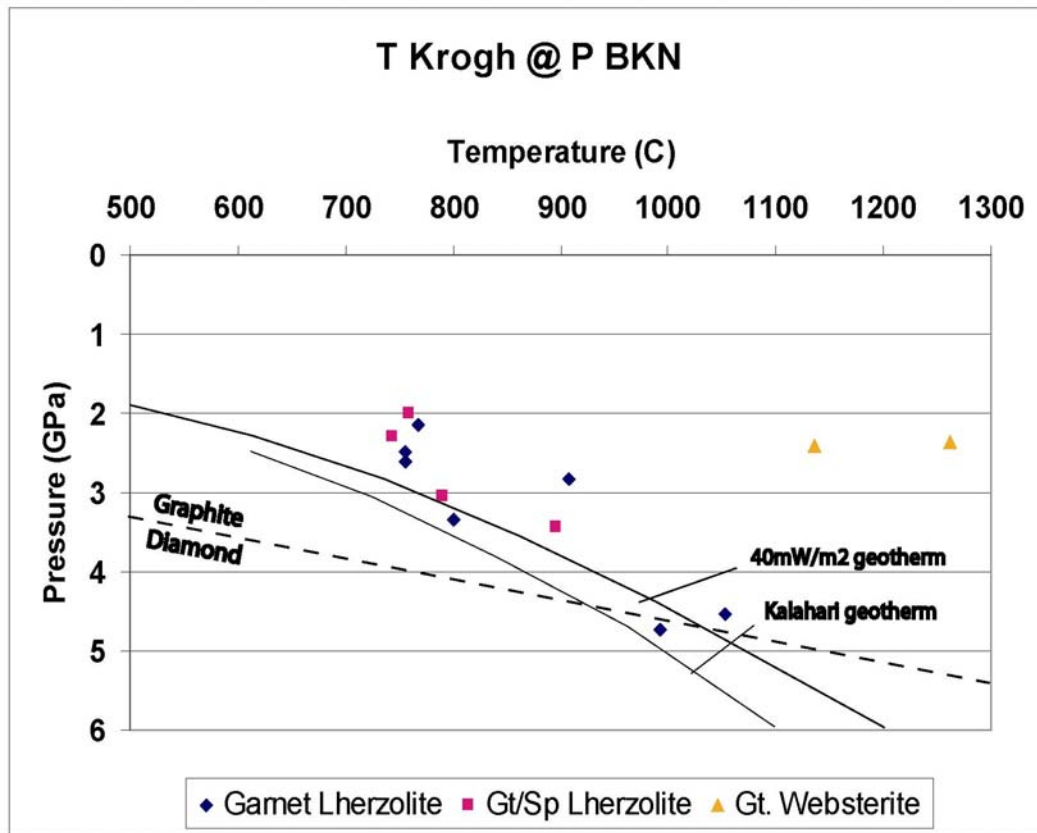


Figure 4-6c: P-T xenolith array utilizing T Krogh @ P BKN. Note that the shallow xenoliths plot above whereas the deep xenoliths plot at or below the 40 mW/m² geotherm.

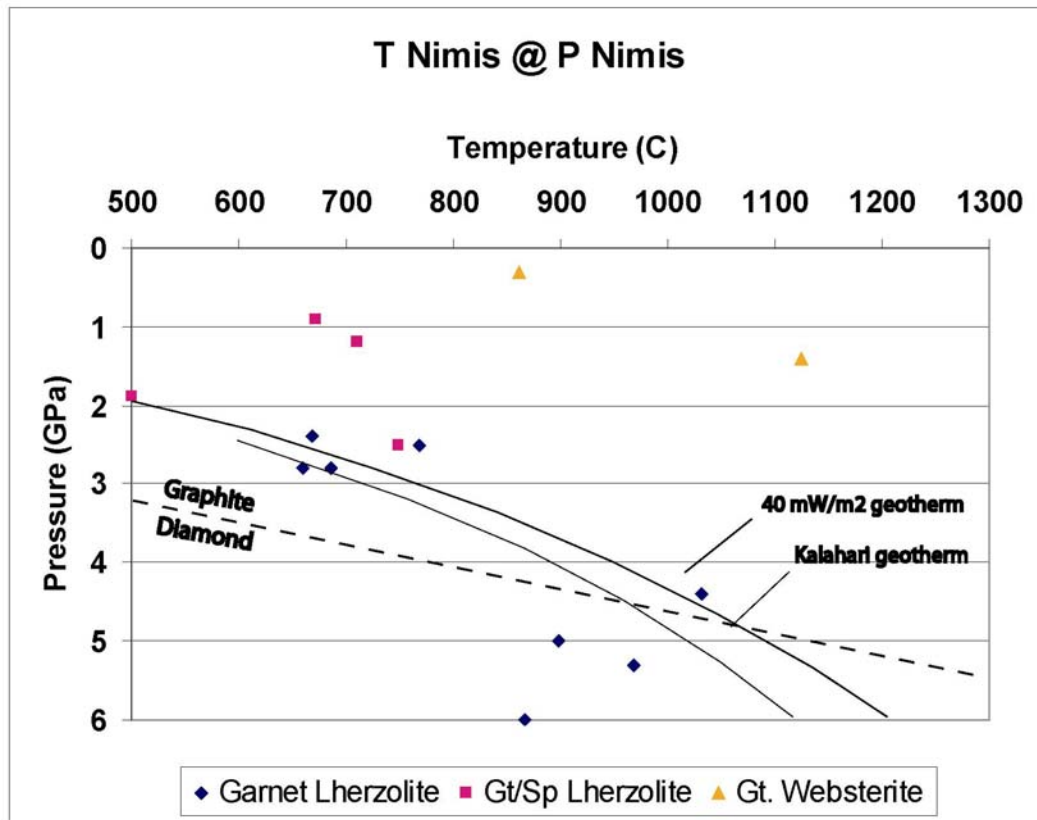


Figure 4-6d: P-T xenolith array utilizing T Nimis @ P Nimis. Note that the shallow xenoliths plot above whereas the deep xenoliths plot at or below the 40 mW/m² geotherm.

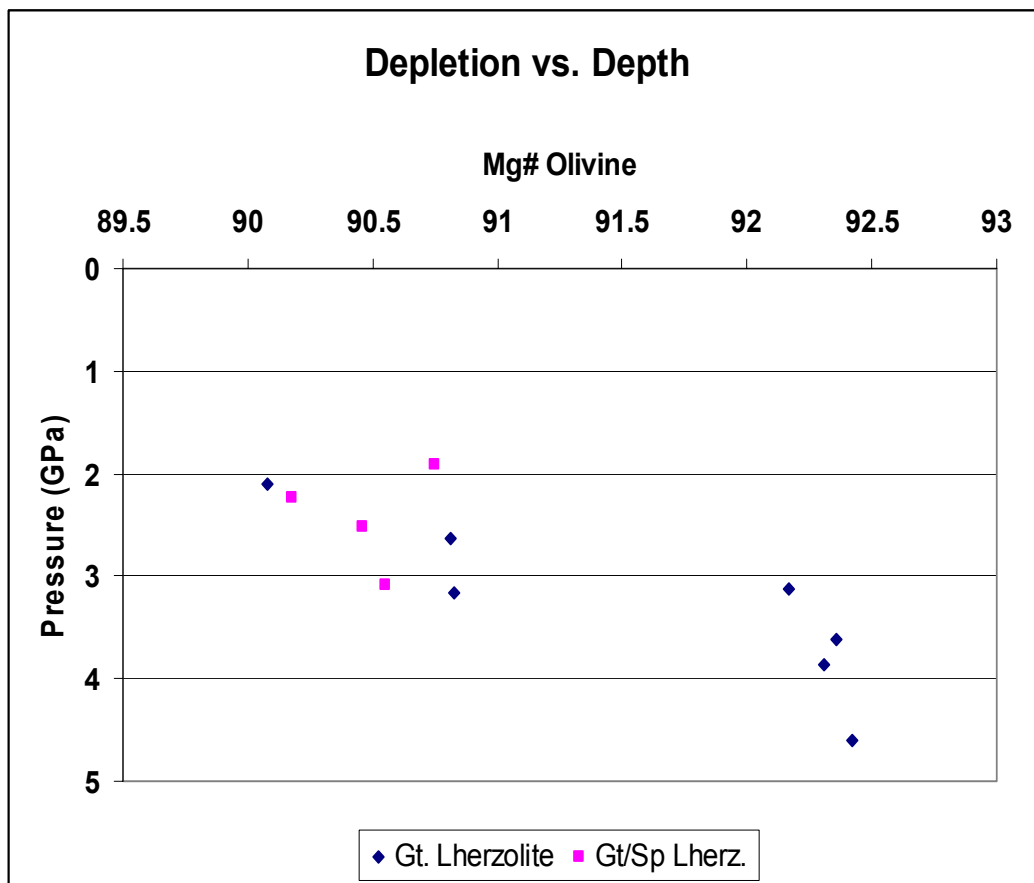


Figure 4-7: Comparison of forsterite content in olivine and pressure. Estimated pressure determined using the T BKN @ P BKN thermobarometer. Note the gap in olivine Mg# between shallow (<3 GPa) and deep (>3 GPa) xenoliths.

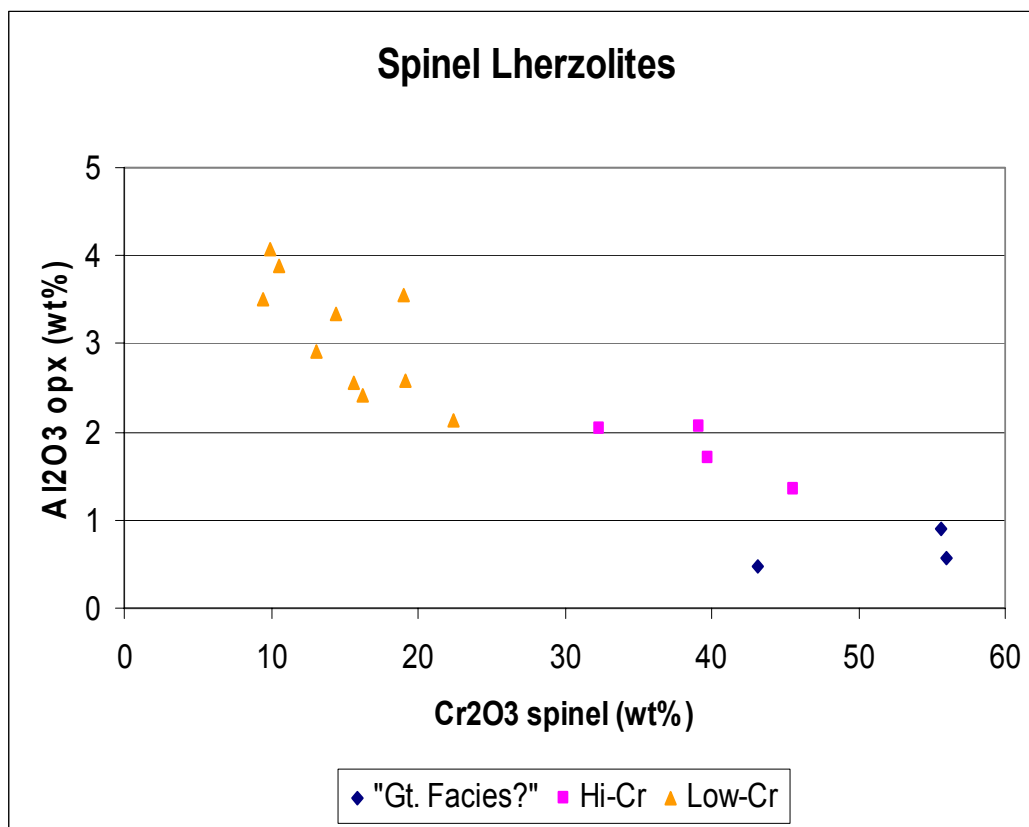


Figure 4-8: Comparison of Cr₂O₃ in spinel and Al₂O₃ in orthopyroxene. Note the rapid increase in Cr₂O₃ of spinel when orthopyroxene falls below ~2 wt % Al₂O₃. Boyd and others (1999) argue that spinel peridotites with less than 1% Al₂O₃ in opx have equilibrated at pressures greater than the garnet/spinel transition.

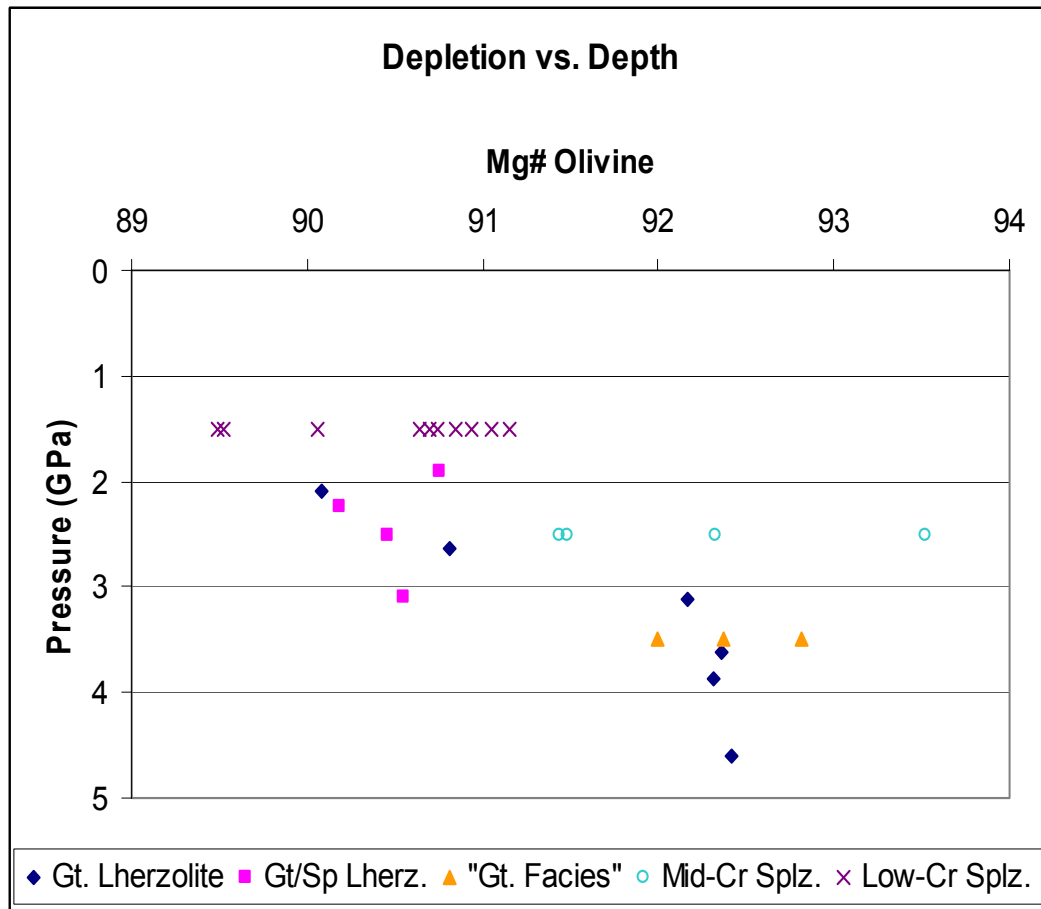


Figure 4-9: Comparison of forsterite content of olivine and pressure (PBKN). Includes the addition of low-Cr spinel lherzolites @ 1.5 GPa, mid-Cr spinel lherzolites @ 2.5 GPa and all high-Cr spinel peridotites @ 3.5 GPa. Note the correlation of increasing Mg-number in olivine with increasing pressure.

Idealized Mantle Petrology

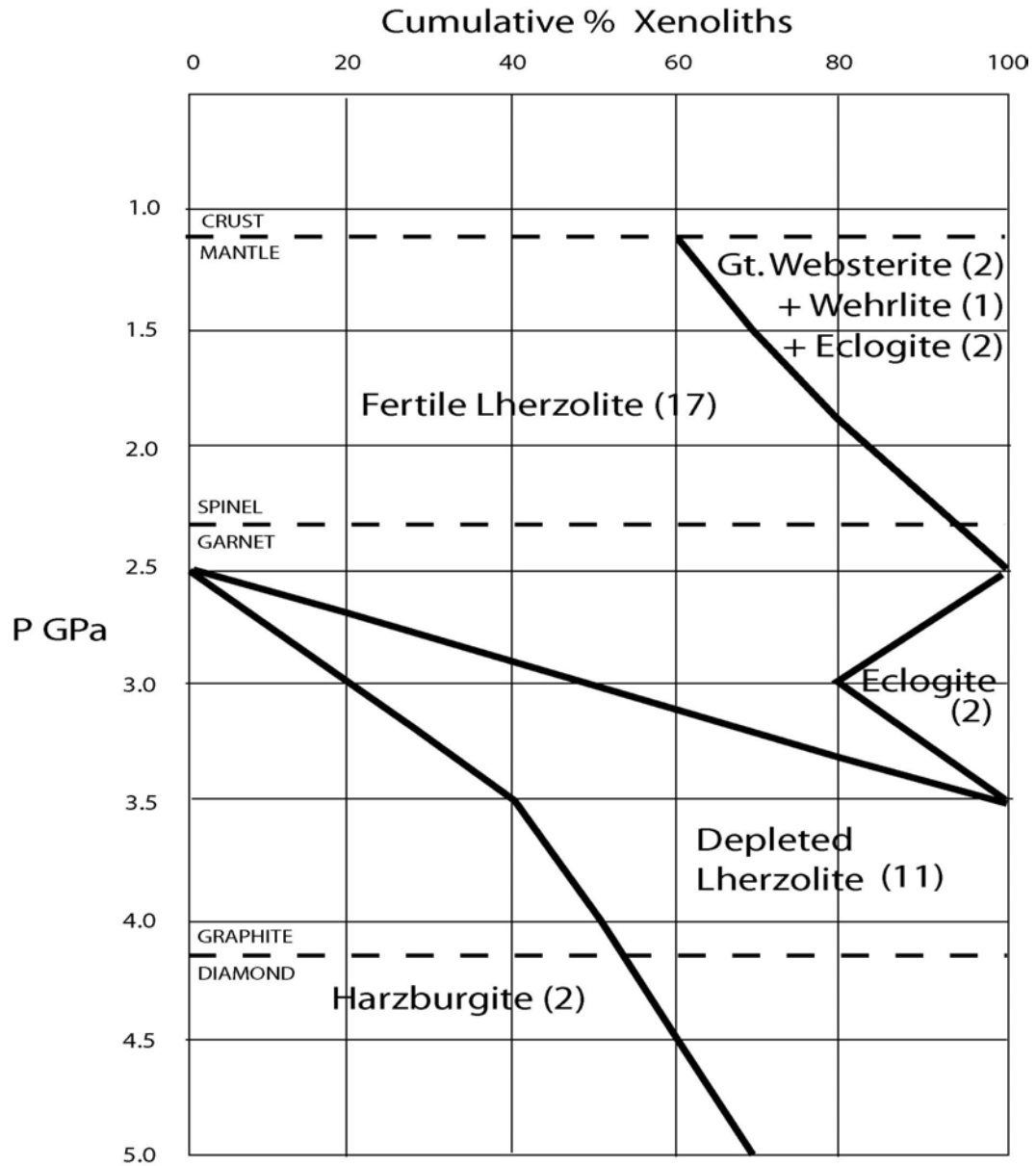


Figure 4-10: Idealized section of sub-continental mantle lithosphere. Section is located beneath the Prairie Creek lamproite province. Number of xenolith type shown in parenthesis.

Chapter 5

CRUSTAL XENOLITHS

XENOLITH PETROLOGY

The crustal xenoliths (1-3 cm in size) were recovered as heavy media concentrates with a density cut-off of $\sim 2.82 \text{ g/cm}^3$. Therefore, the recovery process may result in a sampling bias favoring higher density rock types. Crustal xenoliths were initially sorted by major compositional rock groups. Representative xenoliths of each major compositional group were selected for thin section analysis based on their relative abundance and lack of visible alteration. Crustal xenoliths were divided into shallow near-surface lithologies, which include sedimentary rocks, and deeper lithologies, which include amphibolite, granite, rhyolite, epidote-rich rocks and pelitic metamorphic rocks. Selected polished thin sections representing major compositional groups were analyzed on the JEOL Superprobe 733 at The University of Texas at Austin. Accelerating voltage was maintained at 15keV with a cup current of $\sim 30 \text{ na}$. Nine elements were analyzed on the four crystals. Energy dispersive spectrometry (EDS) was used to confirm the mineral assemblages present and backscattered electron images (BSE) were generated for selected thin sections.

Near-Surface Lithologies

Approximately half of the crustal xenoliths are composed of near surface lithologies which include conglomerate, sandstone, chert and quartzite. The conglomerate consists of coarse sand and gravel which is cemented by iron-oxide rich cement. This rock is similar in appearance to some of the basal conglomerates found in the proximal Cretaceous-age sedimentary rocks into which the host lamproites were intruded. The sandstone, quartzite, and chert are extremely durable and frequently have an abundance of opaque heavy minerals or iron oxide staining. These rock types are similar in appearance to Paleozoic age Ouachita-facies sedimentary rocks which are known to exist in the area at depths greater than ~100 meters (Dunn and Taylor, 2001). There is no visible thermal alteration of these shallow crustal xenoliths, and they are probably derived from documented local lithologies (Miser and Purdue, 1929). Two anomalous pink oolitic dolomite xenoliths with pellets and intraclasts were found that had a density of $\sim 2.77 \text{ g/cm}^3$. These xenoliths are similar to Cambro-Ordovician platform carbonate rocks found throughout the southern mid-continent region (Hardie, 1989).

Amphibolite

The deep crustal xenoliths are about 50% amphibolite consisting of dominant amphibole and lesser amounts of plagioclase. Color ranges from very dark green to a moderate shade of gray. Grain size tends to be fine to medium-grained (~1 mm) although some coarse-grained (~5 mm) varieties have been observed. Weak alignment of mafic minerals indicates a slight foliation is present in the amphibolite (Figures 5-1a). The

density of the amphibolite ranged from 3.01 to 3.16 g/cm³ with an average value of ~3.08 g/cm³.

Amphibole (~50%) in thin section is prismatic and pleochroic from pale olive to dark green in color. The plagioclase (~30%) is equant, anhedral and weakly altered to clay minerals. Albite twinning of the plagioclase is apparent. Accessory minerals range in quantity and type and include biotite, chlorite, microcline, quartz, titanite, ilmenite and apatite. The biotite is subhedral and pleochroic light- to dark brown. The chlorite tends to be an alteration of biotite and amphibole and is blue-green in thin section. The microcline occurs as equant grains generally altered to clay minerals. Some remnant tartan-plaid twinning is observed. The quartz is fresh, equant, anhedral and appears as interstitial grains.

Minerals in representative amphibolites (c1 and c10) were analyzed and the compositions of selected minerals are listed in Table 5-1. The amphiboles generally have between 0.5 and 1.1 wt % K₂O and would be classified as magnesio- and ferro hornblende. Observed plagioclase composition ranges from oligoclase (An₃₁Ab₆₉) through bytownite (An₈₆Ab₁₄). Such calcium-rich plagioclase is uncommon in amphibolites and may indicate some type of calcium enrichment and/or alteration.

Granitic and Rhyolitic Rocks

Felsic composition xenoliths consisting of granitic and rhyolitic rocks are relatively rare making up only ~5% of the deep crustal xenoliths. The coarse-grained (5-10 mm) granites are usually light pink in color and consist of quartz and microcline with lesser amounts of plagioclase, and muscovite (Figure 5-1b). Many of the granitic

xenoliths are iron-stained and have visible hematite and/or magnetite. The quartz is gray, microcline is pink, and the plagioclase is white in color. No foliation is evident within the granite xenoliths. The rhyolite xenoliths are fine-grained (<1mm) and commonly dark pink in color. Alkali feldspar and quartz are the dominant minerals present. The average density of both the granite and rhyolite xenoliths is a surprisingly high $\sim 2.90 \text{ g/cm}^3$. This high density is attributed to the abundance of iron oxides and epidote alteration which may make them more susceptible to concentration within the xenolith recovery process.

When viewed in thin section, the granite has anhedral quartz commonly with undulose extinction. The microcline is equant, subhedral, and has some evident tartan-plaid twinning. The plagioclase is equant with some albite twinning. The Na-rich plagioclase is albite composition. Both feldspars are weakly altered to clay minerals. Both muscovite and biotite are subhedral and the biotite is pleochroic brown-to dark brown. Magnetite and specular hematite are common as iron oxide minerals. The rhyolite consists predominantly of altered potassium feldspar, prismatic epidote and quartz with accessory magnetite, biotite and calcite. Representative mineral compositions of a granite xenolith (c25) are listed in Table 5-1.

Epidote-rich Rocks

Approximately 40% of the recovered deep crustal xenoliths are classified as epidote-rich rocks. Most of the samples are light green, commonly with some pink overtones. Grain size tends to be fine- to medium-grained (1-2 mm) although coarser ($\sim 10 \text{ mm}$) varieties are present. Foliation within the epidote-rich xenoliths is rare except

where epidote growth is concentrated along compositional layering. Densities of epidote-rich rocks are variable depending on the amount of epidote present, but typically range from 3.1 to 3.2 g/cm³.

Most of the granitic xenoliths show evidence of epidote growth. A particularly attractive version of altered granite (c22) is a pink and green rock known as unakite (Figure 5-1c). In thin section, this rock consists of slightly altered equant, microcline with tartan-plaid twinning and subhedral pale green epidote. The clinozoisite appears to be associated with alteration of mafic minerals including amphiboles, biotite and iron oxides. Accessory minerals observed within the unakite include: equant quartz, sub-rounded equant titanite, and hematite which appears to have grain-boundary growth. A similar alteration process of rhyolitic xenoliths has been observed. Some of the felsic xenoliths, especially in the fine-grained varieties, have been so completely replaced by epidote that they could be termed epidotites.

Epidote alteration of the amphibolite is less common but observed. Initial epidote growth seems to occur at the expense of plagioclase leaving a rock consisting mainly of amphibole and epidote (Figure 5-1d). The epidote appears to be produced from an alteration of plagioclase within the rock (c17 and c18). Common accessory minerals include quartz, garnet and hematite. Continued epidotization of an amphibolite protolith appears to result in alteration of the hornblende to a Ca-poor amphibole (c18). Extreme alteration of amphibolite (c23 and c24) may result in a dark colored epidote-rich rock with both zoisite and clinozoisite and lacking amphibole (Figure 5-1e). Common accessory minerals in these highly altered epidote-rich rocks include quartz, biotite, muscovite, chlorite and garnet.

Minerals in representative epidote-rich xenoliths were analyzed and compositions of selected minerals are listed in Table 5-1. Relatively unaltered xenoliths have Ca-rich amphiboles such as hornblende. Increasing epidote alteration appears to result in the conversion of hornblende to monoclinic amphiboles such as grunerite (c23) and finally to the complete elimination of amphiboles from the amphibolite protolith. Epidote alteration of plagioclase-rich amphibolite may result in the growth of garnet. Garnet observed within an epidote-rich xenolith (c18) contains ~65% grossular and ~30% almandine component. A different xenolith contains Mn-rich garnet ~71% grossular, ~12% almandine and ~17% spessartine component (c17).

Pelitic Metamorphic Rocks

Relatively rare (~5%) dark colored xenoliths consist almost exclusively of coarse-grained (~7 mm) micas (Figure 5-1f). These xenoliths show foliation as a weak alignment of the micas (c20 and c21). The density of the micaceous xenoliths averages ~3.10 g/cm³. These micaceous xenoliths consist of ~65% biotite which is elongated, subhedral, and pleochroic in light to dark brown color in thin-section. The muscovite (~20%) is subhedral elongate crystals. Accessory minerals include anhedral interstitial quartz, sub-rounded equant apatite, and equant, opaque ilmenite. Representative mineral compositions in a micaceous xenolith (c20) are listed in Table 5-1. The ilmenite associated with this rock is exceptionally rich in manganese (~16 wt % MnO).

K-AR DATING

Amphibolites were selected for K-Ar isotopic age dating of the hornblende based on their unaltered appearance. Separation of the hornblende was completed by initial crushing of the xenolith and both mechanical (magnetic separation) and visual (microscope) separation to help ensure purity of the sample. One large amphibolite xenolith was supplied to Steve Bergman of the Arco Oil and Gas Research Facility for K-Ar dating in 1990. Three hornblende separates from individual xenoliths were supplied to F. W. McDowell at The University of Texas at Austin facilities for additional K-Ar dating.

The first amphibolite xenolith submitted to Steve Bergman (Tom Bills, Geochron Labs, analyst) for analysis yielded an isotopic age of 1431 \pm 37 Ma. The three isotopic age dates completed at the University of Texas yielded ages of 1478 \pm 144 Ma, 1425 \pm 51 Ma and 1310 \pm 58 Ma with the error range indicated by one standard deviation in the data (Dunn and others, 2000). Data from all K-Ar isotopic analyses are provided in Table 5-2. The four K-Ar isotopic ages indicate an average age of approximately 1.42 Ga for the amphibolites.

DISCUSSION OF RESULTS

Petrology of the crustal xenoliths indicates that about half are near surface sedimentary lithologies and half are deeper igneous and metamorphic rock types. Study of the igneous and metamorphic xenoliths indicates that ~50% are amphibolites, ~5% are pelitic metamorphic rocks, ~5% are granitic/rhyolitic and the remaining ~40% are

epidote-rich varieties. Thin section examination indicates that the majority of the epidote-rich xenoliths were derived from alteration of granitic and rhyolitic protoliths and a lesser number were derived from amphibolite protoliths. The rarity of unaltered felsic igneous rocks is readily explained by sampling bias of the heavy-media recovery process. The densities of felsic rocks are simply too low to permit heavy media concentration unless there is an abundance of epidote or iron oxide to increase the density of the xenoliths. Petrologic observations indicate that the basement rock beneath southwestern Arkansas consists largely of two protoliths: granite/rhyolite and amphibolite.

These petrological data can be used to delineate rock types associated with a lithospheric transect model generated from gravity and seismic data in the region (Mickus and Keller, 1992). This north-south cross section originates in southwest Missouri, passes through southwestern Arkansas (Prairie Creek lamproite province), and approximates the Texas-Louisiana border before extending offshore into the Gulf of Mexico (Figure 5-2). Details of this lithospheric transect in the region of the Prairie Creek lamproite province were derived from COCORP (Consortium for Continental Reflection Profiling) and PASSCAL (Program for Array Seismic Studies of the Continental Lithosphere) data (Figure 5-3). The Prairie Creek lamproite province is located where the Gulf Coast Basin sediments onlap onto the Ouachita-facies rocks of the Ouachita Mountains.

The Mickus and Keller model indicate that the density of the lower cratonal crust is $\sim 3.07 \text{ g/cm}^3$. Density of the amphibolite averaged 3.08 g/cm^3 and is in good agreement with the modeled density of the lower cratonal crust. The modeled density of the upper cratonal crust is $\sim 2.75 \text{ g/cm}^3$. This value is comparable to those expected for the

granite/rhyolite terrane of the southern mid-continent but is lower than those rocks concentrated during the heavy media processing.

The lithospheric transect of Mickus and Keller indicates the majority of deep crustal xenoliths recovered from beneath the Prairie Creek Lamproite province should be derived from “oceanic transition crust” with a density of ~ 2.98 . This transition crust has a thickness and calculated density that could be consistent with either thickened oceanic crust or thinned cratonal crust. The thinned cratonal crust origin is favored based on petrological data showing an abundance of epidote-rich rocks derived from both granite/rhyolite and amphibolite protoliths. A combination of the 3.08 g/cm^3 lower cratonal crust (amphibolite) and the 2.90 g/cm^3 epidote-rich granitic/rhyolitic upper cratonal crust could easily yield an average density of 2.98 g/cm^3 associated with the “oceanic transition crust”. Furthermore, thinning of continental crust might result in fluid mobilization causing epidotization observed in granitic and rhyolitic rocks and the apparent retrograde metamorphism observed in the amphibolite.

A more convincing argument that this “oceanic transition crust” might actually be thinned and altered cratonal crust is provided by the K-Ar isotopic age dating of contained amphibolites. Hornblende separates from four different amphibolite xenoliths yielded K-Ar isotopic ages of $\sim 1.42 \text{ Ga}$. This isotopic age indicates the last time the amphibolite cooled through the blocking temperature of hornblende. The blocking temperature of hornblende is estimated to be $500 \pm 50^\circ\text{C}$ (Hanes, 1991). The $\sim 1.42 \text{ Ga}$ isotopic age of the amphibolite is consistent with the age of the granite/rhyolite province of mid-continental craton and is inconsistent with an expected younger age associated with development of “oceanic transition crust”.

The Mickus and Keller transect suggests the presence of mafic intrusions, with a density of $\sim 3.05 \text{ g/cm}^3$ within the deep crustal section beneath the Prairie Creek lamproite province. The relatively rare pelitic metamorphic xenoliths which consist largely of biotite, muscovite, quartz and ilmenite may be associated with metasomatism by a variety of this igneous rock. The density of the micaceous xenoliths was found to be about $\sim 3.10 \text{ g/cm}^3$ and is comparable with the modeled density of the mafic intrusions.

Approximately half of the crustal xenoliths recovered represent near surface lithologies including the Late Cretaceous sedimentary cover and the Paleozoic Ouachita facies sandstone and chert. Seismic data in southwestern Arkansas show at least 6,000 meters of layered reflectors which were confirmed by drilling to be Carbonaceous flysch (Nicholas and Waddell, 1989). The only modeled rock type not well-represented in the crustal xenoliths are the “lower sediments?” with a density of 2.69 g/cm^3 . These are believed to represent equivalent Lower Paleozoic carbonate rocks found elsewhere in the Ouachita region (Nicholas and Waddell, 1989). Two recovered dolomitized carbonate xenoliths are comparable to these Cambro-Ordovician carbonate rocks (Hardie, 1989) and are believed to be representatives of the “lower sediments?”. These rocks may be under-represented in the crustal xenoliths due to their relatively low density minimizing xenolith recovery or due to extensive epidote alteration masking their true rock association. It is concluded that there is generally good agreement between the rock associations and their densities predicted by the lithospheric transect of Mickus and Keller and observed crustal xenolith petrology.

K-Ar dating of deep crustal amphibolite indicates that they are associated with the granite-rhyolite terrane of the southern mid-continent region. Mosher (1998) has also proposed that the Grenville-Llano deformation front, separating a 1.3-1.5 Ga granite-

rhyolite terrane from the 1.0-1.2 Ga Grenville-Llano terrane to the south, continues northeast from central Texas toward the Arkansas border. This significant age boundary must jog to the south of the Prairie Creek lamproite province due to the 1.42 Ga amphibolite age. The K-Ar age data are significant because it shows no evidence of metamorphism associated with either the Grenville or Ouachita orogenies. The ~1.42 Ga isotopic age indicates that later tectonic events of the region (Grenville or Ouachita) were of insufficient thermal intensity (~500°C) to exceed the hornblende K-Ar blocking temperature in the lower crust (Hanes, 1991). The amphibolite basement rocks indicate that the region was inboard and thermally isolated from the major continent-continent collision associated with the Grenville-Llano orogeny at about 1.1 Ga. It should be noted that there may be some evidence for proximity to the Grenville-Llano deformation front. U-Pb dating of zircons recovered from concentrates of the Prairie Creek lamproite have yielded a 1050 Ma age (Reichenback and Parrish, 1988). The 1050 Ma age is indicative of Grenville terrane suggesting either proximity to the Llano deformation front or basement involvement in later Ouachita deformation.

Xenolith petrology, amphibolite isotopic ages and the lithospheric transect of Mickus and Keller can be used to test two major models proposed for generation of the Ouachita salient and the northern Gulf Coast. The first model is that the Ouachita trough was part of an Early Paleozoic failed rift system that had continental crust with Grenville basement located south of Ouachita trough (Figure 5-4). Evidence supporting this hypothesis is the pre-orogenic sedimentation patterns that suggest the Ouachita trough was a narrow two-sided basin with the southern bounding block providing craton-like detritus well into Ordovician time (Lowe, 1985). The second model is that the southern margin of the mid-continent rifted in late Precambrian-early Paleozoic time along the

Ouachita rift (Figure 5-5). This rift zone extended from south-central Texas northeast to its intersection with the northwest-trending Alabama-Oklahoma transform fault (Thomas, 1991). The large block of continental lithosphere that was rafted out of the Ouachita salient was proposed to have docked with Gondwanaland, becoming part of the Precordillera of Argentina (Astini and others, 1995). Support for a Laurentian origin for the Argentine Precordillera was provided by U-Pb zircon ages indicating a Grenville age (Kay and others, 1996), and by correlation with syn-rift rhyolites of Cambrian age (Thomas, 2000). Expected lithosphere characteristics of these two models for generation of the Ouachita Trough are compared in Table 5-3, and evaluated below.

Data on mantle rocks are provided by xenoliths recovered from the Prairie Creek lamproite province in southwestern Arkansas. These xenoliths record evidence of a two layer subcontinental mantle lithosphere with depletion levels and a geothermal gradient consistent with a Lower Proterozoic age stable craton (Dunn and others, 2000). Furthermore, the relatively high Mg-number of olivine in conjunction with the relative abundance of orthopyroxene within the Arkansas mantle peridotites is typical of subcontinental mantle lithosphere and is inconsistent with depleted oceanic mantle lithosphere (Boyd, 1989).

The hypothesis of depleted, low density mantle lithosphere is reinforced by the lithospheric transect model generated from gravity and seismic data in the region (Mickus and Keller, 1992). The lithospheric transect shows that the Prairie Creek lamproite province falls within the basin structure adjacent to the southern margin of the mid-continent craton (Figure 5-6). This transect shows the presence of depleted (low density) mantle lithosphere beneath the Arkansas lamproite province with a density of 3.30 g/cm^3 . More fertile “oceanic” mantle lithosphere with a density $\sim 3.42 \text{ g/cm}^3$, is observed

approximately 400 km south of the Prairie Creek lamproite province beneath southern Louisiana. Subcontinental mantle lithosphere xenoliths at Prairie Creek record high olivine depletion and low heat flow and therefore are more consistent with the continental rift-Ouachita model than the rifted ocean margin Ouachita model.

Deeper crust xenoliths consist of amphibolite, rare granitic/rhyolitic rock, and significant amounts of altered epidote-rich rock. The 1.42 Ga K-Ar age of the amphibolite establishes an association with the granite-rhyolite terrane of the mid-continent. Furthermore, the K-Ar ages indicate that crustal temperatures did not exceed 500°C since the Proterozoic indicating thermal isolation from the effects of the Grenville and Ouachita orogenies. No petrologic evidence for the presence of Cambrian age ocean crust as predicted by the rifted ocean margin model was observed. Even if the region was located inland of the rifted margin, it is hard to imagine close proximity to a long-standing Early Paleozoic mid-ocean ridge without some evidence of its thermal effects.

The lithospheric transect of Mickus and Keller indicates the presence of “oceanic transition crust” with a density of $\sim 2.98 \text{ g/cm}^3$. This transition crust has a thickness and density that could be consistent with either thickened oceanic crust or thinned lower cratonic crust. However, the 1.42 Ga amphibolite age strongly favors a lower cratonic origin rather than oceanic crust. The composition of the crustal xenoliths and the 1.42 Ga K-Ar amphibolites are consistent with continental extension (structural) of granite/rhyolite terrane and favor the continental rift model for the origin of the Ouachita system. A most interesting observation from the lithospheric transect model is that the “rift pillow”, a thick package of basaltic intrusions associated with oceanic rifts, is found much further south associated with ocean crust within the Gulf of Mexico and not within the structure beneath the Arkansas lamproite province. The lack of Paleozoic age ocean

crust or associated thermal effects, including a “rift pillow” beneath the Arkansas lamproite province, is inconsistent with the rifted ocean margin origin of the Ouachita system. However, the mantle lithosphere transect is consistent with ocean crust within the Gulf of Mexico being a rifted ocean margin of either Lower Paleozoic or Mesozoic age.

The dominant basement rock found in xenoliths from beneath southwestern Arkansas is 1.4 Ga amphibolite of the mid-continent granite-rhyolite terrane. However, projection of the Llano deformation and U-Pb zircon ages of ~ 1050 Ma indicate that the area may be proximal to this structure. Basement continuity is reinforced by the lithospheric transect model which shows both structural symmetry and lateral continuity (Figure 5-6). Cratonal crust north of the Ouachita region consists of an upper crust which is ~ 20 km thick with a density of 2.75 g/cm^3 and a lower crust which is ~ 20 km thick and a density of 3.07 g/cm^3 . This is nearly identical in thickness and density to the two part “micro-continent” south of the Ouachita region. Continuity of basement features across the Ouachita trough is more consistent with the continental rift-basin as opposed to the ocean margin model of genesis.

The structure of the Ouachita metamorphic belt has been described as consisting of a frontal zone, central zone, and southern Carboniferous province. The frontal zone consists of thrusts and folds involving mainly unmetamorphosed Carboniferous flysch. The central zone or core area consists of older pre-Carboniferous rocks, with greenschist-facies metamorphism, and flanked by Carboniferous flysch. The southern province consists of faulted and folded Carboniferous strata, but with deformation decreasing southward until relatively undeformed Carboniferous strata are encountered (Nicholas and Weddell, 1989). The low metamorphic grade within the tectonic zone and the

apparent symmetry of the deformation belt are more consistent with a rift association than with a strongly deformed asymmetrically accreted island arc terrane.

Stratigraphic correlation of the pre-orogenic rocks has not been made because drilling has yet to encounter Lower Paleozoic strata south of the exposed Ouachita Mountains. However, pre-orogenic sedimentation patterns indicate that the Ouachita trough was a narrow two-sided basin with significant detrital input from the southern bounding block. The composition of this southerly derived detritus suggests a craton-derived passive margin sequence (Lowe, 1985). A deep well drilled near Waco, Texas, within the core zone of the Ouachita belt, encountered massive carbonates which have been correlated with Ordovician carbonates of the adjacent foreland (Nicholas and Waddell, 1989). These rocks may correlate with the two dolomitized xenoliths found within the Prairie Creek lamproites.

Stratigraphic correlation of the syn-orogenic Carboniferous flysch is nearly impossible due to the extensive deformation within this sedimentary sequence. Nicholas and Weddell (1989) have made a broad correlation of the Carboniferous flysch across the Ouachita Mountains in stating that the rocks are slightly deformed and unmetamorphosed in the frontal zone, strongly deformed and weakly metamorphosed within the core zone, and slightly deformed and unmetamorphosed in the southern province. Probably the best chance for correlation of rocks across the Ouachita trough lies with dating of intersected volcanic units. Thin volcanic units are found throughout much of the Paleozoic as indicated by exposed tuffs within the Lower Stanley Group (Miser and Purdue, 1929), and drilled volcanic rock of 380 Ma to 255 Ma near Waco, Texas (Nicholas and Waddell, 1989). Another well drilled near Sabine, Texas, within the Texarkana platform, intersected rhyolite porphyry with a Rb-Sr age of 255 +/- 10 Ma (Nicholas and Waddell,

1989). This isotopic age is comparable with a Rb-Sr age of 255 \pm 11 Ma recovered from volcanic rock within the well near Waco, Texas, on the other side of the Ouachita trough and suggests a possible correlation of these rocks. Possible correlation of both pre-orogenic and syn-orogenic volcanic rocks across the Ouachita system would favor the continental rift model for Ouachita development. In addition, the sporadic nature of these thin volcanic units within a thick sedimentary section is more consistent with a rift-related association than that of an accreted volcanic island-arc suggested within the rifted ocean margin model.

Nd isotopes have been used to constrain sediment sources for the Ouachita-Marathon fold belts. Research indicates that Nd depleted mantle model ages (T_{DM}) define three distinct populations: a Lower to Middle Ordovician T_{DM} = 2.0 Ga, an Upper Ordovician to Pennsylvanian T_{DM} = 1.6 Ga, and a Mississippian volcanic tuff T_{DM} = 1.1 Ga (Gleason and others, 1995). The authors interpret the data to imply that there was a shift from craton-derived to Appalachian-derived sediment sources at \sim 450 Ma. They interpret the Mississippian tuffs T_{DM} to have resulted from the isotopic mixing of old crust with young mantle-derived components within a continental margin arc. However, this data is more consistent with the rift-basin model for formation of the Ouachita System. In this model, the \sim 450 Ma shift in sediment sources is from craton-derived to craton-margin derived sediment sources of Grenville age located to the south and consistent with interpreted source directions. The Mississippian tuff T_{DM} = 1.1 Ga, would be expected if these volcanic units were derived from melting of Grenville age crust located in the craton margin to the south. Therefore, Nd isotope data from Ouachita sedimentary assemblages are consistent with the rift-basin Ouachita model of formation.

Xenolith data, geophysical transects, and possible stratigraphic correlation across the Ouachita fold belt support the rift-basin model of the Ouachita Trough as opposed to the rifted continental margin and late Paleozoic development of an exotic island arc terrane. It seems likely that the Ouachita trough was part of an early Paleozoic failed rift system that developed separately from the older Appalachian continental margin (Lowe, 1989). The Ouachita trough was connected to both the Early Paleozoic Wichita and Reelfoot rifts and consisted of two parts; the east-west trending Ouachita Rift in Arkansas and the northeast trending Waco Rift in Texas (Figure 5-7). The Ouachita trough probably formed from distended continental crust with the southern bounding block consisting of a micro-continent of Grenville basement and Lower Paleozoic sediments. Inclusion of this bounding block of Grenville age basement extends the southern margin of the mid-continent craton into southern Louisiana (Figure 5-7).

The rift system apparently deepened rapidly during the Early Carboniferous Period with subsidence ending in the Early Pennsylvanian Period with onset of the Ouachita orogeny. The Ouachita orogeny may have been initiated when the southern margin of the bounding micro-continent was impinged by an Appalachian-type orogeny. Tectonic forces associated with this orogeny at the southern passive margin were transmitted through this stable block causing compression of the Carboniferous flysch and resulting in the thin-skin fold and thrust belt of the Ouachita Mountains.

The Ouachita rift-basin model, through its association with the mid-continent rift-system, helps to explain the shape of the Ouachita salient, the location of the existing Ouachita outcrops, and the lack of high-grade metamorphic rock or plutons within the Ouachita Mountains. This model predicts the existence of a cratonic block with Grenville basement beneath the Texarkana Platform and the resulting bio-stratigraphic

correlation of the Carboniferous flysch across the Ouachita trough. The Ouachita rift model is inconsistent with the hypothesis that the provenance region of the Argentine Precordillera was the Ouachita rifted margin and instead suggests another area further south near the craton margin as a likely provenance region of Laurentia.

The Prairie Creek lamproite xenolith suite, in conjunction with geophysical data, provides important constraints on models of the origin of the Ouachita System. This data provides evidence for the association of the Ouachita trough with a Paleozoic continental rift system and possible extension of the mid-continent craton ~400 km further south than previously suspected. Validation of the aulacogen/rift model would rewrite the basement geology of the Gulf Coast region. In summary, the Prairie Creek lamproite xenolith suite provides important constraints for the regional Paleozoic tectonic evolution of the southern mid-continent and Gulf Coast regions.

TABLE 5-1
Mineral Compositions of Selected Crustal Xenoliths

	c1 amphibolite				c10 amphibolite			
	amph	biotite	plag	titanite	amph	muscov	plag	ilmenite
SiO2	45.33	36.88	60.10	31.17	43.92	48.79	45.48	nd
TiO2	0.68	1.59	nd	36.20	0.76	0.01	0.02	49.52
Al2O3	9.61	15.67	25.35	1.50	10.98	35.08	36.12	nd
FeO*	15.03	14.86	0.10	0.91	18.23	0.57	0.16	45.30
MnO	0.36	0.26	nd	0.08	0.42	0.02	nd	1.93
MgO	11.99	15.86	nd	0.01	9.96	0.37	nd	0.03
CaO	11.95	0.03	6.44	28.90	10.57	0.55	17.62	0.05
Na2O	1.07	nd	7.85	nd	1.36	1.47	1.34	nd
K2O	1.06	8.44	0.14	0.05	0.53	8.69	nd	0.02
Total	97.08	93.58	99.98	98.82	96.73	95.56	100.73	96.86

	c25 granite				c20 micaceous		
	kspar	muscov	plag	biotite	muscov	biotite	ilmenite
SiO2	65.39	46.12	68.16	33.92	46.50	35.11	0.89
TiO2	nd	0.45	nd	0.98	1.07	1.91	48.71
Al2O3	18.61	31.28	20.00	16.62	31.81	16.28	0.17
FeO*	nd	4.89	nd	24.88	3.34	25.92	31.16
MnO	nd	0.04	nd	0.43	nd	0.56	15.98
MgO	nd	1.23	nd	6.90	0.90	5.99	0.08
CaO	nd	nd	0.46	0.16	0.02	nd	0.09
Na2O	0.54	0.33	11.19	0.04	0.38	0.06	0.06
K2O	15.30	10.35	0.10	9.43	10.79	9.63	0.10
Total	99.87	94.69	99.94	93.36	94.82	95.47	97.23

	c22 unakite		c17 epidote-rich			
	epidote	kspar	hem	epidote	amph	garnet
SiO2	37.73	64.34	nd	37.73	49.14	37.42
TiO2	0.07	0.02	0.10	0.13	0.04	0.34
Al2O3	21.89	17.63	nd	23.73	3.55	16.83
FeO*	12.47	0.04	91.95	10.94	20.40	11.45
MnO	0.19	nd	0.15	0.35	1.36	7.31
MgO	0.04	nd	nd	nd	9.93	nd
CaO	22.86	nd	nd	22.53	11.33	24.92
Na2O	0.01	0.40	nd	nd	0.66	nd
K2O	nd	16.20	0.02	nd	0.25	nd
Total	95.26	98.63	92.22	95.42	96.67	98.28

	c18 epidote-rich				c23 epidote-rich		
	epidote	amph	garnet	zoisite	epidote	chlorite	muscov
SiO2	37.07	56.37	38.13	44.02	38.79	21.96	45.91
TiO2	0.31	nd	0.11	nd	nd	0.72	nd
Al2O3	9.42	18.09	22.10	24.4	27.06	20.64	36.16
FeO*	18.08	6.29	13.76	0.36	8.3	41.76	2.22
MnO	2.01	0.02	0.23	0.03	0.24	0.58	nd
MgO	0.08	4.27	0.02	nd	nd	2.53	0.41
CaO	30.96	1.43	22.58	26.22	23.58	0.18	0.05
Na2O	nd	0.11	nd	0.02	nd	0.02	0.22
K2O	nd	0.47	nd	nd	nd	0.03	10.90
Total	97.94	87.07	96.94	95.06	98.01	88.43	95.91

	c24 epidote-rich			
	epidote	chlorite	muscov	titanite
SiO2	39.08	22.13	45.95	30.68
TiO2	nd	0.09	nd	32.95
Al2O3	29.96	20.57	35.97	4.78
FeO*	4.63	40.55	1.70	2.10
MnO	0.09	0.71	nd	0.05
MgO	nd	3.30	0.25	0.07
CaO	23.80	0.02	0.02	27.52
Na2O	nd	0.02	0.27	nd
K2O	nd	0.06	10.82	nd
Total	97.55	87.46	94.97	98.17

FeO*: Total iron as FeO

TABLE 5-2
K-Ar Data

Sample	Mineral	wt % K	% ⁴⁰ *Ar	⁴⁰ *Ar (ppm)	Age (Ma)	+/- 1σ
BL	hornblende	0.95	96	0.1434	1431	37
BL 1	hornblende	0.886	98	0.1428	1478	144
BL 1b	hornblende	0.893	98	0.1326	1425	51
TK 1	hornblende	0.942	98	0.1242	1310	58
Constants:	$\lambda = 4.963 \times 10^{-10}/\text{yr};$ $\lambda = 0.581 \times 10^{-10}/\text{yr};$ $^{40}\text{K}/\text{K} = 1.167 \times 10^{-4}$					

TABLE 5-3
Comparison of Ouachita Model Expectations

	Aulacogen/Rift-Basin	Oceanic Margin/Island Arc
Stratigraphy	regional correlation	no correlation
Volcanic Rocks	sporadic (alkalic)	widespread (calc-alkaline)
Metamorphic Rocks	low-grade (symmetric)	high-grade (asymmetric)
Basement Rocks	structural continuity	no continuity
Lower Crust	altered granite/gabbro	ocean floor/"rift pillow"
Upper Mantle	continental, low-geotherm	oceanic, high-geotherm

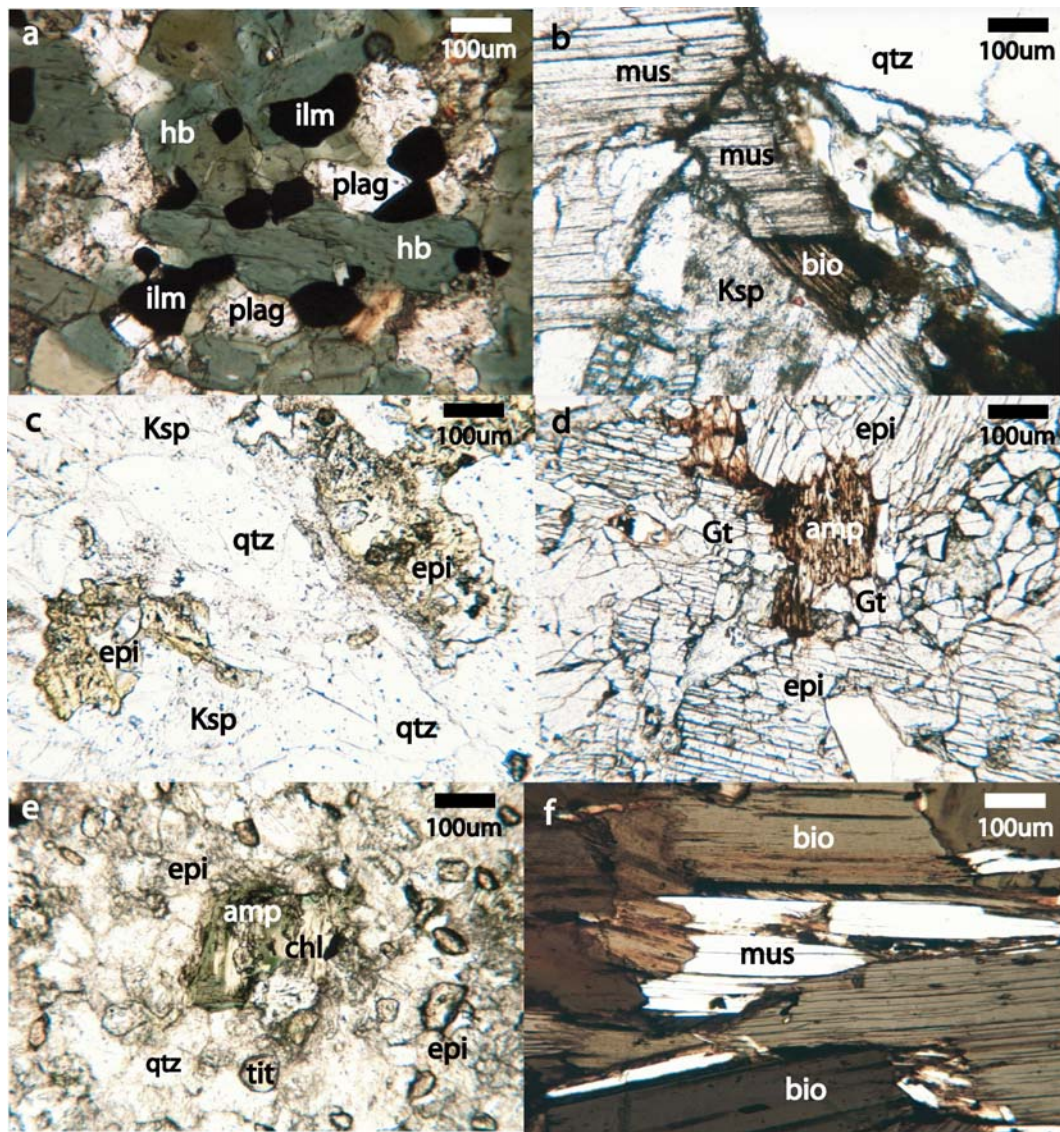


Figure 5-1: Photomicrographs of thin sections in plane polarized light: a) an ilmenite-bearing amphibolite (c10), b) granite with muscovite and biotite (c25), c) Unakite, altered granite consisting of microcline, quartz and epidote (c22), d) epidote-rich rock consisting of epidote, amphibole, and garnet (c17), e) extremely altered epidote-rich rock showing breakdown of amphibole to epidote and chlorite (c23), and f) micaceous rock with biotite, muscovite and ilmenite (c20).

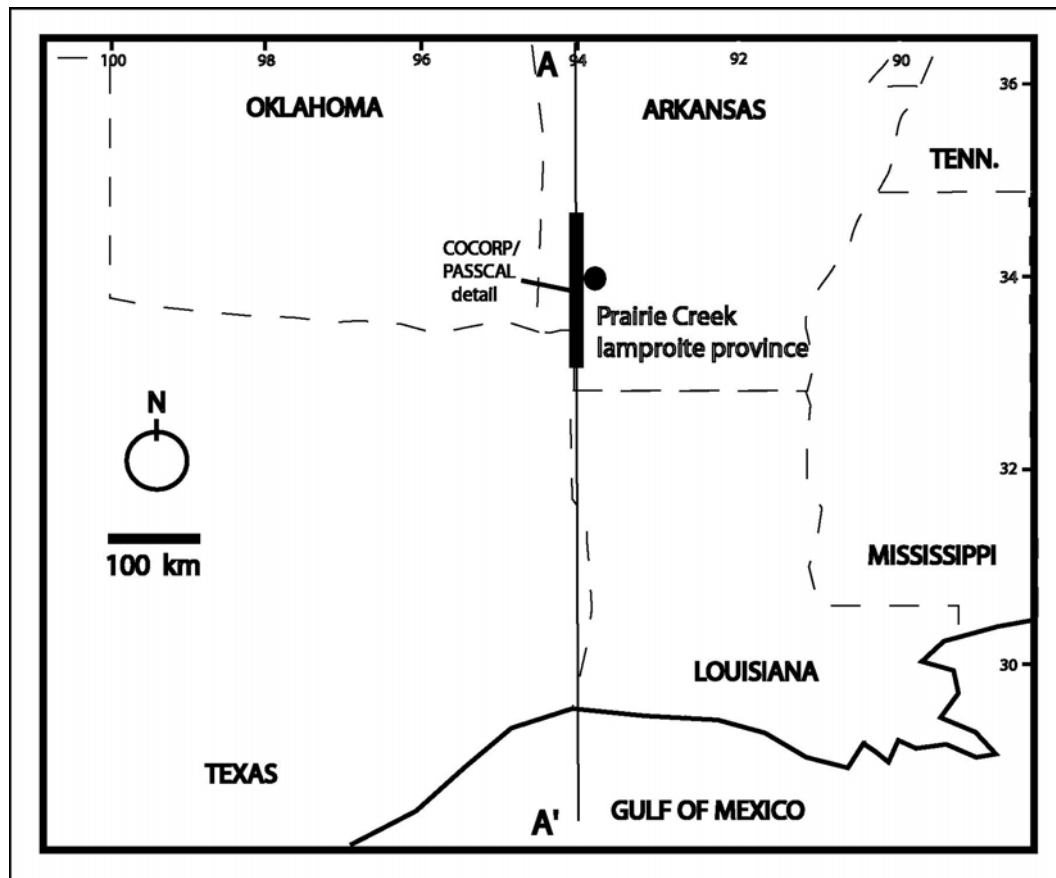


Figure 5-2: Location map of the lithospheric transect of Mickus and Keller, 1992. Sub-surface detail derived from COCORP / PASSCAL gravity and seismic data in the area of the Prairie Creek lamproite province.

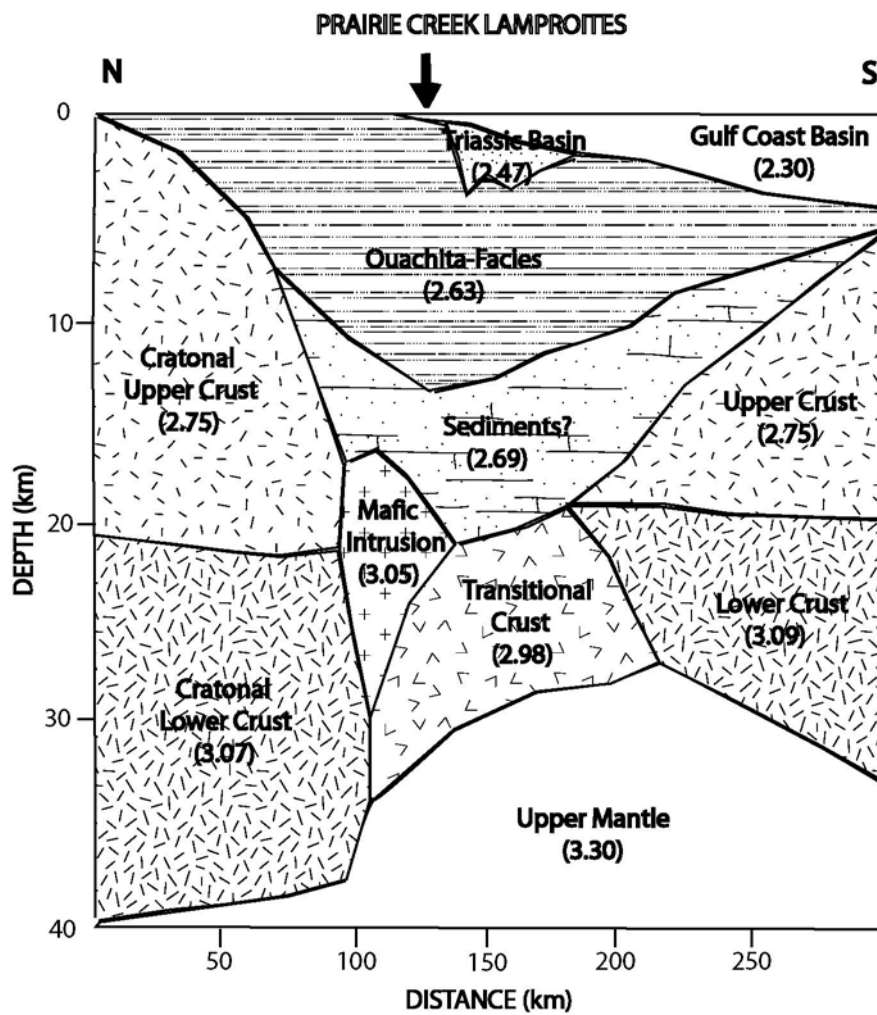


Figure 5-3: Detailed crustal section beneath the Prairie Creek lamproite province. Section modified from the lithospheric transect of Mickus and Keller, 1992. Model is based on seismic and gravity surveys along the PASSCAL/COCORP transect shown in Figure 5-2. Calculated rock density in g/cm^3 is shown in parenthesis.

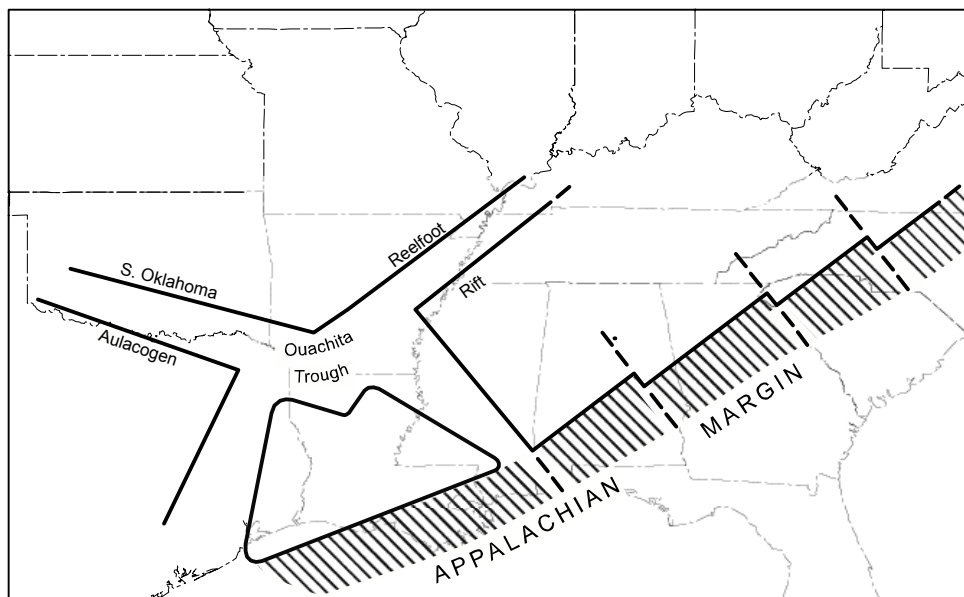


Figure 5-4: Aulacogen model of Ouachita System (Lowe, 1985). The region is associated with a mid-continent rift system in the Early Paleozoic Era.

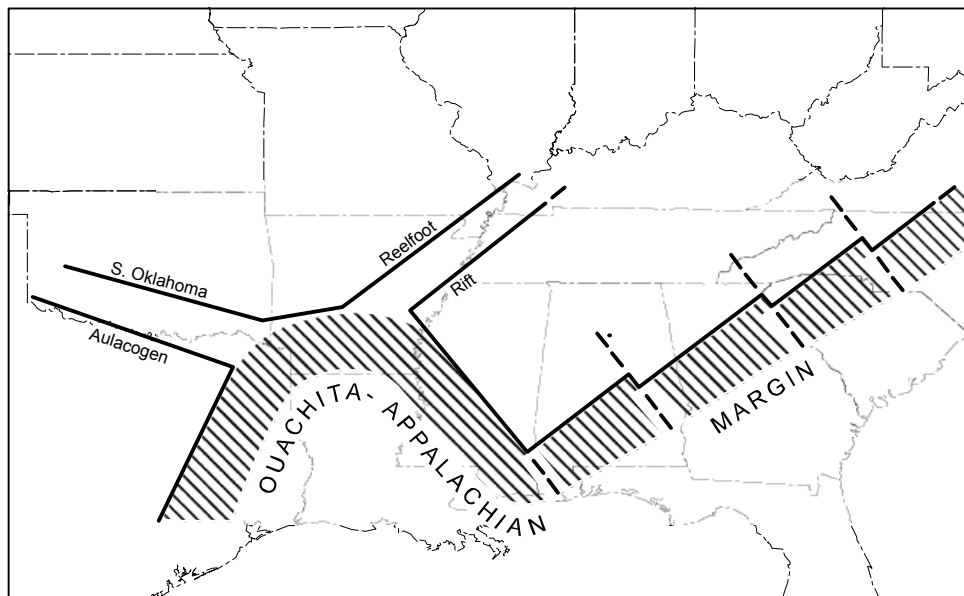


Figure 5-5: Rifted margin model of Ouachita System (Lowe, 1985). The region is associated with a rifted oceanic margin in the Early Paleozoic Era.

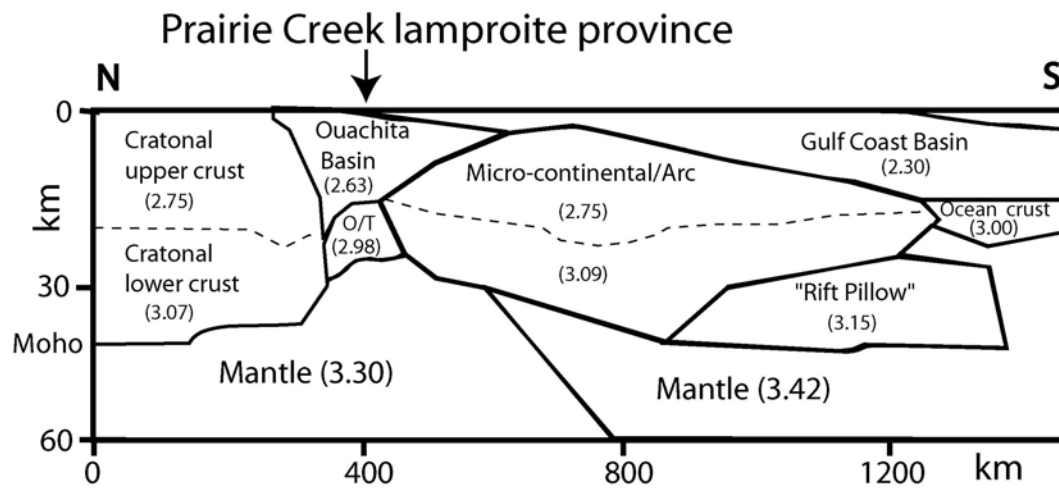


Figure 5-6: Simplified lithospheric transect model (Mickus and Keller, 1992). The approximate location of the Prairie Creek lamproite province is indicated. Calculated rock density in g/cm³ is shown in parenthesis.

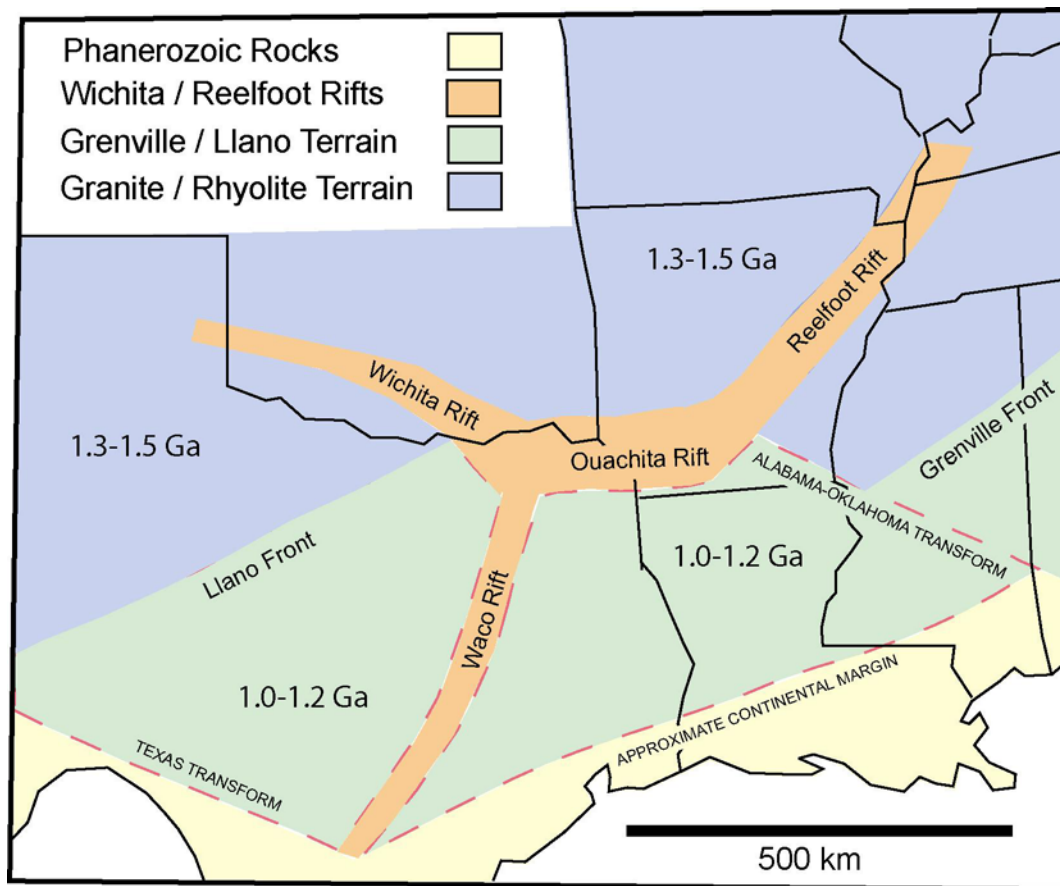


Figure 5-7: Idealized basement geology for the Ouachita aulacogen model.

Chapter 6

SUMMARY AND CONCLUSIONS

Three previously unexplored Arkansas lamproites (satellites to the main Prairie Creek vent) were delineated and evaluated during the 1980's. Exploration programs utilized detailed geophysics, heavy mineral sampling and soil geochemistry. The three vents – Black Lick (10 hectares), Twin Knobs 2 (2 hectares) and Timberlands (<1 hectare) -- were intruded into Early Cretaceous Trinity Fm deposits, and are overlain unconformably by the Late Cretaceous Tokio Fm. This stratigraphy is consistent with published K-Ar phlogopite ages of ~106 Ma for the Prairie Creek vent. Field relationships establish that about 75% of the surface area of the lamproites consist of pyroclastic tuffs, typically with fine-grained sandy tuffs near the margins, and coarse-grained pyroclastics near the cores of the lamproite. Approximately 25% of the vents consist of late stage hypabyssal olivine lamproite which may have reached the surface as extrusive flows.

A 260 tonne bulk sample taken from the two larger lamproites recovered 5 macro diamonds (>0.5mm) yielding a sub-economic average diamond grade of ~0.04 carats per 100 tonnes. This diamond grade is slightly less than that reported for the adjacent Prairie Creek and Twin Knobs 1 lamproites. The bulk sampling yielded a rare suite of mantle and crustal xenoliths.

The recent economic evaluation of the Prairie Creek lamproite has served to advance the understanding of both the geology and history of the Crater of Diamonds

State Park. Although the economic evaluations reveal that the *in-situ* lamproite is not of significant grade to warrant large scale mining operations, they do reveal that the property was a viable economic diamond mine in its time. Commercial diamond grades were initially achieved due to the extreme chemical weathering of the ultramafic rock in the subtropical environment. This unique erosion history allowed for development of economic lag deposits over the vent but also served to minimize downstream accumulation of alluvial diamond deposits. Even though the rich diamondiferous surface soils were rapidly depleted, there is evidence that soils with at least some natural enrichment of diamond remain in the form of small drainages radiating from the intrusion, and as eluvial and alluvial soils adjacent to the intrusion. These deposits are located within the Park boundaries and remain as a future resource to be developed for the tourist industry. All economic evaluations to date have demonstrated the existence of naturally occurring macrodiamonds, and these diamonds, along with the past mining history, are the reason that the State Park was founded and continues in operation today as a tourist attraction.

Both mantle and crustal xenoliths were recovered during diamond bulk testing of various vents within the Prairie Creek lamproite province. Mantle xenoliths include approximately 40 polymineralic xenoliths consisting of eclogite, garnet websterite, wehrlite, harzburgite, spinel lherzolite, garnet/spinel lherzolite and garnet lherzolite. Pressure-temperature calculations based on partitioning of elements between minerals generated a P-T array indicating a geotherm of $\sim 40 \text{ mW/m}^2$; a value typical of Archean or Lower Proterozoic age mantle lithosphere. Two P-T array points with anomalously high temperature values depart from this geotherm and may represent underplating of the

continental crust by magmas associated with the Cretaceous igneous province within southern Arkansas.

Analysis of the Mg-number of olivine within the xenoliths and their recorded pressures indicates the presence of a two layer mantle lithosphere. The shallow mantle lithosphere appears to be relatively fertile consisting of eclogite, wehrlite, websterite, and garnet/spinel lherzolite with an approximate olivine content of Fo_{90.5}. The deeper mantle lithosphere below a depth of ~100 km appears to be relatively depleted consisting of high-Cr spinel lherzolite, harzburgite and garnet lherzolite with an approximate olivine content of Fo_{92.5}. Proposed relationships between average olivine forsterite content and the age of the lithosphere imply that the deeper depleted mantle lithosphere is significantly older than the shallow fertile mantle lithosphere. Two models for tectonic emplacement of this two-layered mantle lithosphere are proposed. The first model suggests incorporation of older allochthonous terrane within the southern margin of the North American craton. Evidence to support this model includes Sm-Nd model ages (Nelson and DePaolo, 1985) and a U-Pb zircon age (Reichenback and Parrish, 1988) which are older than any known rocks in the area. The second model suggests tectonic emplacement of an older continental lithosphere beneath the younger North American craton. This model is supported by the presence of a sharp compositional boundary between the two mantle layers, deep eclogite suite minerals, regional tectonics, and Sr, Nd and Pb isotopic studies. Additional trace, rare-earth element and isotopic studies of these mantle xenoliths may further define the emplacement models for this two-layer mantle lithosphere.

Crustal xenoliths were also recovered during diamond bulk testing within the Prairie Creek lamproite province. More than half of these xenoliths were from near-

surface sedimentary rocks of either Cretaceous or Paleozoic age. The deeper crustal xenoliths are igneous and metamorphic rock types derived from rocks not exposed at the surface. The majority of these deeper xenoliths are amphibolite with rare granite and pelitic metamorphic rocks. Approximately 40% of the deep crustal xenoliths are extensively altered epidote-rich rocks. K-Ar ages of four amphibolite samples average ~ 1.42 Ga. This Proterozoic age indicates the amphibolite is associated with the mid-continent craton and was thermally isolated from later tectonic events associated with both the Grenville and Ouachita orogenies.

Xenolith compositions and isotopic ages in conjunction with published geophysical and drill data are used to test two tectonic models for the development of the Ouachita Mountains. The first model proposed by Lowe (1985) suggests the Ouachita trough is a failed rift basin essentially contained within the North American craton. The second model proposed by Thomas (1991) suggests the Ouachita trough is a rifted continental margin with late Paleozoic accretion of an island arc terrane. Recovered mantle xenoliths are typical of sub-continental mantle lithosphere and record a relatively low geothermal gradient, whereas deep crustal xenoliths indicate 1.42 Ga amphibolite basement rocks. No evidence for the presence of Lower Paleozoic ocean crust or the thermal effects of an ocean rift was observed. A lithospheric transect generated from geophysical data shows symmetry of density and thickness of continental crust across the margins of the Ouachita trough (Mickus and Keller, 1992). Deep drilling has indicated symmetry in the style of structural deformation and low-grade metamorphism within the frontal, core and southern provinces of the Ouachita system (Nicholas and Weddell, 1989). Stratigraphic correlations are inferred for both the pre and syn-orogenic rocks across the Ouachita trough. Application of these data to two models of Ouachita

development suggests that the Ouachita trough is extended and thinned continental lithosphere associated with a Paleozoic rift system that developed separately from the Appalachian continental margin. Tectonic forces associated with the Appalachian orogeny at the distant continental margin were transmitted inland via a crustal block resulting in compression, folding and faulting of the thick Carboniferous flysch developed within the Paleozoic aulacogen.

Appendix A

Microprobe Results for Mantle Xenoliths

Appendix B

Microprobe Results for Crustal Xenoliths

References

- Alibert, C. and Albarede, F. (1988) Relationship between mineralogical, chemical and isotopic properties of some North American kimberlites: Journal of Geophysical Research, v. 93, no. b7, p. 7643-7671
- Astini, R.A., Benedetto, J.L., and Vaccari, N.E. (1995) The early Paleozoic evolution of the Argentine Precordillera as a Laurentian rifted, drifter, and collided terrane: A geodynamic model: Geological Society of America Bulletin v. 107, no. 3, p.253-273
- Atkinson, W.S., Hughes, F.E., and Smith, C.B. (1984) A review of the kimberlitic rocks of western Australia in Kimberlites and related rocks. Proceedings of the Third International Kimberlite Conference, v.1, Washington, D.C., American Geophysical Union, p. 195-224
- Baksi, A.K. (1997) The timing of Late Cretaceous alkalic igneous activity in the northern Gulf of Mexico Basin, southeastern USA., Journal of Geology, v 105, p. 629-643
- Ballhaus, C., Berry R.F., and Green D.H. (1991) High pressure experimental calibration of the olivine-orthopyroxene-spinel-oxygen geobarometer:

implications for the oxidation state of the upper mantle: Contributions to Mineralogy and Petrology, v.107, p. 27-40

Bolivar, S.L. and Brookins, D.G. (1979) Geophysical and Rb-Sr study of the Prairie Creek, Arkansas. kimberlite in Kimberlites, Diatremes, and Diamonds. Proceedings of the Second International Kimberlite Conference, Washington, D.C., American Geophysical Union, v.1, p. 289-299

Boyd, F.R. and McCallister, R.H. (1976) Densities of fertile and sterile garnet peridotites: Geophysical Research Letters, v. 3, p. 509-512.

Boyd, F.R. (1989) Compositional distinction between oceanic and cratonic lithosphere: Earth and Planetary Science Letters, v. 96, p. 15-26

Boyd, F.R., D.G. Pearson, and Mertzman, S.A. (1999) Spinel-facies Peridotites from the Kaapvaal Root: in Fei, Y. et al., eds., Mantle Petrology: Field Observations and High Pressure Experimentations: A Tribute to Francis K. (Joe) Boyd: The Geochemical Society, Special Publication No. 6. p. 40-48

- Brey, G.P. and Kohler, T. (1990) Geothermobarometry in four-phase lherzolites
II. New thermobarometers, and practical assessment of existing
thermobarometers: *Journal of Petrology*, v. 31, p. 1353-1378
- Chulick, G.S. and Mooney, W.D. (1998) New maps of North American crustal
structure. *Seismological Research Letters*, v. 69, 160 p
- Dalziel, I.W.D., Mosher, S. and Gahagan, L.M. (2000) Laurentia-Kalahari
collision and the assembly of Rodinia: *Journal of Geology*, v. 108, p.
499-513
- Dunn, Dennis P. (2000) Erosional diamond distribution at the Prairie Creek
lamproite pipe, Murfreesboro, Arkansas: *Geological Society of America
Abstracts with Programs, South Central Region*, v. 32, no. 3, A-9
- Dunn, D., Smith, D., McDowell, F.W. and Bergman, S.C. (2000) Mantle and
crustal xenoliths from the Prairie Creek lamproite province, Arkansas:
Geological Society of America Abstracts with Programs, v. 32, no. 7,
A-386
- Dunn, D.P. and Taylor, S.D. (2001) Geology of three additional lamproite
occurrences, Pike County, Arkansas: *Geological Society of America
Abstracts with Programs, South Central Region*, v. 33, no. 5, A-56

- Dunn, D.P. and Taylor, S.D. (1988a) Orientation report: Arkansas Diamond Development Company (unpublished), March 1988, 56pp.
- Dunn, D.P. and Taylor, S.D. (1988b) Drilling report: Arkansas Diamond Development Company (unpublished), September 1988, 23pp.
- Dunn, D.P. and Taylor, S.D. (1988c) GCO Timberlands drilling report: Arkansas Diamond Development Company (unpublished), January 1988, 30pp.
- Dunn, D.P. and Taylor, S.D. (1989) Drilling report: Arkansas Diamond Development Company (unpublished), July 1989, 24pp.
- Fuller, John T., (1909) Diamond mine in Pike County, Arkansas. Engineering and Mining Journal, v. 87, p. 152-155
- Fuller, John T., (1931). Reports and information gathered by John T. Fuller from 1908 to 1931, diamond fields in Pike County, Arkansas (unpublished), April 1931, 45pp.
- Gaul, O.F., Griffin, W.L., O'Reilly, S.Y. and Pearson, N.J. (2000) Mapping olivine composition in the lithospheric mantle: Earth and Planetary Science Letters, v. 182, p. 223-235

- Gleason, J.D., Patchett, P.J., Dickinson, W.R. and Ruiz, J. (1995) Nd isotopic constraints on sediment sources of the Ouachita-Marathon fold belt: Geological Society of America Bulletin, v. 107, no. 10, p. 1192-1210
- Gogineni, S.V., Melton, C.E., and Giardini, A.A. (1978) Some petrological aspects of the Prairie Creek diamond-bearing kimberlite diatreme, Arkansas. Contributions to Mineralogy and Petrology, v. 66, p 251-261
- Grand, S.P. (1994) Mantle shear structure beneath the Americas and surrounding oceans: Journal of Geophysical Research, v. 99, no. B6, p. 11,591-11,621
- Gregory, P. and Tooms, J.S. (1969) Geochemical prospecting for kimberlites. Colorado School of Mines Quarterly, v. 64, no. 1, p. 265-305
- Griffin, W.L., O'Reilly, S.Y., Ryan, C.G. and Waldman, M.A., (1994) Indicator minerals from Prairie Creek and Twin Knobs lamproites: Relation to diamond grade: in Proceedings of the Fifth International Kimberlite Conference, CPRM Special Publication, v. 2, p. 302-311
- Griffin, W.L., O'Reilly, S.Y., and Ryan, C.G. Gaul, O. and Ionov, D. (1998a) Secular variation in the composition of sub-continental lithospheric mantle, in Braun J., et al., eds., Structure and evolution of the Australian

continent: Washington, D.C., American Geophysical Union Geodynamics Series, v. 26, p. 1-26

Griffin, W.L., Zhang, A., O'Reilly, S.Y., and Ryan, C.G. (1998b) Phanerozoic evolution of the lithosphere beneath the Sino-Korean craton, in Flower, M., et al., eds., Mantle dynamics and plate interactions in East Asia: Washington, D.C., American Geophysical Union, p. 107-126

Gurney, J.J., Jakob, W.R.O. and Dawson, J.B. (1979) Megacrysts from the Monastery kimberlite pipe, South Africa: in Boyd and Meyer, Proceedings of the Second International Kimberlite Conference, Washington, D.C., American Geophysical Union, v.1, p. 227-243

Hanes, J.A. (1991) K-Ar isotopic age dating in: Short course handbook on applications of radiogenic isotopic systems to problems in geology: editors L. Heaman and J.N. Ludden, Mineralogical Association of Canada

Hardie, L.A. (1989) Cyclic platform carbonates in the Cambro-Ordovician of the Central Appalachians: in Volume 1, Cambro-Ordovician carbonate banks and siliciclastic basins of the United States Appalachians, Hanshw, Penelope M. (editor), p. 51-81

- Howard, J.M. (2000). Summary of the 1990's exploration and testing of the Prairie Creek Diamond-Bearing Lamproite Complex, Pike County, Arkansas, with a Field Guide *in* Contributions to the Geology of Arkansas, Volume IV, J.M. Howard, ed., Arkansas Geological Commission Misc. Pub. 18-D, p. 57-73
- Jordan, T.M., (1978) Composition and development of the Continental Tectosphere: *Nature*, v. 274, p. 594-598
- Kay, S.M., Orrell, S. and Abbruzzi, J.M., (1996) Zircon and whole rock Nd-Pb isotopic evidence for a Grenville age and a Laurentian origin for the basement of the Precordillera in Argentina: *The Journal of Geology*, v. 104, p. 637-648
- Kennedy, C.S. and Kennedy, G.C. (1976) The equilibrium boundary between graphite and diamond: *Journal of Geophysical Research*, v. 81, p. 2167-2170
- Kidwell, A. L., (1990). Famous mineral localities: Murfreesboro, Arkansas. *Mineralogical Record*, v. 21-6, p. 545-555

- Kopylova, M.G., Russell, J.K. and Cookenboo, H., (1998) Upper mantle stratigraphy of the Slave craton, Canada: Insights into a new kimberlite province. *Geology*, v.26, no. 4, p. 315-318
- Krogh, E.J. (1988) The garnet-clinopyroxene Fe-Mg geothermometers-a reinterpretation of existing experimental data: *Contributions to Mineralogy and Petrology*, v. 99, p. 44-48
- Lambert, D.D., Shirey, S.B. and Bergman, S.C., (1995) Proterozoic lithospheric mantle source for the Prairie Creek lamproites: Re-Os and Sm-Nd isotopic evidence: *Geology*, v. 23, no. 3, p. 273-276
- Le Bas, M.J., Le Maitre, R.W., Streckeisen, A. and Zanetti, B. (1986) A chemical classification of volcanic rocks based on the total alkali-silica diagram. *Journal of Petrology*, v. 27, p. 745-750
- Lee, C.T. and Rudnick, R.L. (1999) Compositionally stratified cratonic lithosphere: Petrology and geochemistry of peridotite xenoliths from Labait volcano, Tanzania: *Proceedings of the VII International Kimberlite conference*, v. 2

- Lee, C.T., Yin, Q., Rudnick, R.L., Jacobsen, S.B. (2001) Preservation of ancient and fertile lithospheric mantle beneath the southwestern United States: *Nature*, v. 411, p. 69-73
- Lillie, Robert J. (1985) Tectonically buried continent/ocean boundary, Ouachita Mountains, Arkansas: *Geology*, v. 13, p. 18-21
- Lowe, Donald R. (1985) Ouachita trough: Part of a Cambrian failed rift system: *Geology*, v. 13, p. 790-793
- Lowe, Donald R. (1989) Stratigraphy, sedimentology, and depositional setting of pre-orogenic rocks of the Ouachita Mountains, Arkansas and Oklahoma: in *The Geology of North America, Volume F-2*, The Geological Society of America
- McCandless, T.E., Waldman, M.A. and Gurney, J.J. (1994) Macro- and microdiamonds from Arkansas lamproites: morphology, inclusions, and isotope geochemistry. In *Proceedings of the Fifth International Kimberlite Conference, CPRM Special Publication*, v. 2, p. 264-266
- Mickus, K.L. and Keller, G.R., (1992) Lithospheric structure of the south-central United States. *Geology*, v. 20, p. 335-338

- Miser, H.D. (1913) New areas of diamond-bearing peridotite in Arkansas. U.S. Geological Bulletin 540-U, Contributions to Economic Geology, pt. 1, p. 534-546
- Miser, H.D. and Purdue, A. H. (1929) Geology of the DeQueen and Caddo Gap quadrangles, Arkansas: U.S. Geological Survey Bulletin 808, 191 pp.
- Mitchell, R.H. and Bergman, S.C. (1991) Petrology of lamproites: New York, New York, Plenum Press, 447 pp.
- Mitchell, R.H. and Lewis R.D. (1983) Priderite-bearing xenoliths from the Prairie Creek mica-peridotite, Arkansas: Canadian Mineralogist, v.21, p.59-64
- Moody, C.L. (1949) Mesozoic igneous rocks of northern Gulf Coastal Plain: Bulletin of the American Association of Petroleum Geologists, v. 33, no. 6, p. 1410-1428
- Morgan Mining & Environmental Consultants (1993) Phase I – Evaluation Program, Crater of Diamonds State Park, Project Manager’s Report, Arkansas Department of Parks and Tourism, Little Rock, Arkansas

- Morgan Worldwide Mining Consultants (1997) Crater of Diamonds State Park Evaluation Program, final report, Arkansas State Parks, Recreation and Travel Commission, Little Rock, Arkansas, 108 pp.
- Mosher, S. (1998) Tectonic evolution of the southern Laurentian Grenville orogenic belt: Geological Society of America Bulletin, v. 110, no. 11, p. 1357-1375
- Nelson, B.K., and DePaola, D.J. (1985) Rapid Production of Continental Crust 1.7-1.9 b.y. ago: Nd isotopic evidence from the basement of the North American mid continent: Geological Society of America Bulletin, v. 96, p. 746-754
- Nicholas, R.L. and Waddell, D.F. (1989) The Ouachita system in the subsurface of Texas, Arkansas, and Louisiana, in Hatcher, R.D., Jr., Thomas, W.A. and Viele, G.W., eds., The Appalachian-Ouachita orogen in the United States: Geological Society of America, The Geology of North America, Volume F-2, p. 661-672
- Nimis, P. and Taylor, W.R. (2000) Single clinopyroxene thermobarometry for garnet peridotites: Part I. Calibration and testing of a Cr-in-Cpx barometer and an enstatite-in Cpx thermometer: Contributions to Mineralogy and Petrology, v. 139, p. 541-554

O'Neill, H.S. (1981) The transition between spinel lherzolite and garnet lherzolite, and its use as a geobarometer. *Contributions to Mineralogy and Petrology*, v. 77, p. 185-194

O'Reilly, S.Y., Griffin, W.L. Djomani, Y.H. and Morgan, P. (2001) Are lithospheres forever? Tracking changes in subcontinental lithospheric mantle through time. *Geological Society of America Today*, v. 11, no. 4, p. 4-10

Pantaleo, N.S., Newton, M.G., Gogineni, S.V., Melton, C.E., and Giardini, A.A., (1979) Mineral inclusions in four Arkansas diamonds: Their nature and significance: *American Mineralogist*, v. 64, p. 1059-1062

Pollack, H.N. and Chapman, D.J. (1977) On the regional variation of heat flow, geotherms, and the thickness of the lithosphere. *Tectonophysics*, v. 38, p. 279-296

Poudjom Djomani, Y.H., O'Reilly, S.Y., Griffin, W.L. and Morgan, P. (2001) The density structure of subcontinental lithosphere: Constraints on delamination models, *Earth and Planetary Science Letters*, v. 184, p. 605-621

Reichenbach, I. and Parrish, R. (1988) Age of crystalline basement in BC and NWT, Canada, and CO and AR, U.S.A., as Inferred from U-Pb zircon geochronology of diatremes: Geological Society of America Abstracts with Programs, v. 20, p. A-110

Roden, M.F. and Shimizu, N. (1993) Ion microprobe analysis bearing on the composition of the upper mantle beneath the Basin and Range and Colorado Plateau provinces: Journal of Geophysical Research, v. 98, p. 14091-14108

Rudnick, R.L., and Nyblade, A.A., (1999) The thickness and heat production of Archean lithosphere: Constraints from xenolith thermobarometry and surface heat flow: in Fei, Y. et al., eds., Mantle Petrology: Field Observations and High Pressure Experimentations: A Tribute to Francis K. (Joe) Boyd: The Geochemical Society, Special Publication No. 6. p. 3-12

Scott-Smith, B.H., Danchin, R.V., Harris, J.W. and Stracke, K.J. (1984) Kimberlites near Orroroo, South Australia in Kimberlites II: The mantle and crust-mantle relationships, Elsevier, Amsterdam, p. 121-142

Scott-Smith, B.H. and Skinner, E.M.W. (1984a) A new look at Prairie Creek, Arkansas, in Kimberlites and related rocks: Proceedings of the Third

International Kimberlite Conference, Washington, D.C., American Geophysical Union, v. 1, p. 255-284

Scott-Smith, B.H. and Skinner, E.M.W. (1984b) Kimberlite and American mines near Prairie Creek, Arkansas. Kimberlites III, Annales Scientifique L'Universite de Clermont-Ferrand II, v. 74, p. 27-36

Smith, Douglas (1999) Temperatures and pressures of mineral equilibrium in peridotite xenoliths: Review, discussion and implications: in Fei, Y. et al., eds., Mantle Petrology: Field Observations and High Pressure Experimentation: A Tribute to Francis K. (Joe) Boyd: The Geochemical Society, Special Publication No. 6. P. 171-188

St. Clair, J. (1956) Report on the Arkansas Diamond Property (unpublished), Grand Junction, Colorado, August 14, 1956: 21pp.

Thoenen, J.R., Hill, R.S., Howe, E.G. and Runkek, S.M. (1949). Investigation of the Prairie Creek Diamond Mine Area, Pike County, Arkansas: U.S. Bureau of Mines Report of Investigations 4549: 24pp.

Thomas, William A., (1991) The Appalachian-Ouachita rifted margin of southeastern North America: Geological Society of America Bulletin, v. 103, p. 415-431

Thomas, William A., (2000) Rifting of the Argentine precordillera from southern Laurentia. Palinspastic restoration of basement provinces: Geological Society of America Abstracts with Programs, v. 32, no. 7

Van Schmus, W.R., Bickford, M.E., Sims, P.K., Anderson, R.R., Shearer, C.K. and Treves, S.B., (1986) Proterozoic geology of the western midcontinent basement: geology of North America, v. c.2, p. 239-259

Velde, Danielle (2000) Mineralogy of mafic xenoliths and their reaction zones in the olivine lamproite from Prairie Creek Arkansas and the paragenesis of haggertyite $\text{Ba}(\text{Fe}_6\text{Ti}_5\text{Mg})\text{O}_{19}$. American Mineralogist, v. 85, p. 420-429

Waldman, M.A., McCandless, T.E., and Dummett, H.T. (1987) Geology and petrography of the Twin Knobs #1 lamproite, Pike County, Arkansas in Mantle Metasomatism and Alkaline Magmatism. Geological Society of America Special Paper #215, p. 205-216

Zartman, R.E. (1977) Geochronology of some alkalic rock provinces in eastern and central United States. Annual Review Earth and Planetary Sciences, v. 5, p. 257-286

Vita

Dennis Patrick Dunn was born February 2, 1955 in Philadelphia, Pennsylvania the son of Joseph P. and Margaret E. Dunn. The author received a B.S. in geological sciences from The Pennsylvania State University in 1977 and a M.S. in geology from The Arizona State University in 1980. His first professional position was in diamond exploration with Anaconda Minerals Company. From 1982 through 1984, he participated in a diamond exploration program in Kalimantan, Indonesia. In 1985, the author was trained as a computer exploration geologist with Arco Oil and Gas Company. In 1986, the author took an environmental management position in California with I-Chem Research, but continued his interest in Arkansas diamonds as a consultant. In 1988, the author was appointed as Arkansas Diamond Development Company's technical mining advisor to the Arkansas State Parks Commission on the Crater of Diamonds State Park.

In 1990, the author joined an environmental engineering company (International Technology), ultimately becoming project manager for Travis AFB in Fairfield, California. In 1993, he designed a regional diamond exploration project for Diamond Field Resources (DFR) in Labrador, Canada which ultimately led to the discovery of the Voisey's Bay Ni-Cu-Co deposit. In 1995, the author opened the DFR office in St. John's, Newfoundland and initiated the baseline studies for the project Environmental Impact Study (EIS). In 1996, he

returned to Arkansas to participate in the economic evaluation at the Crater of Diamonds State Park. In 1997, the author married Anita Tobin of Newfoundland, and was accepted into the Ph.D. candidate program at The University of Texas at Austin. Mr. Dunn's permanent address is 5802 Republic of Texas Boulevard, Austin, Texas 78735. The author is a private pilot and owns a Cirrus SR20 single engine aircraft which he enjoys when not working on this dissertation.